HYDROGEN PEROXIDE IN THE HALLS BROOK HOLDING AREA, A SMALL MEROMICTIC LAKE

by

Barbara A. Southworth

B.A., Chemistry
Grinnell College
(1995)

Submitted to the Department of Civil and
Environmental Engineering in Partial Fulfillment of
the Requirements for the Degree of

MASTER OF SCIENCE
in Civil and Environmental Engineering
at the

Massachusetts Institute of Technology

February 1999

Signature of Author_____
Department of Civil and Environmental Engineering
22 December 1998

Certified by_____
Philip M. Gschwend
Professor, Civil and Environmental Engineering
Thesis Supervisor

Accepted by_____
Andrew Whittle, Chairman
Departmental Committee on Graduate Students

HYDROGEN PEROXIDE IN THE HALLS BROOK HOLDING AREA, A SMALL MEROMICTIC LAKE

by

Barbara A. Southworth

Submitted to the Department of Civil and Environmental Engineering on 22 December 1998 in partial fulfillment of the requirements for the Degree of Master of Science in Civil and Environmental Engineering

ABSTRACT

A study of hydrogen peroxide and the processes that control its concentration was carried out at the Halls Brook Holding Area (HBHA) between May 1997 and June 1998. HBHA is a small meromictic lake that receives groundwater contaminated by an adjacent Superfund site. Inflow and outflow rates and depth profiles of temperature, conductivity, dissolved oxygen, pH, and redox potential were measured at HBHA between May 1997 and June 1998. These data were used to characterize the lake structure and chemistry and to calculate groundwater inflow and vertical mixing coefficients.

Hydrogen peroxide was measured at HBHA between May 1997 and February 1998. Large seasonal variations in hydrogen peroxide concentration were observed, with low (< 0.5 micromolar) concentrations in winter and higher than previously reported concentrations in the literature (up to 80 micromolar) in late summer and fall. Additionally, higher concentrations were measured in the afternoon than in the morning on one sampling date (8/14/97). During the late summer and fall, an increase in hydrogen peroxide concentrations with depth in the epilimnion was observed. Below the pycnocline, HBHA is anoxic. Hydrogen peroxide was not detected below the pycnocline on any date, and hydrogen peroxide that was added to samples below the pycnocline was rapidly destroyed. A decay rate of hydrogen peroxide was also measured in samples collected in February. The decay rate was found to be first order with respect to H_2O_2 with a half life of about 30 hours.

Literature values for apparent quantum yields of hydrogen peroxide formation in fresh waters, solar irradiation data, the measured decay rate, and calculated turbulent diffusion coefficients were used to model expected concentrations of hydrogen peroxide in HBHA assuming that abiotic photochemical processes are the only sources. Abiotic photochemical production has been considered to be the only significant source of hydrogen peroxide in most natural fresh waters studied to date. Our modeling results did not fit the observed increase with depth within the epilimnion observed in late summer and fall. This indicates the presence of another, unknown source located near the pycnocline in summer and fall. The size and location of this source were explored using modeling, but the steep observed gradients were not successfully modeled. However, the resulting hydrogen peroxide profiles were highly sensitive to vertical diffusion

coefficient values near the pycnocline, which are not well known due to a lack of data. Based on our observations, we speculate that the unknown source may be biological.

The high concentrations of hydrogen peroxide have significant consequences due to possible Fenton chemistry in HBHA. With high concentrations of hydrogen peroxide in the epilimnion and previously investigated high concentrations of ferrous iron in the hypolimnion, mixing across the pycnocline may result in significant production of hydroxyl radical, which could have a significant impact on the fate of organic pollutants in HBHA.

Thesis Supervisor: Dr. Philip M. Gschwend

Title: Professor of Civil and Environmental Engineering

Acknowledgments

Funding for this thesis was provided by the national Institutes of Environmental Health Sciences Superfund Basic Research Program grant 5-P42-ES04675-10 and a graduate student fellowship from the National Science Foundation. Kris McNeill, Sergi Diez, Lukas Wick, John MacFarlane, Becky Neuschatz, Ellie Kane, and Michael Rojo helped with data acquisition and sample collection. Thanks to Tina Voelker for laboratory space and helpful conversations and to Phil Gschwend for his enthusiasm and encouragement.

Table of Contents

List of Figures

List of Tables

1. Background

1.1 Introduction

Hydrogen peroxide is a ubiquitous constituent of surface waters. Reported values for the concentration of hydrogen peroxide in seawater range from 10 to 300 x 10^{-9} M, while in freshwater, values as high as 3.2 x 10^{-6} M have been reported (Cooper et al., 1988; Shtamm et al., 1991). Hydrogen peroxide, along with superoxide radical anion and hydroxyl radical, is one of the intermediates formed from redox conversions between O_2 and H_2O. It thus tends to be present wherever both water and oxygen are present. Even triple-distilled water generally contains measurable hydrogen peroxide (Bader et al., 1988). Of the reactive oxygen species (ROS), such as hydrogen peroxide, superoxide, peroxy radicals and others, hydrogen peroxide is the most stable and long-lived. Therefore, it accumulates to much higher concentrations than other ROS and is relatively simple to measure and study.

ROS are involved in a multitude of processes affecting surface water ecosystems. They affect the carbon cycle by oxidizing organic matter to form smaller organic compounds that are more bio-available (Mopper et al., 1991; Miller and Zepp, 1995). Some researchers have proposed that this is the rate-limiting step in the recycling of organic matter in the oceans (Mopper et al., 1991). Degradation of colored organic matter can control the optical transparency of surface waters, affecting photosynthesis and limiting the production of additional ROS (Morris and Hargreaves, 1997). ROS may also degrade anthropogenic pollutants, forming less or, occasionally, more toxic compounds, more or less tractable to further degradation (Cooper and Zika, 1989; Hoigné et al., 1989). These reactions have been applied to engineered systems for use in wastewater treatment and groundwater remediation using ROS in "advanced oxidation processes" (Bauer and Fallmann, 1997; Bhattacharjee and Shah, 1998). Metal speciation and redox chemistry are also affected by ROS, potentially controlling the bioavailability and/or toxicity of trace metals in aquatic environments. For example, the oxidation of ferrous iron by dissolved

oxygen is kinetically limited; it is oxidized at much higher rates by hydrogen peroxide (Moffett and Zika, 1987). Finally, ROS are themselves toxic to organisms and can affect the species composition of ecosystems. For example, high concentrations of hydrogen peroxide can inhibit the growth of certain algal species in favor of other species (Shtamm et al., 1991).

The major source of hydrogen peroxide in surface waters (both fresh and marine) is believed to be photochemical, although other sources may be important in some cases (Cooper et al., 1994 and references therein). Superoxide radical anion is formed by photochemical reactions involving the sunlight-absorbing fraction of dissolved organic carbon (DOC) and molecular oxygen, and it has been generally assumed that hydrogen peroxide forms from the reaction of superoxide with itself (dismutation). In natural waters, reactions of superoxide with metal species that form hydrogen peroxide are probably more important than dismutation (Zafiriou et al., 1998) (see section 1.4). In either case, hydrogen peroxide production is directly related to photochemical production of superoxide and may also act as an indicator of related photochemical reactions, such as the production of singlet oxygen or aqueous electrons. Photochemically formed ROS mediate the indirect photolysis of organic matter, and may be a significant sink for organic pollutants. One of the most reactive ROS, hydroxyl radical, is often not photochemically produced at fast enough rates for it to accumulate to high enough concentrations to have a significant impact on the fate of organic pollutants in surface waters. However, under certain conditions where reduced iron is present, hydrogen peroxide may undergo Fenton's reaction, producing hydroxyl radical by oxidation of Fe(II) (see section 1.6). Identification and quantification of the factors that control the formation and degradation of hydrogen peroxide are essential for understanding its distribution in natural waters and the role it plays in reactive oxygen species chemistry.

1.2 Measurement

A wide variety of analytical methods have been employed to measure low concentrations of hydrogen peroxide in aquatic media. These include titration, electrochemical procedures, and spectral methods. Many of these methods suffer from strong interferences with common constituents of natural waters. Simple titration methods generally have low sensitivity and/or high detection limits unless laborious procedures are followed. Kieber and Helz (1986) have developed a method involving iodometric titration to an amperometrically determined end point with a detection limit of 20 nM. Interference of common oxidants necessitates comparison with samples treated with catalase for 25 min. Hydrogen peroxide measurements using amperometric electrodes have been the focus of intense research for biological applications. Detection limits have been lowered to the nanomolar range by use of modified electrodes, especially peroxidase-coated glassy carbon electrodes (Ruzgas et al., 1996). To date, these methods have mainly been applied to clean aqueous solutions. Oxygen, trace metals, and certain organic compounds can all interfere with the signal produced by hydrogen peroxide, severely reducing the sensitivity when high concentrations of these species are present. No attempt to use these methods for the detection of hydrogen peroxide in surface freshwater or seawater has been reported in the literature, although two studies measured H_2O_2 in rainwater using voltammetry (Lagrange and Lagrange, 1991; Zhang and Wong, 1994).

Spectral methods have been more widely employed in natural waters research. These include chemiluminescent, fluorimetric, and photometric methods. Other than the chemiluminescent luminol method, which suffers from severe interference problems (Kok et al., 1978), the majority of these methods are based on the peroxidase oxidation of a specific substrate, often a phenol or aromatic amine. Of these methods, the scopoletin fluorimetric method has been the most widely employed in both seawater and freshwater (Zika and Salzman, 1982). Kieber and Helz (1986) verified this method against the independent iodometric method described above. Detection limits of 10^{-9} M have been achieved using the fluorimetric method, but it is

best used with relatively clean water samples due to the interference of natural organic matter. Cooper et al. (1988) found it necessary to dilute samples by 1:20 or 1:40 for samples with total organic carbon exceeding 2 mg C L^{-1}. Bader et al. (1988) devised a photometric method in which N,N-diethyl-p-phenylenediamine (DPD) is stoichiometricly oxidized by hydrogen peroxide in a reaction catalyzed by horseradish peroxidase to form a colored species. The DPD method has a slightly higher detection limit than the scopoletin method (10^{-8} M), but it is simple and quick to perform. Most importantly, DOC does not interfere with DPD analysis of hydrogen peroxide. This method was chosen for use in this study and will be discussed in detail in Chapter Two.

1.3 Occurrence

Hydrogen peroxide has been known to exist in the atmosphere and in precipitation for over a century. In rain, the concentration varies widely and has been found as high as nearly 1 mM (Shtamm et al., 1991). The concentration of hydrogen peroxide in surface water was first determined by van Baalen and Marler (1966) in the Gulf of Mexico. Hydrogen peroxide in the photic zone of seawater is typically on the order of 10^{-7} M (Van Baalen and Marler, 1966; Zika et al., 1985a; Zika et al., 1985b; Kieber and Helz, 1986; Kieber and Helz, 1995). The first measurements of hydrogen peroxide in freshwater were carried out by V. E. Sinel'nikov (1971) using chemiluminescent and iodometric methods in Russia, mainly in the Volga (Shtamm et al., 1991). Typical values ranged from 3×10^{-7} M to 3×10^{-6} M. In the zone of contamination of reservoirs by domestic effluent, the hydrogen peroxide concentration was up to 10^{-5} M. It was believed that this increase was due to microorganisms, in particular, to algae. In North America, Cooper and Zika (1983) were the first to report hydrogen peroxide concentrations in surface freshwater. These concentrations range from 90-170 nanomolar, which is similar to the concentrations previously found in seawater. They also reported a rapid increase in H_2O_2 concentrations in both surface and ground waters upon exposure to sunlight. They proposed that H_2O_2 is formed

from superoxide that is produced photochemically from dissolved organic carbon (DOC) (Cooper and Zika, 1983). Since then, reported values for H_2O_2 concentrations in surface freshwaters have typically ranged between about 50 and 500 nM. Hydrogen peroxide has also been reported in groundwater at a concentration of approximately 20 nM (Holm et al., 1987).

Abiotic photochemical formation has been considered to be the primary, if not the only, significant source of H_2O_2 in most of the surface freshwaters studied to date. This view is supported by the wide diel variation in H_2O_2 concentrations found in several lakes, the rapid formation of hydrogen peroxide in natural water samples upon exposure to light, and by a lack of evidence for other formation processes. For example, Cooper et al. (1994) have observed a reduction in the decay rate of samples upon filtration with 0.45 μm filters. This indicates that microorganisms contributed more to the decay of H_2O_2 than to its production in their samples, at least in the dark.

Diel cycles of two orders of magnitude change in H_2O_2 concentration have been observed in freshwater (Cooper and Lean, 1989) as compared to less than a factor of two in marine surface water (Zika et al., 1985a). Minimum concentrations occur in the early morning hours and maximum concentrations occur in the mid to late afternoon. Variations with meteorological conditions, such as a decrease in concentration with cloud cover and an increase with rain (Cooper et al., 1987), have also been observed. Cooper and Lean found that H_2O_2 concentrations in Jack's Lake varied with the photosynthetic active radiation over a period of several days (Cooper and Lean, 1989). Scully and co-workers have calculated *in situ* formation rates of hydrogen peroxide formation by measuring H_2O_2 concentration profiles over time and correcting by dark decay rates (Scully et al., 1995; Scully et al., 1997).

1.4 Photochemical Formation

When UV radiation (280-400 nm) is absorbed by dissolved organic matter, superoxide is formed. Superoxide may then dismutate (react with itself) to form H_2O_2. Cooper et al. (1994) proposed the following simplified reaction mechanism:

$$^1DOC + h\upsilon \rightarrow {}^1DOC^* \rightarrow {}^3DOC^* \quad (1)$$

$$^3DOC^* + {}^3O_2 \rightarrow DOC^{\bullet-} + O_2^{\bullet-} \quad (2)$$

$$O_2^{\bullet-} + H^+ = HO_2 \quad (3)$$

$$HO_2 + HO_2 \rightarrow H_2O_2 + O_2 \quad (4)$$

$$HO_2 + O_2^{\bullet-} + H_2O \rightarrow H_2O_2 + O_2 + OH^- \quad (5)$$

Equations 1 and 2 show that superoxide is formed from dissolved organic carbon, oxygen, and light. First, ground state DOC absorbs a photon to reach its first singlet excited state. Through inter-system crossing, it is transformed to the triplet excited state. Triplet DOC then reacts with triplet oxygen to form superoxide radical anion, which dismutates to form hydrogen peroxide. Other mechanisms for the formation of superoxide from DOC have been proposed. For example, singlet or triplet DOC could lose an election to form an aqueous electron that could react with O_2 to form superoxide. Aqueous electrons react with O_2 at diffusion controlled rates, so this pathway could be dominant if aqueous electrons were in fact formed to a significant extent. Spectroscopic evidence for the formation of aqueous electrons in humic substance solutions has been observed by several researchers, but the quantum yield of formation is low because expelled electrons react faster than they can be solvated to form aqueous electrons (Fischer et al., 1987; Power et al., 1987; Zepp et al., 1987a). In certain circumstances, singlet oxygen, formed from triplet DOC, could also react with DOC to form superoxide (Cooper and Zika, 1989).

Superoxide radical anion is in equilibrium with its conjugate acid, HO_2 (pK_a 4.5-4.9) (Cooper and Zika, 1989 and references therein). At circumneutral pH, the conjugate acid of superoxide forms hydrogen peroxide at a much faster rate than superoxide does. Thus, the reaction, $2\ O_2^{\bullet-} + 2H_2O \rightarrow H_2O_2 + O_2 + 2OH^-$ is negligible ($k = 0.3\text{-}6\ M^{-1}s^{-1}$), and does not appear in the above mechanism. Over a pH range of 7-9, the disproportionation rate has been evaluated as $\log k = 12.681 - 0.998(pH)$ ($M^{-1}s^{-1}$) in pure water (Bielski et al., 1985). This rate is probably not applicable to

natural freshwaters for two reasons. First, redox couples or enzymes present in natural waters may catalyze the di- mutation reaction. In order to evaluate the second order superoxide dismutation rate in pure water, care was taken to exclude trace metals, which are known to catalyze a first order dismutation (Bielski and Allen, 1977). Copper species, in particular, can be even more efficient than superoxide dismutase at catalyzing the dismutation of superoxide (Allen and Bielksi, 1982). A recent study determined the reaction rates of $O_2^{\bullet-}$ with Cu(I) and with Cu(II) in seawater (Zafiriou et al., 1998):

$$Cu(I) + O_2^{\bullet-} + 2H^+ \rightarrow Cu(II) + H_2O_2 \qquad k = 1.98(\pm 0.05) \times 10^9\ M^{-1}s^{-1} \qquad (6)$$

$$Cu(II) + O_2^{\bullet-} \rightarrow Cu(I) + O_2 \qquad k = 0.663(\pm 0.071) \times 10^9\ M^{-1}s^{-1} \qquad (7)$$

Reaction 6, which leads to the formation of hydrogen peroxide, was found to be dominant over the dismutation reactions, 4 and 5 in seawater. The oxidation kinetics of ferrous iron in freshwater samples was recently studied by Emmenegger et al. (1998). They showed that the ferrous iron oxidation rate by superoxide was independent of the initial iron concentration, indicating that superoxide was primarily reacting with Fe(II) in an analogous reaction to reaction 6. In low ionic strength water (2-3 mM), the oxidation of superoxide by Cu^+ is faster than oxidation by Fe^{2+} (Rush and Bielski, 1985; von Piechowski et al., 1993):

$$Fe^{2+} + O_2^{\bullet-} + 2H^+ \rightarrow Fe^{3+} + H_2O_2 \qquad k = 1.0(\pm 0.1) \times 10^7\ M^{-1}s^{-1},\ pH>6 \qquad (8)$$

$$Cu^+ + O_2^{\bullet-} + 2H^+ \rightarrow Cu^{2+} + H_2O_2 \qquad k = 9.4(\pm 0.8) \times 10^9\ M^{-1}s^{-1} \qquad (9)$$

In freshwaters with very high ferrous iron concentrations, iron may also catalyze the dismutation of superoxide; other reduced metals also potentially contribute.

A second reason why the dismutation rate of superoxide in pure water may not indicate the hydrogen peroxide production rate in natural waters is that not all superoxide in natural waters forms hydrogen peroxide. In coastal seawater, Petasne

and Zika (1987) found that 24-41% of the superoxide formed did not produce hydrogen peroxide. The alternative pathways for superoxide consumption were not investigated. One possibility is the formation of molecular oxygen from oxidized metals, such as Cu(II), as in reaction 7.

Scully et al. (1996) irradiated a wide variety of filtered natural freshwater samples with a solar simulator, measured the accumulation rates of hydrogen peroxide, and found a positive correlation between the concentration of DOC in the sample and the accumulation rate. The fluorescence of the samples and their absorbance at 310 nm were both linearly correlated with the hydrogen peroxide accumulation rate. However, this effect may be due almost entirely due to differences in light absorption by the samples. Weighted quantum yield measurements indicate that most of the H_2O_2 is formed by light of about 400 nm in wavelength. The percentage of light near 400 nm absorbed in their experiment would be expected to vary widely over the DOC concentrations in their samples. They found no relationship between "formation efficiencies" (accumulation rates divided by the number of photons absorbed by the sample) and DOC concentrations. Field studies confirm the lack of a relationship between DOC concentrations and formation rates, since nearly all of the 400 nm light is absorbed within a few meters even in lakes with relatively low DOC contents (Scully et al., 1995). The pH was not found to significantly affect the peroxide accumulation rate (Scully et al., 1996) despite the greater than two orders of magnitude difference in dismutation rates over the equivalent range of pH values (6.1 to 8.4) found in pure water (Bielski et al., 1985). This lends support to the possibility that pH-independent catalysis of dismutation due to the presence of extracellular superoxide dismutase or metal species, e.g., copper, is the dominant mechanism of hydrogen peroxide production in natural freshwater.

1.5 Other Possible Formation Processes

Other processes that can produce hydrogen peroxide in natural waters have been investigated to a lesser degree. Patterson and Myers (1973) were the first to

observe continuous photosynthetic production of H_2O_2 in the extracellular medium by intact cells by irradiating the cyanobacterium, *Anacysitis nidulans,* with light from 620-675 nm. Photosynthetic production of H_2O_2 has since been observed in several, but not all, species of green and blue-green algae. This production is due to reduction of O_2 in photosystem I or to photorespiration. Secretion of superoxide, hydrogen peroxide, or a compound that can reduce dissolved oxygen may result in the observed H_2O_2 production. Zepp and co-workers (1987b) studied the production rate of hydrogen peroxide in pure culture exposed to light for several species of algae and cyanobacteria. In their experiments, up to about 2 µM / hr of H_2O_2 was produced at cell concentrations of about 1000 (mg chl *a*) m^{-3}. Algal species with low catalase activity can also result in higher H_2O_2 accumulation. Zepp and co-workers (1987b) found that prior exposure of *Chlamydomonas* to sunlight resulted in a subsequently decreased ability to degrade H_2O_2, suggesting that part of the accumulation of H_2O_2 in sunlight is due to inhibition of H_2O_2-degrading enzymes. Production of H_2O_2 from immobilized algal cells using methyl viologen as a redox catalyst has been investigated as a method for producing H_2O_2. Methyl viologen is reduced by photosynthetic activity and reoxidized by oxygen to form superoxide (Morales and de la Rosa, 1992; Scholz et al., 1995). This illustrates the possibility that algae produce hydrogen peroxide indirectly by releasing reducing equivalents into their environment.

The dark biological production of hydrogen peroxide has been investigated in pure culture and observed in seawater samples. Palenik and Morel (1990) discovered a system by which some marine phytoplankton oxidize L-amino acids on their surfaces to produce H_2O_2, NH_3, and an α-keto acid extracellularly. A previous study found evidence for net biological dark production at depths of 40-60 m in the Sargasso Sea (Palenik and Morel, 1988). The maximum rate observed was 11 nM hr^{-1}. Moffett and Zafiriou (1990) used ^{18}O-labled O_2 and H_2O_2 to determine absolute rates of hydrogen peroxide production and decay in surface seawater. They found no evidence for photosynthetic production of hydrogen peroxide, but did observe particle-dependent dark production of H_2O_2 at rates ranging from 0.8 to 2.4 nM h^{-1}. Biologically mediated

production of hydrogen peroxide has not been shown to be significant in any natural freshwater to date. In most cases, filtration, poisoning or heating of natural water samples to remove or inhibit microorganisms is an effective way to dramatically slow the degradation rate of H_2O_2. Thus, it is generally assumed that the production of peroxide by microorganisms is insignificant compared to biologically mediated decay in lakes (Cooper et al., 1994).

Redox processes that result in the production of hydrogen peroxide have been proposed. If a reduced metal, such as Cu^+, reacted more efficiently with dissolved oxygen than with hydrogen peroxide at ambient concentrations, accumulation of peroxide could occur with superoxide as an intermediate.

$$Me^{n+} + O_2 \rightarrow Me^{n+1} + O_2^{\bullet-} \quad (10)$$

$$Me^{n+} + H_2O_2 \rightarrow Me^{n+1} + OH^{\bullet} + OH^- \quad (11)$$

Reaction 10 results in the production of superoxide radical, which then undergoes fast reactions to form hydrogen peroxide (see section 1.4), whereas reaction 11, the Fenton reaction (see section 1.6), results in the destruction of hydrogen peroxide. A given reduced metal, therefore, could be either a source or a sink of hydrogen peroxide depending on the relative rates of reactions 10 and 11 and the ambient concentrations of O_2 and H_2O_2. Kinetic studies with copper in seawater indicate that copper could contribute to hydrogen peroxide production in seawater (Moffett and Zika, 1983), but comparable studies have not been done for freshwater. Emmenegger et al. (1998) found that for a freshwater sample spiked with ferrous iron, reaction 10 was faster than reaction 11 under typical conditions in Lake Greifen (pH 8-8.5, $[O_2] = 3 \times 10^{-4}$, H_2O_2 = 50-200 nM). Whether ferrous iron acts as a source or a sink of hydrogen peroxide in a given freshwater is dependent on the relative concentrations of O_2 and H_2O_2, pH, ionic strength (Millero et al., 1987), and iron complexation to organic ligands (Harris and Aisen, 1973; Liang et al., 1993). Additionally, the rates of

reaction may be influenced or controlled by catalysis on iron oxide surfaces and/or by iron-oxidizing bacteria (Tamura et al., 1976; Barry et al., 1994).

In addition to the above formation processes, hydrogen peroxide can also be introduced into a lake with rainwater. The concentration of H_2O_2 in rain can be up to nearly 10^{-4} M and is commonly 10^{-7} to 10^{-5} M (Shtamm et al., 1991 and references therein). As this is greater than typical concentrations in surface waters (10^{-8} to 10^{-7} M), it is possible for rain to be a significant input, even when diluted over the entire mixed layer of a lake.

1.6 Decay Processes

The decay of hydrogen peroxide in both freshwater and seawater has been attributed primarily to biologically mediated decay. The half life of hydrogen peroxide in a water sample can typically be extended from a few hours to over two days by filtration (0.45 or 0.2 μm), autoclaving, sonication, or poisoning with Hg^{2+} or azide (Cooper and Zepp, 1990; Cooper et al., 1994; Petasne and Zika, 1997). The effect of filtration using different size filters was studied in a freshwater sample (Cooper et al., 1994). Removal of large particles, including zooplankton and large algae, with a 12 μm filter decreased the decay rate only slightly. Most of the decay was due to particles smaller than 1.0 μm - small algae and bacteria. The decay of hydrogen peroxide by algae and bacteria in pure culture is typically first order in $[H_2O_2]$ and first order in either bacteria cell number or [chlorophyll *a*] (Zepp et al., 1987b; Cooper et al., 1994). Zepp et al. (1987b) collected kinetic data for the degradation of hydrogen peroxide in pure culture for several cyanobacteria and green algae. Using an initial concentration of 5 μM H_2O_2 and varying the chlorophyll *a* concentration, second order rate constants were determined for each species. The rate constants for four species of cyanobacteria ranged from 2.2±0.5 x 10^3 to 8.8±2.0 x 10^3 m^3 (mg chl *a*)$^{-1}$ h^{-1}, and the rate constants for five species of green algae ranged from 0.18±0.04 x 10^3 to 6.3±0.9 x 10^3 m^3 (mg chl *a*)$^{-1}$ h^{-1}. In natural waters, H_2O_2 decay is usually pseudo-first order with respect to H_2O_2, although inhibition of the rate has been observed at high

concentrations of H_2O_2 (Cooper et al., 1994). However, no simple relationship between bacterial cell numbers and decay rate exists, probably due to species differences (Cooper et al., 1994).

Biologically mediated decay of hydrogen peroxide probably occurs through the action of the enzymes, catalase and/or peroxidase. A peroxidase enzyme substrate can be added to natural water samples to test for peroxidase activity. Cooper and Zepp (1990) found 0.7 moles of *p*-anisidine oxidized per mole of hydrogen peroxide added in a lake water sample. Since two moles of *p*-anisidine are oxidized for every mole of hydrogen peroxide catalyzed by peroxidase, these results imply that 35% of the hydrogen peroxide in the sample was degraded by peroxidase. Because the products of catalase degradation of H_2O_2 are H_2O and O_2, whereas the product of peroxidase degradation of H_2O_2 is H_2O alone, Moffett and Zafiriou (1990) were able to distinguish between the two pathways of degradation by using ^{18}O labeled H_2O_2. In surface water samples from Vineyard Sound, they found that 65-80% of the hydrogen peroxide decay is due to catalase and the rest to peroxidase. Biological decay rates in this study were not influenced by light.

Reduction by metals, Fe(II) in particular, has also been suggested as a possible sink of H_2O_2, although particle-dependent (biological) decay has generally been found to be dominant (Cooper and Zepp, 1990; Cooper et al., 1994; Petasne and Zika, 1997; Moffett and Zafiriou, 1990). Manganese oxides and reduced copper could also potentially act as sinks for hydrogen peroxide, but little work has been done in freshwater. Hydrogen peroxide and reduced iron can undergo Fenton's reaction, resulting in the production of hydroxyl radical (Haber and Weiss, 1934):

$$H_2O_2 + Fe(II) \rightarrow OH\bullet + Fe(III) \qquad (12)$$

This is of particular interest since hydroxyl radical reacts at near diffusion-controlled rates with many organic compounds. Fe^{2+} and other reduced species could be introduced into a lake from anoxic groundwater or could be present in an anoxic

hypolimnion. In a natural freshwater sample, the rate constant of reaction 12 was determined as a function of pH to be log $k \cong 0.8(pH)$ (Emmenegger et al., 1998). Some decay of hydrogen peroxide is also associated with sunlight. Moffett and Zafiriou (1993) found that light-associated decay was about 5% of the net H_2O_2 production in eastern Caribbean and Orinoco River surface water samples using ^{18}O-labeled H_2O_2 as a marker. The decomposition was due to an oxidant in the seawater samples and a reductant, probably photo-produced Fe(II), in the river water.

In summary, the hydrogen peroxide cycle in most natural surface waters studied to date is controlled by three major processes: photochemical production, rainwater input, and biologically-mediated decay. Photochemical production is dependent on the DOC absorbance of the water, the quantum yield of hydrogen peroxide formation, and the incident sunlight. Decay is proportional to bacterial numbers in pure culture, but it is probably a function of both cell numbers and species in natural samples. Under certain circumstances, biological production and production and/or decay of H_2O_2 due to redox chemistry may also play a role in the hydrogen peroxide cycle in natural waters. However, field studies have not shown any of these processes to be significant in the surface freshwaters studied to date.

1.7 Motivation

Our research group has been interested in studying the factors that control the fates of organic pollutants in the Halls Brook Holding Area (HBHA), a small lake located north of Boston in Woburn, MA [Figure 1]. The lake is close to the Industri-plex Superfund Site, a former industrial area with a long history (1853-1967) of chemical manufacturing. Some of the chemicals that were produced include acids, dyes, phenolic compounds, lead arsenate pesticides, tanning materials, solvents, and explosives (Wick and Gschwend, 1998 and references therein). Waste from these chemical manufacturing processes has entered the groundwater that flows into HBHA. As a result, HBHA is now heavily contaminated with both toxic inorganic pollutants, such as arsenic, chromium, and lead (Davis et al., 1996), and organic compounds,

such as benzene, diphenyl sulfone, and hydroxybiphenyls (Wick and Gschwend, 1998). HBHA flows out to the Aberjona river, which flows by Wells G and H, the sources of drinking water alleged to cause leukemia in a civil lawsuit (Harr, 1995). The river eventually enters the Upper Mystic Lake, which is used for recreational purposes.

One of the possible degradation mechanisms for organic compounds in HBHA is reaction with reactive transients, including the reactive oxygen species (ROS). Studying hydrogen peroxide in HBHA should help us understand and eventually quantify the effect of ROS on organic pollutants in HBHA in two ways. First, since the production of hydrogen peroxide is controlled by similar factors (e.g., incident light intensity, DOC absorbance, and the quantum yields), it may be possible to use hydrogen peroxide as an indicator of photochemical processes affecting organic compounds. Second, the chemistry of HBHA could lead to significant production of hydroxyl radical that could oxidize organic pollutants. HBHA contains high (up to 10^{-3} M) concentrations of Fe(II) in its hypolimnion (Diez and Gschwend, 1996). HBHA is also high in DOC, such that most of the light that could produce hydrogen peroxide is absorbed within the oxic epilimnion. Mixing across the pycnocline should bring hydrogen peroxide and iron (II) in contact, resulting in the production of hydroxyl radical. An understanding of the factors that control hydrogen peroxide distribution in HBHA could, therefore, lead to the understanding and quantification of the indirect photochemical processes affecting organic pollutants in the Halls Brook Holding Area.

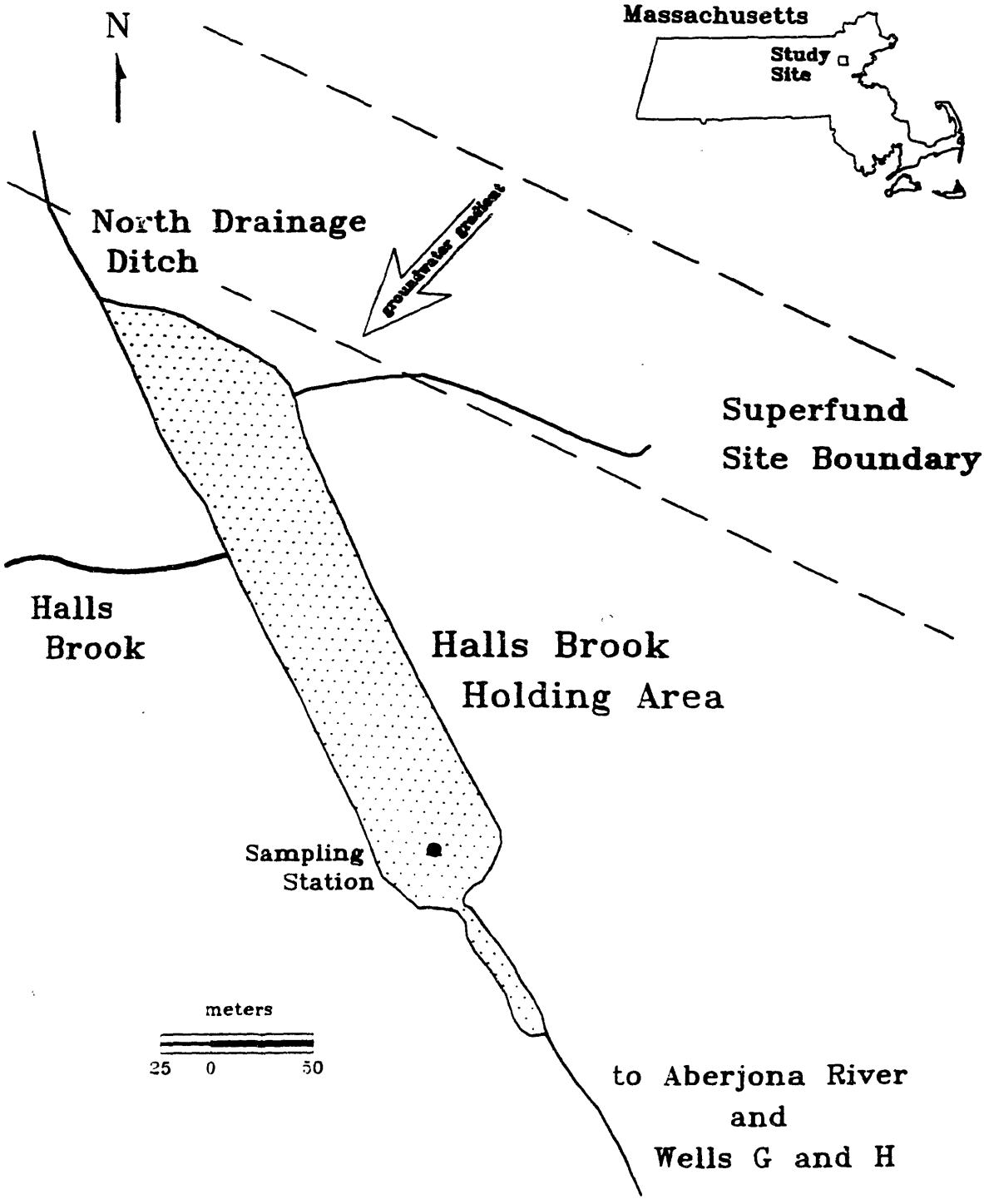

Figure 1.1. Map of the Halls Brook Holding Area and surroundings.

1.8 References

Allen, A. O. and Bielksi, B. H. J., 1982. Formation and disappearance of superoxide radicals in aqueous solutions. Superoxide Dismutase. L. W. Oberley. Boca Raton, CRC Press. **1:** 125-141.

Bader, H., Sturzenegger, V. and Hoigné, J., 1988. Photometric method for the determination of low concentrations of hydrogen peroxide by the peroxidase catalyzed oxidation of N, N-diethyl-p-phenylenediamine (DPD). *Wat. Res.*, **22**(9): 1109-1115.

Barry, R. C., Schnoor, J. L., Sulzberger, B., Sigg, L. and Stumm, W., 1994. Iron oxidation kinetics in an acidic alpine lake. *Wat. Res.*, **28**(2): 323-333.

Bauer, R. and Fallmann, H., 1997. The Photo-Fenton oxidation - A cheap and efficient wastewater treatment method. *Res. Chem. Intermed.*, **23**(4): 341.

Bhattacharjee, S. and Shah, Y. T., 1998. Mechanisms for advanced photooxidation of aqueous organic waste compounds. *Rev. Chem. Eng.*, **14**(1): 1-46.

Bielski, B. H. J. and Allen, A. O., 1977. Mechanism of the disproportionation of superoxide radicals. *J. Phys. Chem.* , **81**: 1048-1050.

Bielski, B. H. J., Cabelli, D. E., Ravindra, L. A. and Ross, A. B., 1985. Reactivity of HO_2/O_2^- radicals in aqueous solution. *J. Phys. Chem. Ref. Data*, **14**(4): 1041--1051.

Cooper, W. J. and Lean, D. R. S., 1989. Hydrogen-peroxide concentration in a northern lake - photochemical formation and diel variability. *Environ. Sci. Technol.*, **23**(11): 1425-1428.

Cooper, W. J., Saltzman, E. S. and Zika, R. G., 1987. The contribution of rainwater to variability in surface ocean hydrogen peroxide. *J. Geophys. Res.*, **92**(C3): 2970-2980.

Cooper, W. J., Shao, C., Lean, D. R. S., Gordon, A. S. and Scully, F. E., Jr., 1994. Factors affecting the distribution of H_2O_2 in surface waters. Environmental Chemistry of Lakes and Reservoirs. L. A. Baker. Washington D.C., ACS. **237:** 390-422.

Cooper, W. J. and Zepp, R. G., 1990. Hydrogen peroxide decay in waters with suspended soils: Evidence for biologically mediated decay. *Can. J. Fish. Aquat. Sci.*, **47**: 888-893.

Cooper, W. J. and Zika, R. G., 1983. Photochemical formation of hydrogen peroxide in surface and ground waters exposed to sunlight. *Science*, **220**: 711-712.

Cooper, W. J. and Zika, R. G., 1989. Sunlight-induced photochemistry of humic substances in natural waters: major reactive species. Aquatic humic substances: influence on fate and treatment of pollutants. I. H. Suffet and P. MacCarthy. Washington, D.C., ACS. **219:** 332-362.

Cooper, W. J., Zika, R. G., Petasne, R. G. and Plane, J. M. C., 1988. Photochemical formation of H_2O_2 in natural waters exposed to sunlight. *Environ. Sci. Technol.*, **22**: 1156-1160.

Davis, A., Sellstone, C., Clough, S., Barrick, R. and Yare, B., 1996. Bioaccumulation of arsenic, chromium, and lead in fish: constraints imposed by sediment geochemistry. *Appl. Geochem.*, **11**: 409-423.

Diez, S. and Gschwend, P. M. unpublished results, 1996.

Emmenegger, L., King, D. W., Sigg, L. and Sulzberger, B., 1998. Oxidation kinetics of Fe(II) in a eutrophic Swiss lake. *Environ. Sci. Technol.*, **32**: 2990-2996.

Fischer, A. M., Winterle, J. S. and Mill, T., 1987. Primary photochemical processes in photolysis mediated by humic substances. Photochemistry of Environmental Aquatic Systems. R. G. Zika and W. J. Cooper. Washington, D.C., American Chemical Society: 141-156.

Haber, F. and Weiss, J., 1934. The catalytic decomposition of hydrogen peroxide. *Proc. Roy. Soc. London, Ser. A*, **147**: 332-351.

Harr, J. 1995. A Civil Action. New York, Random House.

Harris, D. C. and Aisen, P., 1973. Facilitation of Fe(II) autoxidation by Fe(III) complexing agents. *Biochim. Biophys. A.*, **329**: 156-158.

Hoigné, J., Faust, B. C., Haag, W. R., Scully, F. E. and Zepp, R. G., 1989. Aquatic humic substances as sources and sinks of photochemically produced transient reactants. Aquatic Humic Substances, ACS: 363-381.

Holm, T. R., George, G. K. and Barcelona, M. J., 1987. Fluorometric determination of hydrogen peroxide in groundwater. *Anal. Chem.*, **59**: 582-586.

Kieber, R. J. and Helz, G. R., 1986. Two-method verification of hydrogen peroxide determinations in natural waters. *Anal. Chem.*, **58**(11): 2312-2315.

Kieber, R. J. and Helz, G. R., 1995. Temporal and seasonal variations of hydrogen peroxide levels in estuarine waters. *Estuar. Coast. Shelf Sci.*, **40**: 495-503.

Kok, G. L., Darnall, K. R., Winer, A. M., Pitts, J. N., Jr. and Gay, B. W., 1978. Ambient air measurements of hydrogen peroxide in the California south coast air basin. *Environ. Sci. Technol.*, **12**: 1077-1080.

Lagrange, J. and Lagrange, P., 1991. Voltammetric method for the determination of H_2O_2 in rainwater. *Fresen. J. Anal. Chem.*, **339**(7): 452-454.

Liang, L. Y., McNabb, J. A., Paulk, J. M., Gu, B. H. and McCarthy, J. F., 1993. Kinetics of Fe(II) oxygenation at low partial pressure of oxygen in the presence of natural organic matter. *Environ. Sci. Technol.*, **27**(9): 1864-1870.

Millero, F. J., Sotolongo, S. and Izaguirre, M., 1987. The oxidation kinetics of Fe(II) in seawater. *Geochim. Cosmochim. Acta*, **51**: 793-801.

Miller, W. L. and Zepp, R. G., 1995. Photochemical production of dissolved inorganic carbon from terrestrial organic matter: Significance to the oceanic organic carbon cycle. *Geophys. Res. Lett.*, **22**(4): 417-420.

Moffett, J. W. and Zafiriou, O. C., 1990. An investigation of hydrogen peroxide chemistry in surface waters of Vineyard Sound with $H_2{}^{18}O_2$ and $^{18}O_2$. *Limnol. Oceanogr.*, **35**(6): 1221-1229.

Moffett, J. W. and Zafiriou, O. C., 1993. The photochemical decomposition of hydrogen peroxide in surface waters of the eastern Caribbean and Orinoco River. *J. Geophys. Res.*, **98**(C2): 2307-2313.

Moffett, J. W. and Zika, R. G., 1983. Oxidation kinetics of Cu(I) in seawater: implications for its existence in the marine environment. *Mar. Chem.*, **13**: 239-251.

Moffett, J. W. and Zika, R. G., 1987. Reaction kinetics of hydrogen peroxide with copper and iron in seawater. *Environ. Sci. Technol.*, **21**(8): 804-810.

Mopper, K., Zhou, Z., Kieber, R. J., Keiber, D. J., Sikorski, R. J. and Jones, R. D., 1991. Photochemical degradation of dissolved organic carbon and its impact on the oceanic carbon cycle. *Nature*, **353**: 60-62.

Morales, I. and de la Rosa, F. F., 1992. Hydrogen peroxide photoproduction by immobilized cells of the blue-green alga *Anabaena variabilis* : a way to solar energy conversion. *Sol. Energy*, **49**(1): 41-46.

Morris, D. P. and Hargreaves, B. R., 1997. The role of photochemical degradation of dissolved organic carbon in regulating the UV transparency of three lakes on the Pocono Plateau. *Limnol. Oceanogr.*, **42**(2): 239-249.

Palenik, B. and Morel, F. M. M., 1988. Dark production of H_2O_2 in the Sargasso Sea. *Limnol. Oceanogr.*, **33**(6): 1606-1611.

Palenik, B. and Morel, F. M. M., 1990. Amino acid utilization by marine phytoplankton: A novel mechanism. *Limnol. Oceanogr.*, **35**(2): 260-269.

Patterson, C. O. P. and Myers, J., 1973. Photosynthetic production of hydrogen peroxide by *Anacysits nidulans*. *Plant Physiol.*, **51**: 104-109.

Petasne, R. G. and Zika, R. G., 1987. Fate of superoxide in coastal seawater. *Nature*, **325**: 516-518.

Petasne, R. G. and Zika, R. G., 1997. Hydrogen peroxide lifetimes in south Florida coastal and offshore waters. *Mar. Chem.*, **56**: 215-225.

Power, J. F., Sharma, D. K., Langford, C. H., Bonneau, R. and Joussot-Dubien, J., 1987. Laser flash photolytic studies of a well-characterized soil humic substance. Photochemistry of Environmental Aquatic Systems. R. G. Zika and W. J. Cooper. Washington, D.C., American Chemical Society: 157-173.

Rush, J. D. and Bielski, B. H. J., 1985. Pulse radiolytic studies of the reactions of HO_2/O_2^- with Fe(II)/Fe(III) ions. The reactivity of HO_2/O_2^- with ferric ions and its implication on the occurrence of the Haber-Weiss reaction. *J. Phys. Chem.* , **89**: 5062-5066.

Ruzgas, T., Csoregi, E., Emneus, J., Gorton, L. and Marko-Varga, G., 1996. Peroxidase-modified electrodes: Fundamentals and application. *Anal. Chim. Acta.*, **330**(2-3): 123-138.

Scholz, W., Galvan, F. and Delarosa, F. F., 1995. The microalga *Chlamydomonas reinhardtii* CW-15 as a solar cell for hydrogen peroxide photoproduction: Comparison between free and immobilized cells and thylakoids for energy conversion efficiency. *Sol. Energ. Mater.*, **39**(1): 61-69.

Scully, N. M., Lean, D. R. S., McQueen, D. J. and Cooper, W. J., 1995. Photochemical formation of hydrogen peroxide in lakes: effects of dissolved organic carbon and ultraviolet radiation. *Can. J. Fish. Aquat. Sci.*, **52**: 2675-2681.

Scully, N. M., McQueen, D. J. and Lean, D. R. S., 1996. Hydrogen peroxide formation: the interaction of ultraviolet radiation and dissolved organic carbon in lake waters along a 43-75°N gradient. *Limnol. Oceanogr.*, **41**(3): 540-548.

Scully, N. M., Vincent, W. F., Lean, D. R. S. and Cooper, W. J., 1997. Implications of ozone depletion for surface-water photochemistry: Sensitivity of clear lakes. *Aquat. Sci.*, **59**(3): 260-274.

Shtamm, E. V., Purmal, A. P. and Skurlatov, Y. I., 1991. The role of hydrogen peroxide in natural aquatic media. *Rus. Chem. Rev.*, **60**(11): 1228-1248.

Sinel'nikov, 1971. *Gidrobiol. Zh.*, **7**: 115. (as reported in Shtamm et al., 1991)

Tamura, H., Goto, K. and Nagayama, M., 1976. The effect of ferric hydroxide on the oxygenation of ferrous ions in neutral solutions. *Corr. Sci.*, **16**: 197-207.

Van Baalen, C. V. and Marler, J. E., 1966. Occurrence of hydrogen peroxide in seawater. *Nature*, **211**: 951.

von Piechowski, M., Nauser, T., Hoigne, J. and Buhler, R. E., 1993. O_2^- decay catalyzed by Cu^{2+} and Cu^+ ions in aqueous solutions: a pulse radiolysis study for atmospheric chemistry. *Ber. Bunsenges. Phys. Chem.*, **97**(6): 762-771.

Wick, L. Y. and Gschwend, P. M., 1998. Source and chemodynamic behavior of diphenyl sulfone and *ortho*- and *para*-hydroxybiphenyl in a small lake receiving discharges from an adjacent Superfund site. *Environ. Sci. Technol.*, **32**: 1319-1328.

Zafiriou, O. C., Voelker, B. M. and Sedlak, D. L., 1998. Chemistry of the superoxide radical (O2-) in seawater: reactions with inorganic copper complexes. *J Phys. Chem. A*, **102**: 5693-5700.

Zepp, R. G., Braun, A. M., Hogné, J. and Leenheer, J. A., 1987a. Photoproduction of hydrated electrons from natural organic solutes in aquatic environments. *Environ. Sci. Technol.*, **21**: 485-490.

Zepp, R. G., Skurlatov, Y. I. and Pierce, J. T., 1987b. Algal-induced decay and formation of hydrogen peroxide in water: its possible role in oxidation of anilines by algae. Photochemistry of Environmental Aquatic Systems. R. G. Zika and W. J. Cooper. Washington, D.C., American Chemical Society: 215-224.

Zhang, L. S. and Wong, G. T. F., 1994. The determination of hydrogen-peroxide in aqueous-solutions by square-wave voltammetry. *Talanta*, **41**(11): 1853-1859.

Zika, R. G., Moffett, J. W., Petasne, R. G., Cooper, W. J. and Saltzman, E. S., 1985a. Spatial and temporal variations of hydrogen peroxide in Gulf of Mexico waters. *Geochim. Cosmochim. Acta*, **49**: 1173-1184.

Zika, R. G., Saltzman, E. S. and Cooper, W. J., 1985b. Hydrogen peroxide concentrations in the Peru upwelling area. *Mar. Chem.*, **17**: 265-275.

Zika, R. G. and Salzman, E. S., 1982. Interaction of ozone and hydrogen peroxide in water: implications for analysis of H_2O_2 in air. *Geophys. Res. Lett.*, **9**: 231-234.

2. Hydrogen Peroxide Measurement Methodology

2.1 Background

2.1.1 DPD Oxidation

The "DPD" method of hydrogen peroxide analysis was developed by Bader et al. (1988) as a simple and selective alternative to existing H_2O_2 measurement methods. The method relies on the stoichiometric oxidation of DPD (N,N-diethyl-*p*-phenylenediamine) by hydrogen peroxide in the presence of peroxidase catalyst (Bader et al., 1988):

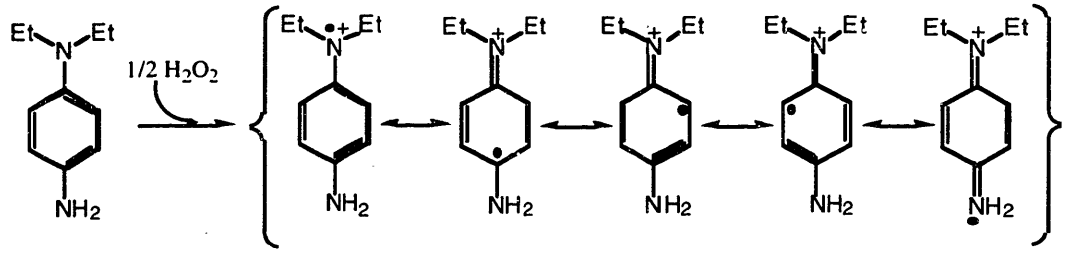

(1)

Two moles of DPD are oxidized to resonance-stabilized radical cations for every mole of hydrogen peroxide present. The oxidized product has a structure similar to Wurster's salts, radical cations of phenylenediamines that are some of the most stable radical species known (Forrester et al., 1968).

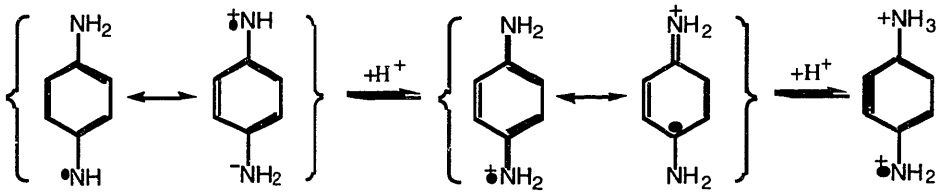

a b c

(2)

Wurster's salts are the major stable species in the pH range of 3.5-6 (2b). In strong acid, a di-cation (2c) forms and in basic solution the neutral radical (2a) is formed. Both the di-cation and the neutral radical are unstable at all pH values. Wurster's salts

typically show two strong absorption peaks between 450 and 610 nm (Forrester et al., 1968).

In general, peroxidase oxidation is thought to occur by the following mechanism (George, 1952; Bruice, 1988):

$$E + H_2O_2 \rightarrow E\text{-}I + H_2O \quad (3)$$

$$E\text{-}I + AH_2 \rightarrow E\text{-}II + AH\bullet \quad (4)$$

$$E\text{-}II + AH_2 \rightarrow E + AH\bullet + H_2O \quad (5)$$

where E is peroxidase and AH_2 is a "hydrogen donor". The active site of the peroxidases contains an iron protoporphyrin IX with a proximal-bound histidine. The iron is in a (+III) oxidation state when the peroxidase is in the resting state (E). In the first step (3), peroxidase (E) reacts with hydrogen peroxide, releasing water and forming an activated peroxidase complex (E-I). The active site of E-1 is an Fe(IV) porphyrin cation radical (Bruice, 1988; Traylor, 1984 and references therein):

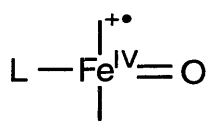

In the second step (4), E-I abstracts a hydrogen atom from the hydrogen donor, AH_2, which is typically a phenol or an aromatic amine, forming a second activated enzyme complex, E-II, and a radical species, AH•. The active site of E-II is generally written as (Bruice, 1988; Traylor, 1984 and references therein):

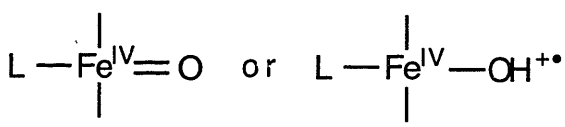

In the case of the first structure shown, a proton is also released. Finally, E-II abstracts a second hydrogen from a hydrogen donor, regenerating the enzyme and producing

another radical species, AH•, and a second water molecule. The neutral radical, then, is in equilibrium with its conjugate bases $AH_2^{\bullet+}$ ($DPD^{\bullet+}$) and $AH_3^{\bullet 2+}$, analogous to equation 2:

$$AH\bullet + H^+ = AH_2^{\bullet+} \quad (6)$$

$$AH_2^{\bullet+} + H^+ = AH_3^{\bullet 2+} \quad (7)$$

The species, $DPD^{\bullet+}$, has an absorption spectrum with two peaks, one at 510 nm and the other at 551 nm (Bader et al., 1988). Over a period of minutes to hours, the absorbance peak gradually disappears. On the time scale of hours to days, a dark purple color appears and purple solid precipitates. This may be the result of dimerization or polymerization of the radical species.

2.1.2 DPD Analysis of Hydrogen Peroxide

The absorptivity of $DPD^{\bullet+}$ at 551 nm is 21,000 ± 500 M^{-1} cm^{-1}. In distilled water, calibration curves plotting A vs. added H_2O_2 concentration obtained by Bader et al. using the DPD method were linear from 20 nM to 100 µM H_2O_2. Standard additions were performed in several natural lakewater samples with similar results (Bader et al., 1988).

Measured samples need to be compared to blanks due to some absorbance by the reagents and the possibility of interferences. Manganese dioxide can oxidize DPD, leading to the formation of color in the absence of peroxidase. Filtration though a 0.1 µm filter has been shown to eliminate the problem. Sulfite ions can reduce the oxidized DPD species, but this can be masked by the addition of formaldehyde. If other interfering oxidants are present, color will form in the absence of peroxide (e.g., when manganese dioxide is present) or color may increase with time (e.g., alkyl peroxides are present). In either case a blank may be prepared by selectively destroying hydrogen peroxide. This is done by lowering the pH to 4, adding bisulfite to eliminate H_2O_2, and then formaldehyde to mask the bisulfite (Bader et al., 1988).

Ferrous iron decreases the observed signal from the DPD reaction by either reducing the oxidized DPD species or by reducing hydrogen peroxide directly. Additionally, iron (III) can affect the observed blank signal. Voelker and Sulzberger (1996) have measured hydrogen peroxide in the presence of iron by adding bipyridine to bind with Fe^{2+} and EDTA to bind Fe^{3+}. Using bipyridine to bind Fe^{2+} has the advantage of allowing for simultaneous measurement of Fe^{2+} concentrations, as the bipyridine-iron(II) complex is also colored (ε = 8650 M^{-1} cm^{-1} at 522 nm). In this procedure, the absorbance of the sample at 551 nm must be measured before and after the addition of DPD and peroxidase to correct for the absorbance of the bipyridine-iron(II) complex (Voelker and Sulzberger, 1996).

2.2 Experimental

2.2.1 Materials

All solutions were prepared using 18 MΩ Milli-Q water (Q-H_2O) from a Millipore system consisting of a pre-filter cartridge and two ion exchange cartridges. Chemicals were used as received. N,N-diethyl-p-phenylenediamine, peroxidase (type II from horseradish), catalase (from bovine liver), and hydrogen peroxide (30%) were obtained from Sigma. 2,2'-dipyridyl (bipyridine), sodium EDTA, formaldehyde, and perchloric acid were obtained from Aldrich. Other reagents used included sodium phosphate dibasic and monobasic and sodium sulfite from Mallinckrodt.

2.2.2 Hydrogen Peroxide Analysis

Hydrogen peroxide was measured using the DPD method as developed by Bader et al. (1988) and modified by Voelker and Sulzberger (1996). The procedure followed in this study consisted of the following steps. First, 0.3 mL of pH 6 phosphate buffer (0.5 M), 75 µL of bipyridine stock solution (0.01 M bipyridine in 10^{-3} M $HClO_4$), and 25 µL of EDTA stock solution (10^{-2} M Na_2EDTA) were mixed in a 1 cm pathlength cuvette. Next, 1.5 mL of sample was added and the cuvette was covered and inverted

several times to mix. A background measurement was taken on a HP 8453 diode array spectrophotometer or at 552 nm on a Beckman Model DU 640 spectrophotometer. 25 µL of DPD reagent (3.8×10^{-2} M in 0.1 N H_2SC_4 and 25 µL of horseradish peroxidase (100 units/mL) were then added to the cuvette, the cuvette was tipped to mix, and the absorbance at 552 nm was measured after a timed interval (typically 60 seconds).

For natural water samples, a blank measurement was also taken by following the above procedure but omitting the peroxidase. Blanks were occasionally also measured by selectively eliminating hydrogen peroxide with bisulfite as described by Bader et al. (1988). Prior to the addition of DPD and peroxidase, 25 µL of 1 mM bisulfite stock solution were added to the cuvette. After about 30 seconds, 25 µL of 1 mM formaldehyde stock solution were added and the procedure was completed as above.

Standard additions of hydrogen peroxide stock solution to natural water samples were usually performed. Stock solution was prepared by dilution of 30% H_2O_2 solution, to approximately 1 mM. The absorbance at 240 nm was measured for the 1 mM solution and several dilutions with Q-H_2O and plotted as the absorbance vs. the dilution factor. The concentration is the fitted slope divided by $\varepsilon = 40.0\ M^{-1}\ cm^{-1}$ (Bader et al., 1988). This was compared with a standard addition of the stock solution in Q-H_2O using the DPD method to check for a result of $\varepsilon = 21000 \pm 500\ M^{-1}\ cm^{-1}$. The two methods correspond within two significant figures.

2.2.3 Samples Treatment

Samples collected from the Halls Brook Holding Area (HBHA) were treated in the following way: water samples were pumped up using a peristaltic pump through Cole-Parmer Kynar (polyvinylidene fluoride) tubing and filtered through two in line filters, a type AP Millipore prefilter and a type HA Millipore membrane filter (0.45 µm). Alternatively, cellulose acetate syringe filters (0.45 µm) were used. Samples were measured in the field by following the above procedure using a Spec 20 portable

spectrophotometer. Samples were prepared in the field for later laboratory analysis by adding aliquots of filtered sample water to acid-washed polypropylene and/or glass bottles containing proportional amounts of stock solution. The stock solution consisted of 0.2 mL pH 6 buffer, 50 μL of bipyridine stock and 16.7 μL of EDTA stock solution for every 1 mL of sample. Samples were placed on ice in the dark. Hydrogen peroxide was measured within 5 hours using the DPD method.

2.3 Results and Discussion

2.3.1 Standard Curves

Standard curves (absorbance vs. added [H_2O_2]) for the measurement of hydrogen peroxide using the DPD method in Q-H_2O were linear with slopes of 21000±500 for concentrations less than about 40 micromolar [Figure 2.1]. At higher concentrations, the slope began to fall off. It should also be noted that the Q-H_2O typically contained between 200 and 500 nM H_2O_2. Standard additions to HBHA water samples usually yielded slopes of 21000±1000. For HBHA samples with high concentrations of hydrogen peroxide present (greater than about 20 micromolar), the slopes of the standard curves were often lower by up to a factor of two. This leads to calculated concentrations of H_2O_2 up to a factor of two lower than calculated using the literature value (see, for example, Table 3.7).

For a set of samples collected from HBHA in September 1997, there appears to be an inverse relationship between the absorbance measured by the DPD method of each sample and the slope of its standard curve [Figure 2.2]. If this relationship was due to a curved standard curve in HBHA water, we would expect that dilution of sample before adding standard hydrogen peroxide should increase the slope. This was indeed the case for a sample obtained Oct. 28, 1997. Figure 2.3 and Table 2.1 show the increase in slope with increase in dilution. The increases are, however, small, and it is not certain that the slope would approach the literature value of 21,000 M^{-1} cm^{-1} at very high dilution. Usually the hydrogen peroxide stock solution was

calibrated within 24 hours of use, but in this case, it had not been calibrated in a week. It's possible that the low slopes partially represent degradation of hydrogen peroxide in the stock solution, though in my experience degradation of the stock solution was very slow except on rare occasions when degradation was rapid, probably due to contamination. Curvature of the standard curve will tend to overestimate the concentration of hydrogen peroxide if both the best fit slope and intercept of a standard addition are used, but will underestimate the concentration of hydrogen peroxide if the literature value for the slope is used. Table 2.1 shows the concentrations of hydrogen peroxide calculated from the slope and intercept of the best fit line for the standard additions of each dilution. The differences between the calculated concentrations of hydrogen peroxide were, however, not much larger than the standard deviation of the best fit lines.

If something in HBHA samples was competing with DPD as a peroxidase / hydrogen peroxide substrate, causing less DPD to be oxidized to the colored species, adding more DPD should increase the absorbance. If something in HBHA samples was inhibiting peroxidase, adding more peroxidase should increase the absorbance. However, increasing both DPD and peroxidase had no effect on the absorbance. It is possible that something in HBHA water samples reacts with the DPD-radical cation, either reducing it back to DPD or decreasing its stability and causing it to dimerize or polymerize more quickly. It remains unclear why we see a nonlinear Beer's Law response in HBHA samples.

2.3.2 Sample Preservation

In order to examine our ability to preserve HBHA samples for analysis in the lab, a single sample of HBHA surface water (7/22/97) was filtered with syringe filters (0.45 μm), divided into 4 x 10 mL portions and "preserved" by adding samples to vials containing stock solutions used for the DPD analysis of hydrogen peroxide. The stock solution consisted of 0.2 mL pH 6 buffer, 50 μL of bipyridine stock and 16.7 μL of EDTA stock solutions for every 1 mL of sample. Additions of stock hydrogen peroxide

solution were made in the field as shown in row one of Table 2.2. Hydrogen peroxide measurements were made approximately 4 hours later by standard additions. Hydrogen peroxide standard additions are shown in row two of Table 2.2. Table 2.3 shows the absorbance measured using the DPD method for each total amount of added hydrogen peroxide (the amount added in the field plus the amount added in the lab ~4 hours later adjusted by the dilution factor due to added reagents). The standard error between samples with the same total amount of added hydrogen peroxide is substantial (up to 10%), but first order degradation can be ruled out as the cause. If hydrogen peroxide was quickly degrading in transit, we would expect lower concentrations in samples with a greater portion of hydrogen peroxide added at the earlier time in the field. There is no trend towards lower measured hydrogen peroxide concentrations from sample 1 to sample 4. Each value of equal added $[H_2O_2]$ concentration was averaged and each of these averaged points were plotted as average absorbance vs. added $[H_2O_2]$ [Figure 2.4]. The best fit line has a slope of 17,000 M^{-1} cm^{-1}, but a slope of 20,300 M^{-1} cm^{-1} was found if the last point is excluded. This compares well to the literature slope of 21,000 M^{-1} cm^{-1}. The last point was only measured once and may be low due to curvature of the standard curve. This procedure was repeated for three samples analyzed Aug. 14 with similar results.

The degradation of H_2O_2 in samples preserved by following the above procedure was first order with respect to H_2O_2 and slow enough that transportation of preserved field samples to the lab should not have lead to degradation that was significant compared to the experimental error. Two sets of HBHA water samples were collected on February 27, 1998, one at a depth of 1.0 m and the other at 3.0 m, and spiked with hydrogen peroxide stock solution. Each set of samples consisted of one bottle with preserved sample, another with unfiltered preserved sample, and a third with unfiltered, unpreserved sample. The concentrations of hydrogen peroxide over time are shown in Figure 2.5 and the first order linearizations in Figure 2.6. Half lives in hours are shown below in Table 2.4. At both depths, the preserved samples (A and B) have significantly longer half lives than the unpreserved samples (C). For the half

lives listed for the 1 m and the 3 m samples, preserved samples would lose about 2% and 6% of their hydrogen peroxide, respectively, within the four hours needed to transport and analyze them. Since the half-lives for hydrogen peroxide degradation were similar for both filtered and unfiltered samples, but substantially lower for samples containing metal-binding ligands (preserved samples), the major degradation process was probably abiotic at that time of year.

2.3.3 Blank Measurements and the Effect of Sunlight

Blank absorbances (no peroxidase) measured on the Spec 20 instrument at HBHA were variable and large, similar in magnitude to sample absorbances. For example, on May 27, hydrogen peroxide measurements were made in the field and the average absorbance of all blank measurements made that day was 0.083 ± 0.025 (37 measurements). The total absorbance was less than twice the blank absorbance for all samples measured on that date. For preserved samples taken the afternoon of Aug. 14, however, the average absorbance of all blank measurements measured was only 0.0050 ± 0.0012 (19 measurements), and blank absorbance was always less than 0.01 for all HBHA samples taken between August and October. The absorbance of each blank measured in the field also tended to rise slightly with time, but blank absorbances in general fell over the course of the afternoon sampling period [Figure 2.7]. This general decrease in blank absorbance could have been due to change associated with depth or with decreasing sunlight intensity.

To test whether sunlight exposure during the hydrogen peroxide measurement was influencing the blank measurement, HBHA surface water collected several days previously was placed in two plastic cuvettes and left uncovered and exposed to sunlight for 60 sec. DPD was added to one of the samples outdoors and to the other after being brought indoors. The outdoor sample was exposed to sunlight for an additional 45 sec upon addition of DPD. Absorbance was measured indoors as a function of time since addition of DPD. The results are shown in Figure 2.8. The absorbance at 552 nm of the sample exposed to sunlight after DPD was added was

approximately three times the absorbance of the sample handled indoors. The blanks that were not exposed to light after the addition of DPD had similar absorbances at 552 nm as the Aug. 14 samples. The blanks that were exposed to sunlight had lower absorbances than the May 27 samples, but variations due to the amount of radiation absorbed by the samples would be expected. Generation of peroxy radicals in sunlight-exposed samples may explain these results. Peroxy radicals generally react by abstracting hydrogen atoms, as does hydrogen peroxide in the presence of peroxidase (see Section 2.1), so that peroxy radicals could react with DPD to form the colored DPD product. Peroxy radicals are also known to form photochemically and to have very short lifetimes (Schwarzenbach et al., 1993). Once DPD is added to a sample, photochemically generated peroxy radicals could oxidize it to form the same colored species formed by hydrogen peroxide and peroxidase. However, peroxy radicals may have too short a lifetime to persist after samples have been placed in the dark.

Blank signals were also high in samples obtained between December and February 1997-98. The blank signals tended to fall over a period of hours [Figure 2.9] and were typically higher in preserved, that is, bipyridine and EDTA amended, samples than in unpreserved samples [Table 2.5]. The samples were not filtered with filters with pore sizes less than 0.45 μm to see if high blank signals were due to particulate matter, though blanks of samples from the summer of 1998 were unchanged by filtration with 0.05 μm filters.

Addition of bisulfite to selectively destroy hydrogen peroxide as a blank measurement has been suggested by Bader et al. (1988). Bisulfite blanks in HBHA samples were generally comparable to blanks measured by omitting peroxidase. The pH must be lowered to 4 in order for bisulfite to react with hydrogen peroxide, but the concentration of DPD-radical cation is pH dependent. For example, for the same sample, the absorbance of $DPD^{+}\bullet$ was 0.0049±0.0005 at pH 6, while it was 0.0217±0.0008 at pH 4. To avoid this discrepancy, the pH of bisulfite blanks should be raised to 6 after enough time has passed to eliminate hydrogen peroxide. The bisulfite

method of blank measurement was suggested in part because catalase can take a long time to eliminate hydrogen peroxide. This is not a problem for field samples which are stored for several hours before analysis, so catalase blanks may be a good option for preserved sample blanks if confirmation of catalase-omitted blanks is desired.

Sunlight may also produce hydrogen peroxide in samples exposed to light. Preserved samples (0.4 m) from Oct. 22 (approximately 60 mL in uncapped polypropylene bottles) were left in sunlight for varying lengths of time before placing them in the dark and taking them back to the lab. Figure 2.10 shows the hydrogen peroxide measured in each sample vs. the amount of time each sample vial was left in sunlight. The hydrogen peroxide concentration stayed fairly constant over the first half hour of sunlight exposure, but approximately doubled after an hour of sunlight exposure.

Hydrogen peroxide can also be produced by sunlight in the stock solutions used for preservation in the absence of sample. A vial containing preservation reagents exposed to noon sunlight in July under cloudy skies for 1 hour contained more than 50 μM hydrogen peroxide. This could have serious consequences since care was not taken to exclude sunlight from stock solutions prior to addition of field samples collected for hydrogen peroxide analysis between August 1997 and February 1998 (see Chapter Three). In July 1998, field samples were collected in the same manner as samples collected the previous summer and fall. A set of samples was simultaneously collected in which the reagent bottles were protected from sunlight before, during and after filling with sample. These were compared to method blanks in which Q-H_2O was added to vials containing preservation reagents in lieu of sample that were also shielded from sunlight. Samples shielded from light were all less than 0.5 μM and not significantly different than method blanks. Samples treated in the same manner as field samples collected between Aug. 1997 and Jan 1998 were exposed to light for less than five minutes. There was some production of hydrogen peroxide, shown in Table 2.6. The samples were collected between noon and 1 p.m.

During this time, the weather conditions changed from sunny to cloudy, but the results were similar in all three samples. Notice that there was not a large increase in hydrogen peroxide with depth as was seen with field samples collected in Aug., Sept., and Oct. 1997 (see Chapter Three).

2.4 Discussion and Conclusions

Although the precision of the DPD method in HBHA water samples was typically less than 10%, there were problems affecting accuracy. Several of these difficulties have been mentioned. These include non-ideal and possibly non-linear standard addition curves and production of both hydrogen peroxide and other oxidants capable of oxidizing DPD in sunlight. Another factor influencing the detection limit was the presence of small amounts of hydrogen peroxide in stock solutions and Q-H_2O stored in the dark. These problems should be kept in mind when interpreting the data in Chapter Three. Low concentrations of hydrogen peroxide (less than ~ 4 μM) should be approached with skepticism, since concentrations of 2-3 μM were produced by sunlight during the sampling procedure when this was checked on one occasion. Hydrogen peroxide concentrations in samples with non-ideal standard addition curves can not be determined accurately. Using both the best fit slope and intercept of a standard curve with a lower than ideal slope results in an overestimate of the hydrogen peroxide concentration, while using the ideal slope to calculate the concentration results in an underestimate. The actual value should lie in between, so both numbers are reported for data in Chapter Three.

In the future, several things can be done to overcome the problems discussed in this chapter. First, during field sampling, all reagents, vials and samples must be protected from sunlight. Method blanks in which Q-H_2O is added in lieu of sample should be used to check for inadvertent sunlight exposure. In order to measure small (< 0.5 μM) concentrations of hydrogen peroxide, hydrogen peroxide-free water and stock solutions should be prepared. Distillation can reduce the concentration of hydrogen peroxide in water to less than about 25 nM (Holm et al., 1987). To reduce

the hydrogen peroxide concentration further, small amounts of catalase, allowed to act overnight, have been used. Additionally a method for eliminating hydrogen peroxide from distilled water by pumping it through a MnO_2 column has been described (Hwang and Dasgupta, 1986). Ideally, samples should be analyzed immediately using a flow injection system, but hydrogen peroxide decay in preserved samples is typically slow enough to allow for transport to the laboratory. Non-ideal standard addition curves poses a problem if precise values for hydrogen peroxide concentrations are desired. One way this problem could be solved is by using the following procedure. Hydrogen peroxide could be selectively destroyed by bisulfite at pH 4, which is then masked by formaldehyde as described above. The pH should then be brought to 6 before adding standard additions of hydrogen peroxide and measuring H_2O_2 using the DPD method. The absorbance of the sample could then be compared to this standard curve. Alternatively, a series of dilutions with hydrogen peroxide-free water can be performed. With these methodological improvements, it should be possible to measure hydrogen peroxide in HBHA more selectively, more precisely and with a lower limit of detection.

2.5 References

Bader, H., Sturzenegger, V. and Hoigné, J., 1988. Photometric method for the determination of low concentrations of hydrogen peroxide by the peroxidase catalyzed oxidation of N,N-diethyl-p-phenylenediamine (DPD). *Wat. Res.*, **22**(9): 1109-1115.

Bruice, T. C., 1988. Chemical studies related to iron protoporphyrin-IX mixed function oxidases. Mechanistic Principles of Enzyme Activity. J. F. Liebman and A. Greenberg. New York, VCH: 227-277.

Forrester, A. R., Hay, J. M. and Thomson, R. H. (1968). Organic Chemistry of Stable Free Radicals. London, Academic Press.

George, P., 1952. Chemical nature of the secondary hydrogen peroxide compound formed by cytochrome-C peroxidase and horseradish peroxidase. *Nature*, **169**: 612-613.

Holm, T. R., George, G. K. and Barcelona, M. J., 1987. Fluorometric determination of hydrogen peroxide in groundwater. *Anal. Chem.*, **59**: 582-586.

Hwang, H. and Dasgupta, P. K., 1986. Fluorometric flow injection determination of aqueous peroxides at nanomolar level using membrane reactors. *Anal. Chem.*, **58**: 1521-1524.

Schwarzenbach, R. P., Gschwend, P. M. and Imboden, D. M., 1993. Photochemical Transformation Reactions. Environmental Organic Chemistry. New York, Wiley: 436-484.

Traylor, T. G., Lee, W. A. and Stynes, D. V., 1984. Model compound studies related to peroxidases. Mechanisms of reactions of hemins with peracids. *J. Am. Chem. Soc.*, **106**: 755-764.

Voelker, B. M. and Sulzberger, B., 1996. Effects of fulvic acid on Fe(II) oxidation by hydrogen peroxide. *Environ. Sci. Technol.*, **30**(4): 1106-1114.

2.6 Figures and Tables

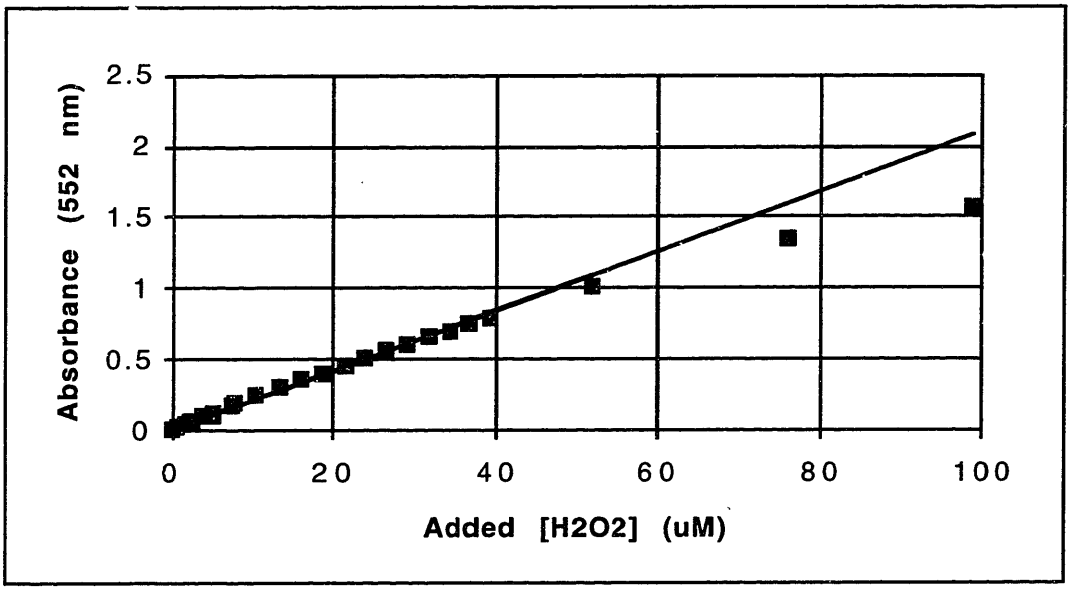

Figure 2.1. Standard curve in Q-H_2O. The line corresponds to values calculated using the literature value for the absorptivity. Points agree well with the literature value below about 50 micromolar hydrogen peroxide.

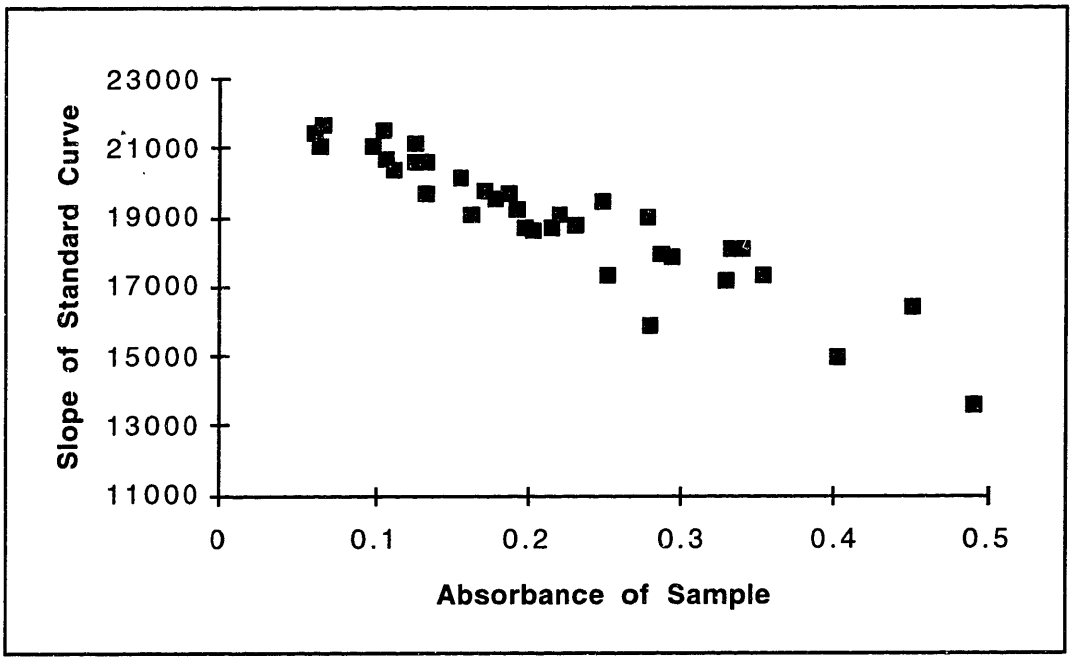

Figure 2.2. Relationship between absorbance (552 nm) and slope of the standard curve for HBHA samples collected in September 1997.

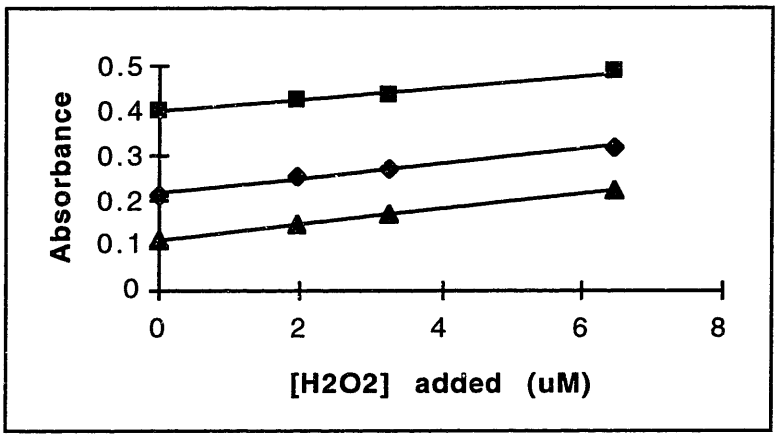

Figure 2.3. Dilution experiment. The top curve is a standard addition curve for undiluted sample. The second curve is for the same sample diluted by a factor of 1.9. The bottom curve is for the sample diluted by a factor of 3.8.

Dilution Factor	Slope	Calculated $[H_2O_2]$ (μM)	Standard Deviation (μM)
1	13500	38.3	2.2
1.9	16000	33.8	2.0
3.8	17300	32.5	0.9

Table 2.1. Dilution experiment. As the dilution factor rises, the slope of the best fit line rises and the calculated value for the hydrogen peroxide concentration falls slightly.

	Vial1				Vial 2			
$[H_2O_2]$ (μM) added in field	0	0	0	0	1.32	1.32	1.32	1.32
$[H_2O_2]$ (μM) added in lab	0	1.32	3.96	6.6	0	1.32	3.96	6.6
Total $[H_2O_2]$ (μM) added	0	1.32	3.96	6.6	1.32	2.64	5.28	7.92

	Vial 3				Vial 4			
$[H_2O_2]$ (μM) added in field	3.96	3.96	3.96	3.96	6.6	6.6	6.6	6.6
$[H_2O_2]$ (μM) added in lab	0	1.32	3.96	6.6	0	1.32	3.96	6.6
Total $[H_2O_2]$ (μM) added	3.96	5.28	7.92	10.56	6.6	7.92	10.56	13.2

Table 2.2. Field preservation positive control. One HBHA sample was divided into four vials containing stock solutions for preservation. An aliquot of hydrogen peroxide stock solution was immediately added in the field to vials 2 - 4. Additional hydrogen peroxide stock solution was added to samples from each vial during analysis in the lab several hours later.

Total H_2O_2 added (μM)	Vial 1	Vial 2	Vial 3	Vial 4	Average
0.00	0.052				0.052
1.02	0.068	0.073			0.071
3.05	0.096	0.114	0.112		0.11
5.08	0.148	0.151	0.145	0.164	0.15
7.11		0.194	0.177	0.204	0.19
9.14			0.241	0.236	0.24
15.23				0.299	0.30

Table 2.3. Sample preservation experiment data. Total added hydrogen peroxide concentrations vs. the absorbance using the DPD method for each vial is shown.

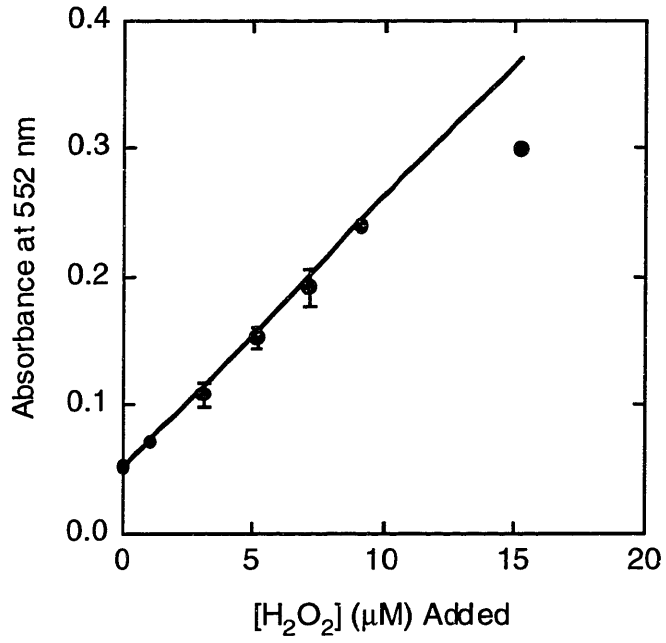

Figure 2.4. Sample preservation experiment results. The points are average values from Table 2.3 above. The line represents the literature value for the slope.

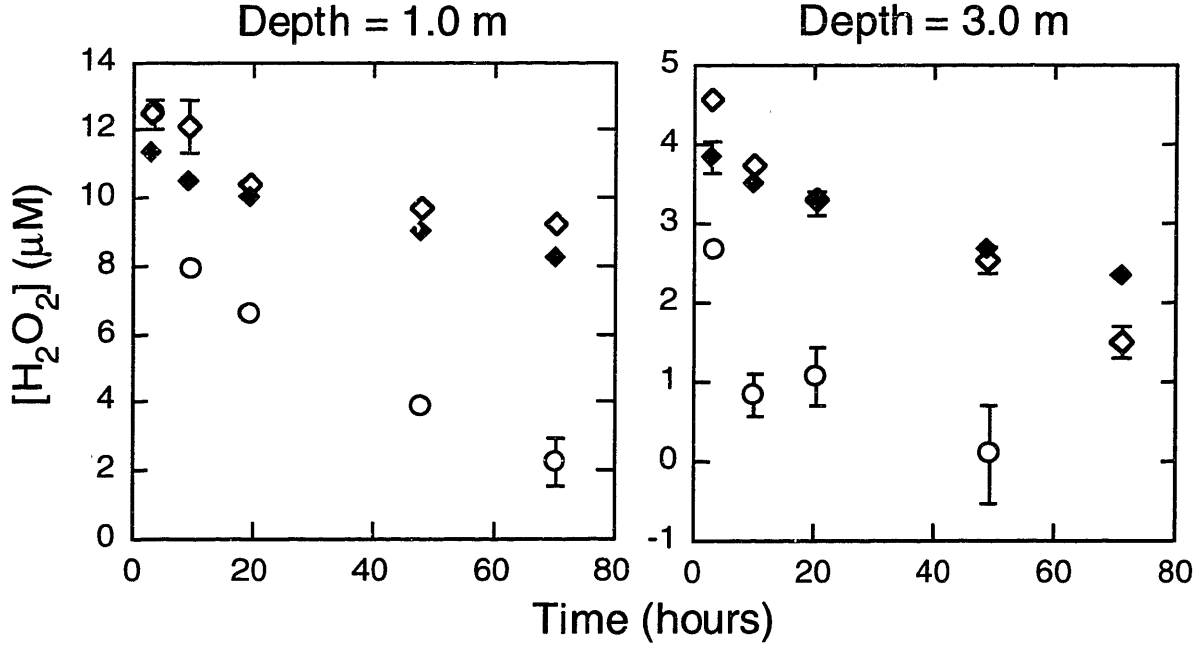

Figure 2.5. Degradation of hydrogen peroxide vs. time. Open circles are unpreserved, unfiltered samples. Open diamonds are filtered, preserved samples. Filled diamonds are unfiltered, preserved samples. Degradation is faster in the unpreserved samples than in either of the preserved samples.

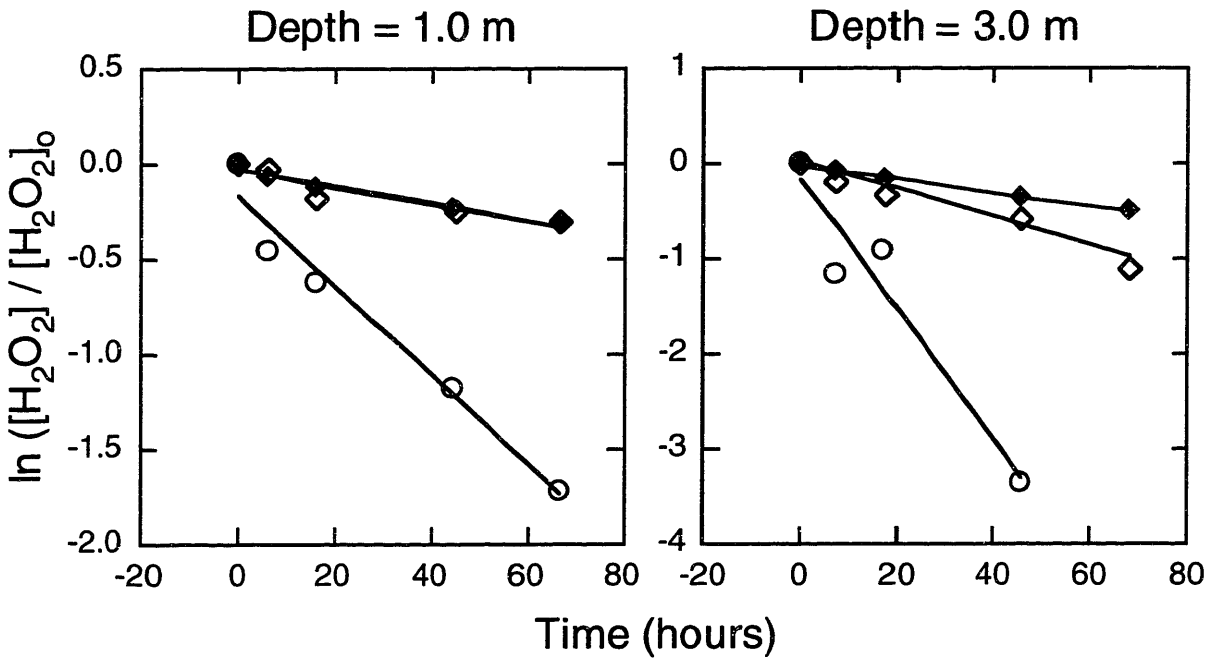

Figure 2.6. First order decay of hydrogen peroxide. Shown are plots of the natural log of the hydrogen peroxide concentration divided by the initial H_2O_2 concentration vs. time. Open circles are unpreserved, unfiltered samples. Open diamonds are filtered, preserved samples. Filled diamonds are unfiltered, preserved samples.

	1.0 m	*3.0 m*
A	157	47
B	157	97
C	30	10

Table 2.4. Half lives for the degradation of hydrogen peroxide. The half lives in hours were calculated using the best fit lines shown in Figure 2.6. A is unpreserved, unfiltered sample, B is filtered, preserved sample, and C is unfiltered, preserved sample. Filtration appears to have little effect on the degradation rates, whereas preservation by adding metal-binding ligands slows the degradation rate. This indicates that the major degradation processes at this time of year were abiotic.

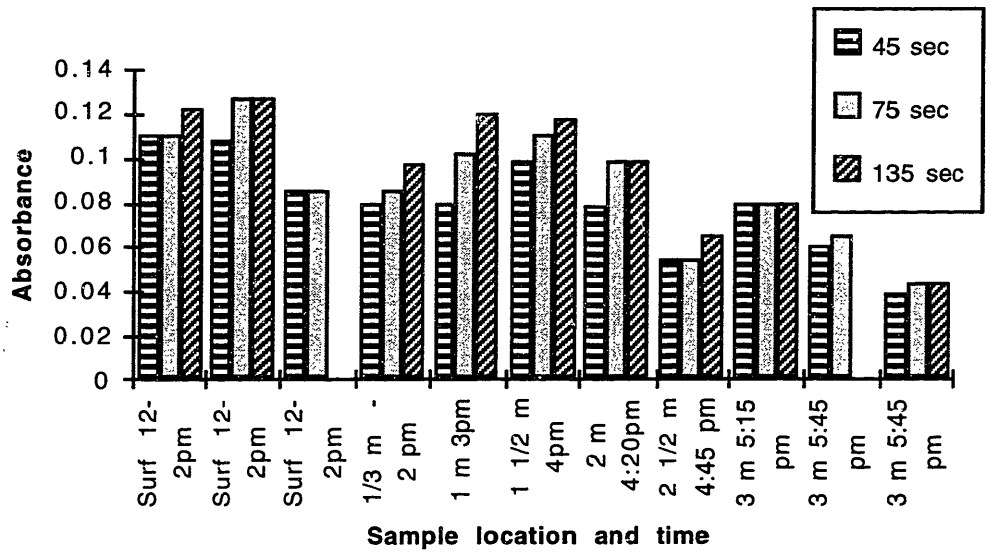

Figure 2.7. Blank signals measured at HBHA. Blanks were no-peroxidase blanks measured on site at HBHA using a Spec 20 spectrophotometer (5/27/97). Notice both the rise from 45 to 135 sec for each sample and the general fall with depth and time of day.

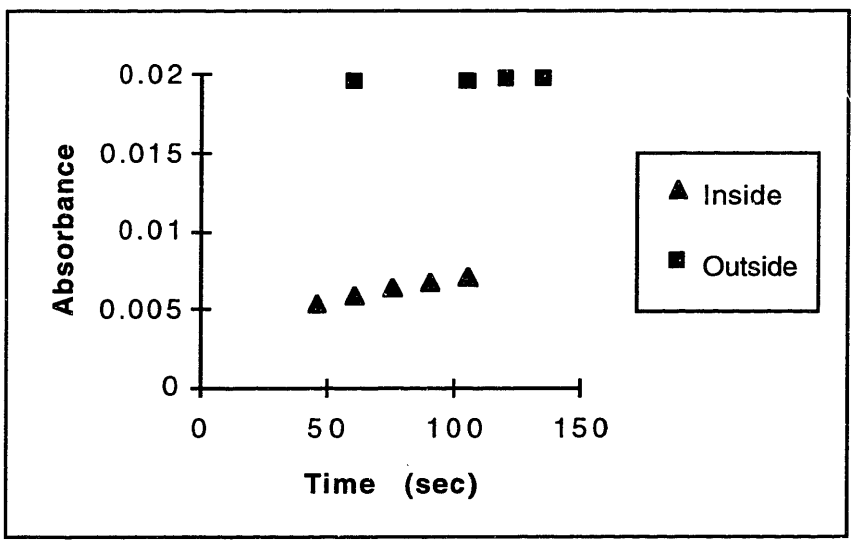

Figure 2.8. Blanks processed indoors vs. outdoors. The blank processed indoors was not exposed to sunlight after the addition of DPD. The blank processed outdoors was exposed to sunlight for 45 sec. after the addition of DPD. Time on the y-axis is time since the addition of DPD.

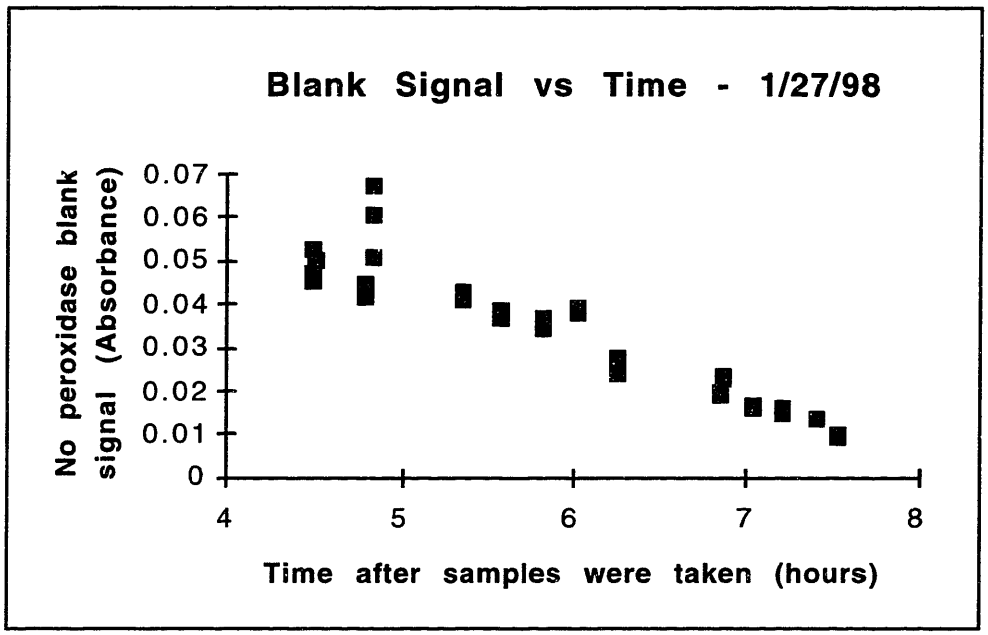

Figure 2.9. Blank signal decline over 8 hours. Points are for all samples collected from HBHA on 1/27/98.

Feb. 27, 1998

Sample	Blank	Stand. Dev.
A-preserved	0.0511	0.0008
B-preserved	0.0532	0.0013
A-unfiltered; preserved	0.0559	0.0027
B-unfiltered; preserved	0.0443	0.0031
A-unpreserved	0.0184	0.0005
B-unpreserved	0.0124	0.0007

Table 2.5. Blanks of preserved vs. unpreserved samples. A and B are two different samples collected 2/27/98. Preserved samples were added to EDTA, bipyridine, and phosphate buffer stock solutions as described in the text. Unpreserved samples were also unfiltered. Blanks were no-peroxidase blanks. Blank absorbance (552 nm) is significantly higher in preserved samples than in unpreserved samples.

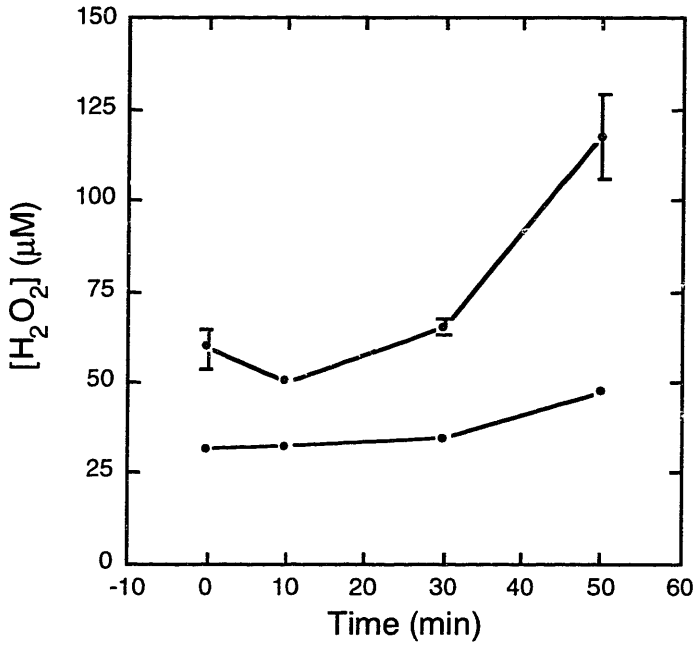

Figure 2.10. Hydrogen peroxide production in sunlight. Each point is for one polypropylene bottle containing approximately 60 mL of preserved sample (10/22/98; 0.4 m). The top curve shows the calculated concentrations of hydrogen peroxide based on the best fit slope and intercept of standard addition curves. The bottom curve shows the calculated concentrations of hydrogen peroxide based on the literature value for the slope (21,000 M^{-1} cm^{-1}). Bottles were left uncapped and exposed to sunlight for the time indicated on the graph before closing, placing on ice in the dark and returning to lab for analysis.

Depth	*Weather*	*Time*	*$[H_2O_2]$*	*Std. Dev.*
0.0	Cldy	12:59	2.5	0.1
1.0	Sunny	12:07	2.2	0.3
2.0	Mstly Sun	12:13	3.4	0.3

Table 2.6. Hydrogen peroxide produced by sunlight during sampling procedure. Samples collected simultaneously, but protected from light, contained undetectable (<0.5 μM) concentrations of hydrogen peroxide.

3. Field Work

3.1 Introduction

The physical characteristics of the Halls Brook Holding Area (HBHA) must be understood in order to understand the distribution and fate of hydrogen peroxide. Several of HBHA's physical characteristics are known, including the surface area, the area at three depths, volume, maximum depth, and mean depth [Table 3.1] (Roux Associates, 1992). The lake is both quite small (17,400 m^2 surface area) and shallow (2.2 m mean depth). Highly variable flow conditions though this small lake led to variable residence times of water in the lake that were typically low (~3 days in the epilimnion of HBHA) during a study period from Sept. '95 to Sept. '96 (Wick and Gschwend, 1998). Surface outflows were consistently larger than surface inflows during this period, and the difference between the two was used to estimate groundwater inflow (Wick and Gschwend, 1998).

The structure of a lake also affects the lake chemistry, since it controls vertical mixing and the residence time of water in the lake. In a typical dimictic lake, temperature determines the water density and characterizes the lake structure. In a saline lake, temperature and salinity together determine the density. In saline lakes, conductivity is often used to characterize the "salt" profile. If conductivity acts as a conservative tracer, that is, it is affected by mixing processes only, it can be used to characterize lake structure. Previous work has shown that the major ionic species in high conductivity HBHA water (4000 µmho/cm) are Na^+, Ca^{2+}, SO_4^{2-}, and Cl^- at concentrations of about 17 mM, 6 mM, 11 mM, and 4 mM, respectively (Wick and Gschwend, 1998). The conductivity has been shown to proportional to Na^+ concentration (McNeill and Gschwend, 1998). Since Na^+ is inert and generally conservative in natural waters, conductivity can be assumed to be conservative in HBHA as well.

Hydrogen peroxide distribution is a function of mixing, production, and decay processes. Mixing can be understood by using temperature and conductivity as

tracers of turbulent mixing processes. Photochemical production is controlled by incident light intensity, the absorptivity of dissolved organic carbon (DOC) in the lake, and the apparent quantum yield of H_2O_2 formation from DOC. These parameters are, therefore, needed in order to understand hydrogen peroxide distributions and to quantify the production function for hydrogen peroxide. Hydrogen peroxide decay may occur by biological degradation or redox reactions with reduced metal species. Metal speciation is controlled by the redox potential and the pH of the system, so that both of these parameters are important indicators of lake chemistry. Dissolved oxygen is also an important indicator of lake chemistry that determines the type of biota that may be present. Chlorophyll or other measures of biological activity could also be useful indicators of decay or production. Chlorophyll *a* and turbidity were not measured during the course of this study, but they were measured at HBHA in October of 1998, revealing a dense layer of photosynthetic activity near the pycnocline (see section 3.3.1). The processes controlling the hydrogen peroxide distribution in HBHA, including photochemical production, turbulent vertical mixing, decay processes, etc., will be quantified and used to model hydrogen peroxide profiles in Chapter Four.

3.2 Experimental

3.2.1 Description of Field Site

All field work was carried out at the Halls Brook Holding Area (HBHA), a small meromictic lake in the Aberjona watershed in Woburn, MA [Figure 1.1; Table 3.1] between May 1997 and June 1998. HBHA receives seasonally variable inflows from the Halls Brook stream and from a constructed drainage ditch to the north. The lake also receives a groundwater inflow from the adjacent Industriplex Superfund site that is highly saline, high in organic matter and heavily contaminated with organic pollutants. This inflow causes the lake to be permanently stratified, with fresh water from Halls Brook overlying a dense, saline anoxic monimolimnion (hypolimnion) with dissolved organic matter concentrations of up to 100 mg/L (Wick and Gschwend,

1998) and ferrous iron concentrations greater than 10^{-3} M (Diez and Gschwend, 1996). The outflow empties into a marsh that drains into the Aberjona River, which flows by the Wells G and H Superfund site before reaching the Upper Mystic Lake. The Mystic Lakes, located about 5 miles south of HBHA, are used for recreational purposes, including boating, fishing, and swimming.

3.2.2 Measurement of Chemical Parameters

Conductivity (μmho/cm), dissolved oxygen (mg/L), temperature (°C), pH, and E_H (mV vs. SHE) were measured *in situ* with a Hydrolab MiniSonde probe connected to a Hydrolab Surveyor 4 (Hydrolab Corporation, Austin, TX). Conductivity was calibrated at two points, one at zero μmho/cm using Q-H_2O and at known conductivity using a KCl solution. Dissolved oxygen was calibrated in water-saturated air. The pH meter was calibrated at pH 4 and at pH 7. Alternatively, on the May, October, and November sampling dates, conductivity and temperature were measured with a YSI model 33 S-C-T meter and dissolved oxygen with a YSI 57 oxygen meter. The YSI conductivity meter was not calibrated on either of the September sampling dates. This means that relative conductivity on each of these dates should be correct, but that the conductivity is not comparable to conductivity measured on other dates. In October 1998, a Hydrolab DataSonde 4 equipped with a turbidity meter and a chlorophyll *a* fluorescence detection system, in addition to the meters in the MiniSonde described above, was used. Both the turbidity and chl *a* detection systems were left at their factory-calibrated settings. Water velocities in Hall's Brook and in the outflow stream were measured with a Marsh and McBirney model 201 portable water current meter at 4 to 8 locations at approximately regular intervals across the streams. The arithmetic means of both the measured velocities and the measured depths were calculated. Flow was calculated as the average velocity times the average depth times the width of the stream. Lakewater absorptivity was measured using 1 cm quartz cuvettes in a HP 8453 spectrophotometer.

3.2.3 Measurement of Hydrogen Peroxide and Iron (II)

Samples collected for the analysis of hydrogen peroxide were preserved for later laboratory analysis in the following way. Water samples were pumped up using a peristaltic pump through Cole-Parmer Kynar (polyvinylidene fluoride) tubing and filtered through two in line filters, a type AP Millipore prefilter and a type HA Millipore membrane filter (0.45 μm). Alternatively, cellulose acetate syringe filters (0.45 μm) were used. In order to preserve samples (see section 2.3.2), aliquots were removed and added to acid-washed polypropylene and/or glass bottles containing proportional amounts of stock solution. The stock solution consisted of 0.2 mL pH 6 phosphate buffer (0.5 M), 50 μL of bipyridine stock (0.01 M bipyridine in 10^{-3} M $HClO_4$), and 16.7 μL of EDTA stock solution (10^{-2} M Na_2EDTA) for every 1 mL of sample. Samples were placed on ice in the dark. Sample vials containing the stock solutions were exposed to sunlight for less than approximately 5 min. while samples were added. Hydrogen peroxide was measured using the DPD spectrophotometric method of Bader et al. (1988) and refined for use in the presence of inorganic interferants including Fe(II) by Voelker and Sulzberger (1996) within 5 hours of sampling as described in Chapter Two. Blanks were treated identically to samples except that peroxidase was not added during the analysis. Blank absorbance was subtracted from the sample absorbance when calculating hydrogen peroxide concentrations in samples.

The presence of ferrous iron in samples collected for hydrogen peroxide analysis was indicated by an orange-pink color upon addition of sample to the stock solution described above. The color is due to the formation of an Fe^{2+} - bipyridine complex with a maximum absorbance at 522 nm. Assuming that an absorbance greater than 0.01 is visible in a 1 cm vial, concentrations greater than 10^{-6} M Fe^{2+} are visible using this procedure. On the Aug. 14, 1997 sampling date, the absorbance using this procedure with samples from several depths was measured at 522 nm within 5 minutes using a portable Spec 20 spectrophotometer. The ferrous iron concentrations were calculated according to Beer's law using the literature absorptivity of 8650 M^{-1} cm^{-1} (Voelker and Sulzberger, 1996).

3.3 Results and Discussion

3.3.1 Typical Lake Structure and Chemistry in HBHA

The vertical structure of HBHA was revealed by the conductivity vs. depth profile, assuming that conductivity acted as a conservative tracer in HBHA. The water column in HBHA consisted of three layers analogous to the epilimnion, metalimnion and hypolimnion of a thermally stratified lake. The layer of relativity low, constant conductivity defined the epilimnion (or mixolimnion), the layer of rising conductivity defined the metalimnion, and the bottom layer of relatively constant (±5%) maximum conductivity defined the hypolimnion (or monimolimnion) [Figure 3.1]. The pycnocline is the plane at the depth of the maximum density (conductivity) gradient, where vertical turbulent mixing is the slowest. The pycnocline was usually near the top of the metalimnion in HBHA. The dissolved oxygen concentration was typically constant in the epilimnion, falling rapidly with depth in the top of the metalimnion, to a minimum constant concentration below the pycnocline. Conductivity continued to rise below the pycnocline with a smaller gradient. In spring and fall, the conductivity rose with depth all the way to the bottom of the lake. In summer and fall, the conductivity reached a maximum of about 4400 μmho/cm in the hypolimnion.

On all sampling dates, a well-defined epilimnion existed, below which conductivity rose with depth, often with a steep gradient. In summer and fall, the epilimnion was typically less than 2 m deep [Figure 3.2], and a hypolimnion of relatively constant high conductivity existed in the bottom meter or two of the lake. In winter and spring, the epilimnion was 3 or more meters deep and included most of the volume of the lake. The metalimnion of increasing conductivity extended all the way to the bottom of the lake, leaving no defined hypolimnion [Figure 3.3]. Some fine structure defined by the temperature profile could also sometimes be observed within the "epilimnion" as defined by the conductivity profile. This fine structure was probably transitory, forming after time periods with low wind speed and a large difference in air

temperature as compared to water temperature [Figure 3.2]. If the fine structure persisted, it should eventually be reflected in the conductivity profile as well.

The conductivity of the HBHA epilimnion was about double that of Hall's Brook in the summer and fall when the inflows were small. It was similar to or slightly higher than that of Halls Brook and the North Ditch in winter and spring when the inflow was large [Table 3.2]. This is consistent with the idea that salt enters HBHA below the surface with groundwater and diffuses upwards to mix with water from Halls Brook in the epilimnion. Salinity, more than temperature, controls the structure of the lake and reduces vertical mixing in HBHA. Assuming salt behaves conservatively, conductivity can be used as a tracer for vertical mixing.

Temperature gradients reinforced the stability of the density gradient caused by salinity when the epilimnion temperature was higher than that of the hypolimnion (spring and summer). The converse was typically true in winter and fall. In summer and fall, the hypolimnion temperature was between 10 and 15 °C. In winter and spring, the isolated hypolimnion had been flushed out, leaving a small metalimnion less resistant to mixing. The temperature at the bottom of the lake fell below 10 °C. Thus, for a typical summer profile, temperature was high with a slight gradient in the epilimnion, fell steeply in the metalimnion, and was constant at about 12 °C in the hypolimnion [Figure 3.2]. In a typical winter profile, temperature was constant through the epilimnion and rose slightly to 7 °C at the bottom of the lake (metalimnion) [Figure 3.3]. The redox potential (E_H) profile was typically a mirror image of the conductivity profile throughout the year, indicating the presence of a uniformly oxidized epilimnion and a hypolimnion with a redox potential of less than 100 mV [Figure 3.2 and Figure 3.3]. The dissolved oxygen profile reflected the redox conditions. It showed high, relatively constant DO concentrations in the epilimnion and a steep negative gradient with depth as conductivity began to rise and E_H began to fall with depth. Below the pycnocline, the DO concentration was less than 0.5 mg/L [Figure 3.2 and Figure 3.3]. Additionally, ferrous iron concentrations rose rapidly with depth through the metalimnion as E_H and DO fell [Figure 3.2]. The pH in HBHA was typically

circumneutral, between 6.5 and 7.5, though the hypolimnion was generally higher in pH than the epilimnion [Figure 3.2 and Figure 3.3]. Often, a slight dip in pH was observed in the metalimnion, probably due to the oxidation of Fe^{2+} to form $Fe(OH)_3$, and possibly due to respiration of organic matter as well [Figure 3.2].

Although chlorophyll *a* concentrations were not measured during the course of this study, they were measured once in October 1998. The depth profiles of other parameters such as conductivity, dissolved oxygen, pH and E_H measured on this date were similar to profiles observed in fall of 1997 [Figure 3.4]. Additionally, a large peak of both chlorophyll *a* and turbidity was seen just below the epilimnion, at the pycnocline [Figure 3.5]. This is consistent with research done on other meromictic lakes. Chlorophyll *a* often reaches a peak near the chemocline of stratified lakes, along with various bacteriochlorophylls used in anoxic photosynthesis by purple and green bacteria (Venkateswaran et al., 1993 and references therein). Much of the peak in HBHA occurred within a depth range in which conditions were still oxic despite lower dissolved oxygen concentrations than existed in the epilimnion. Although turbidity fell off with depth to its near-surface value in the hypolimnion, "chl *a*" remained relatively high. Chlorophyll *a* containing organisms such as green algae and cyanobacteria generally cannot grow under the anoxic conditions prevailing in the hypolimnion. The elevated "chl *a*" concentrations in the epilimnion may be due to the fluorescence of an additional fluorophore that comes in with the groundwater and interferes with the chl *a* measurement. This potential fluorophore could be a pollutant or dissolved organic matter at high concentration (up to 80 mg/L in the hypolimnion on this date). More work will need to be done to determine whether the "chl *a*" concentrations are due entirely to chlorophyll *a* or whether an additional fluorophore interferes.

3.3.2 Seasonal Changes of Lake Structure and Chemistry in HBHA

Conductivity profiles underwent seasonal changes caused by changes in inflow volume [Table 3.2]. From July to December 1997, the epilimnion was less than 2 m

deep and the maximum conductivity was greater than 4000 µmho/cm [Figure 3.6]. (The September profiles are similar to other summer and fall profiles, but the probe was not calibrated, so the numbers are not absolute [Figure 3.7]) Higher conductivities than the 4000 µmho/cm observed at the sampling station between July and December (up to 18,000 µmho/cm) have been observed at the bottom of the northern, more shallow (3 m) basin of the lake (Wick et al. 1998). This indicates that the stable maximum of 4400 µmho/cm observed in summer and fall in the southern basin probably did not represent the groundwater conductivity. It may have represented a stable situation in which the groundwater entering the lake from the northeast mixed with lakewater as it flowed along the bottom of the lake. This diluted groundwater may eventually have flowed to the deepest point in the lake, the southern basin where our field measurements were made.

From July to December, the pycnocline gradually moved deeper, so that in January, the depth of the epilimnion was greater than 3 m, a well mixed hypolimnion no longer existed, and the maximum conductivity of the lake had dropped slightly [Figure 3.6]. These trends of deepening mixed layer and lowered maximum conductivity continued through February. In March, the profile showed a rise all the way to the bottom of the lake with no defined hypolimnion. Then in April and June 1998, consistent with May 1997, the epilimnion become shallower and the metalimnion, the zone of increasing conductivity, increased in size. No hypolimnion was observed in May 1997 or April 1998.

In winter and early spring, the hypolimnion was presumably flushed out by high flow conditions, allowing greater mixing between incoming groundwater and water in the epilimnion, and leading to lower maximum conductivities at the bottom of the lake. The volume of inflow was generally much higher and the residence time of the lake was smaller on dates when the epilimnion was deep. Turbulence generated by influx of storm runoff may induce vertical mixing and flush out most of the lake, but incoming saline groundwater rapidly re-induces stratification. In fact, there was an inverse relationship between the log of the volume of inflow and the log of total salt present in

HBHA [Table 3.2 and Figure 3.8]. "Total salt" was calculated by dividing HBHA into 0.1 m horizontal layers and defining the area of the lake at each layer as a linear extrapolation between known areas at defined depths. The amount of "salt" in each layer is the conductivity multiplied times the area of the lake at the depth of the layer times 0.1 m. "Total salt" is the sum of "salt" in all of the layers. Large inflows may lead to increased turbulent mixing that results in a proportionate flushing out of the salt in the hypolimnion.

In the epilimnion, seasonal changes in temperature profiles reflected equilibration with changing air temperatures. In the metalimnion and hypolimnion, temperature profiles were determined by the degree of vertical mixing; that is, when vertical mixing was limited, the temperature of the hypolimnion was isolated from seasonal change. From May to November 1997 the temperature in the epilimnion varied from a low of 4 degrees C in November to a high of 23 degrees C in July, while the hypolimnion varied only between 10 to 14 degrees during this period [Figure 3.9]. After November, the hypolimnion began to be flushed out, so that the bottom of the lake was no longer thermally isolated. The temperature at the bottom of the lake dropped to a low of 5 degrees C in February before warming again from March to June 1998. By June the temperature at the bottom of the lake had risen to about 12 degrees C, within the 10 to 14 degree range observed for the summer and fall of 1997 [Figure 3.9]. This temperature may represent the temperature of incoming groundwater and/or the temperature of the lake just before the hypolimnion developed enough to remain thermally isolated from the epilimnion.

Dissolved oxygen was fairly constant through the epilimnion (except in July, when there was a peak above the pycnocline) [Figure 3.10]. The solubility of oxygen at equilibrium with the atmosphere is a function of temperature and salinity; solubility is lower at higher temperature and salinity. Since the conductivity of the epilimnion is low, the solubility of dissolved oxygen is primarily a function of temperature. On all dates, the measured concentration of DO was lower than the solubility at the measured temperature [Figure 3.11]. This indicates that loss of oxygen due to mixing

across the pycnocline was faster than equilibration of the epilimnion with the atmosphere. In July, the DO concentration had a large peak (100% saturation) just above the pycnocline that may be due to photosynthetic activity. Dissolved oxygen rapidly dropped to less than 0.2 mg/L (6 μM) just below the epilimnion, near the top of the metalimnion on all sampling dates. The drop from maximum dissolved oxygen concentration to a concentration less than 0.2 mg/L occurred in less than 10 cm on all dates except May 1997 and June 1998. These two dates also had the smallest conductivity gradient observed over the course of this study and the thus the greatest vertical mixing [Figure 3.6; Figure 3.10].

The pH showed little clear seasonal variation, always remaining between 6.1 and 7.6, with the higher values in the hypolimnion [Figure 3.12]. A slight dip in value just below the epilimnion, probably due to ferrous iron oxidation, was detected on most dates. E_H profiles usually looked like the inverse of the conductivity profile and thus show the same sort of seasonal variation as conductivity [Figure 3.12]. The E_H measuring system was slow to recover from extreme measurements. For example, if the probe was lowered into the bottom water where the E_H was low or negative, subsequent measurements in the epilimnion were low, and only gradually recovered. Thus the rise in E_H with depth in the epilimnion shown for some dates (December and March) was probably simply an artifact of the gradual recovery of the E_H meter after being subjected to a low E_H.

3.3.3 Hydrogen Peroxide Profiles

Hydrogen peroxide was detected in epilimnion samples on all sampling dates except in February 1998. In February, care was taken to shield all reagents and samples from sunlight. On other dates, reported concentrations must be compared to hydrogen peroxide concentrations found in method blanks measured in July 1998 (see section 2.3.3). In May 1997, hydrogen peroxide was measured in the field with exposure to sunlight. The concentrations were similar to those of the method blanks (2

to 3 μM) and were, therefore, possibly artifacts of sunlight exposure [Figure 3.13, Table 3.3].

Concentrations of hydrogen peroxide well above the method blanks (above 1 to 4 μM) were detected in samples from the epilimnion in August (afternoon), September and October. In August, the observed hydrogen peroxide concentrations were similar to and slightly greater than those seen in method blanks, but there was a clear increase in concentration with depth [Figure 3.14 and Table 3.4]. Deeper samples would have been exposed to less light during sample processing than shallower samples since they were processed later in the afternoon. So the increase with depth can not be explained by increased photo-production during sampling, although there is uncertainty in the absolute values of hydrogen peroxide concentration in these samples. These results can be compared to early morning samples in which hydrogen peroxide was not detectable (<0.25 μM) near the surface, and only 0.5 μM at 1.3 m, which could be an artifact of production during collection [Figure 3.15 and Table 3.5]. The higher concentrations in the afternoon suggest that if hydrogen peroxide decay is constant, then production increases during the day. If the primary source was not abiotic photochemical, biological production associated with photosynthesis would be consistent with this data. However, hydrogen peroxide concentrations were not monitored over time on any other date, so we lack confirmation of a diurnal cycle of hydrogen peroxide concentrations in HBHA.

In September, both epilimnion samples had hydrogen peroxide levels well above that of method blanks [Figure 3.16 and Table 3.6]; and in October, the deeper sample contained a large and significant amount of hydrogen peroxide, while the surface sample was within the range observed for method blanks [Figure 3.17 and Table 3.7]. The reported concentrations for September and October have large error bars due to possible curvature of the standard curve in these samples (see section 1.3.1). The concentrations reported for August, September and October are higher than any previously reported in the literature for surface water. Interestingly, the highest reported concentrations (up to 3 μM) in the literature are for Russian lakes

high in organic matter and polluted with domestic effluent (Sinel'nikov, 1971; Shtamm et al., 1991). Most of the research on hydrogen peroxide in North American lakes has been done in relatively pristine or large lakes with relatively low (< 10 mgC/L) organic matter concentrations (Cooper and Lean, 1989; Cooper et al., 1989; Scully et al., 1995; Scully and Vincent, 1997). However, a study comparing the hydrogen peroxide profiles in several lakes and an oxidation pond of varying trophic status in New Zealand did not report any concentrations of H_2O_2 greater than 0.75 μM (Herrmann, 1996). All of their data could be explained by a photochemical source, wet deposition, mixing and decay processes. This was true even for a hypereutrophic oxidation pond with DOC concentrations of 24-28 mg/L.

On all three dates with high hydrogen peroxide concentrations, hydrogen peroxide increased with depth. However, it was not detectable below the pycnocline. This kind of profile has not been previously reported and seems to indicate a source below the surface of the lake, that is, a source other than an abiotic photochemical source. This possibility will be explored in Chapter Four. Below the pycnocline, Fe^{2+} concentrations were high enough to be observed as an orange-pink color upon addition of the sample to the stock solution described above, indicating the complexion of iron(II) with bipyridine [Tables 3.4, 3.5 and 3.8-3.10]. When hydrogen peroxide stock solution was added to samples collected from below the pycnocline, it was quickly degraded (first order decay at least 1 min^{-1} in a 8/14/97 sample). Lakewater samples were also analyzed for hydrogen peroxide in December and January, but concentrations were less than 1.5 μM, not significant compared to method blanks due to possible production of hydrogen peroxide during sampling [Figure 3.18, Figure 3.19, Table 3.8, and Table 3.9]. In February, care was taken to isolate samples and stock solutions from sunlight, and hydrogen peroxide was of the same order of magnitude as the standard error [Figure 3.20 and Table 3.10].

3.4 Conclusions

The structure of Halls Brook Holding Area was controlled by the salt concentration (indicated by conductivity). In summer and fall the water column was strongly stratified and could be divided into three distinct layers. The epilimnion was the oxic surface mixed layer characterized by low conductivity and DOC concentration. The metalimnion was the anoxic layer below the epilimnion of increasing conductivity with depth. It typically had a steep conductivity gradient just below the epilimnion. Ferrous iron concentrations also rose rapidly in the metalimnion as E_H values fall. The metalimnion also appeared to contain a peak of photosynthetic activity. The hypolimnion was the anoxic bottom layer of relatively constant, high conductivity, characterized by high DOC and ferrous iron concentrations. In winter, flow though the lake generally increased and temperature destabilized the stratification, resulting in greater vertical mixing and a gradual washout of the isolated hypolimnion. However, due to constant inputs of high density groundwater, the lake never became well mixed over the entire water column. In late spring, as surface flows decreased and temperature profiles reinforced stratification, stratification of the water column increased.

High and significant (compared to method blanks) concentrations of hydrogen peroxide were observed in the epilimnion in August, September and October. These concentrations (as high as 30 - 60 μM in October) were higher than previously reported in the literature. These concentrations may be too high to be due entirely to abiotic photochemical production. Concentrations increased with depth on all dates despite constant conductivity, dissolved oxygen, and redox potential in the epilimnion on these dates. This suggests that the dominant source of hydrogen peroxide in HBHA may lie below the surface, as opposed to an abiotic photochemical source, which would be localized at the surface. Concentrations of hydrogen peroxide in HBHA were not significant compared to method blanks in the months both before (May) and after (December - February) the period in which high concentrations were observed. The maximum observed concentration also increased from August to

October, even as sunlight intensity was decreasing over this period. This lack of a seasonal relationship between light intensity and measured concentrations indicated that incident sunlight was not the only important variable for hydrogen peroxide production in HBHA. On the other hand, the increase in concentrations from morning to afternoon in August suggested that there may be a diurnal cycle with production during the day, that is, a light-associated source. A source which could be consistent with all of the data is a seasonally variable (present in late summer and fall only), light-dependent source localized just above the pycnocline. Photosynthetic microorganisms could fit this description if they produced large amounts of hydrogen peroxide in sunlight and become dominant in the lake ecosystem in late summer and fall. This possibility will be considered further in Chapter Four.

3.5 References

Bader, H., Sturzenegger, V. and Hoigné, J., 1988. Photometric method for the determination of low concentrations of hydrogen peroxide by the peroxidase catalyzed oxidation of N, N-diethyl-p-phenylenediamine (DPD). *Wat. Res.*, 22(9): 1109-1115.

Cooper, W. J. and Lean, D. R. S., 1989. Hydrogen-peroxide concentration in a northern lake - photochemical formation and diel variability. *Environ. Sci. Technol.*, **23**(11): 1425-1428.

Cooper, W. J., Lean, D. R. S. and Carey, J. H., 1989. Spatial and temporal patterns of hydrogen-peroxide in lake waters. *Can. J. Fish. Aquat. Sci.*, **46**(7): 1227-1231.

Diez, S. and Gschwend, P. M., 1996. Unpublished results.

Herrmann, R., 1996. The Daily Changing Pattern of Hydrogen Peroxide in New Zealand Surface Waters. *Environ. Toxicol. Chem.*, **15**(5): 652-662.

McNeill, K. and Gschwend, P. M., 1998. Unpublished results.

Roux Associates, Inc. Environmental Science & Engineering, Inc.; PTI Environmental Services "Ground-Water/Surface-Water Investigation Plan. Phase 2 Remedial Investigation Draft Report. Volume III of III, Appendix D," Industriplex Site Remedial Trust, 1992.

Scully, N. M., Lean, D. R. S., McQueen, D. J. and Cooper, W. J., 1995. Photochemical formation of hydrogen peroxide in lakes: effects of dissolved organic carbon and ultraviolet radiation. *Can. J. Fish. Aquat. Sci.*, **52**: 2675-2681.

Scully, N. M. and Vincent, W. F., 1997. Hydrogen peroxide: A natural tracer of stratification and mixing processes in subarctic lakes. *Arch. Hydrobiol.*, **139**(1): 1-15.

Shtamm, E. V., Purmal, A. P. and Skurlatov, Y. I., 1991. The role of hydrogen peroxide in natural aquatic media. *Rus. Chem. Rev.*, **60**(11): 1228-1248.

Sinel'nikov, 1971. *Gidrobiol. Zh.*, **7**: 115. (as reported in Shtamm et al., 1991)

Venkateswaran, K., Shimada, A., Maruyama, A., Higashihara, T., Sakou, H. and Maruyama, T., 1993. Microbial characteristics of Palau Jellyfish Lake. *Canadian Journal Of Microbiology*, **39**(5): 506-512.

Voelker, B. M. and Sulzberger, B., 1996. Effects of fulvic acid on Fe(II) oxidation by hydrogen peroxide. *Environ. Sci. Technol.*, 30(4): 1106-1114.

Wick, L. Y. and Gschwend, P. M., 1998. Source and chemodynamic behavior of diphenyl sulfone and *ortho*- and *para*-hydroxybiphenyl in a small lake receiving discharges from an adjacent Superfund site. *Environ. Sci. Technol.*, **32**: 1319-1328.

Wick, L. Y., McNeill, K., Diez, S., Southworth, B. and Gschwend, P.M., 1996-1998, Unpublished results.

3.6 Figures and Tables

Latitude		42°30'
Longitude		71°
Volume		39,000 m^3
Area	surface	17,400 m^2
	1.5 m	11,600 m^2
	3 m	5990 m^2
	4 m	2250 m^2
Maximum depth		4.9 m
Mean depth		2.2 m

Table 3.1. Physical characteristics of HBHA (Roux Associates, 1992).

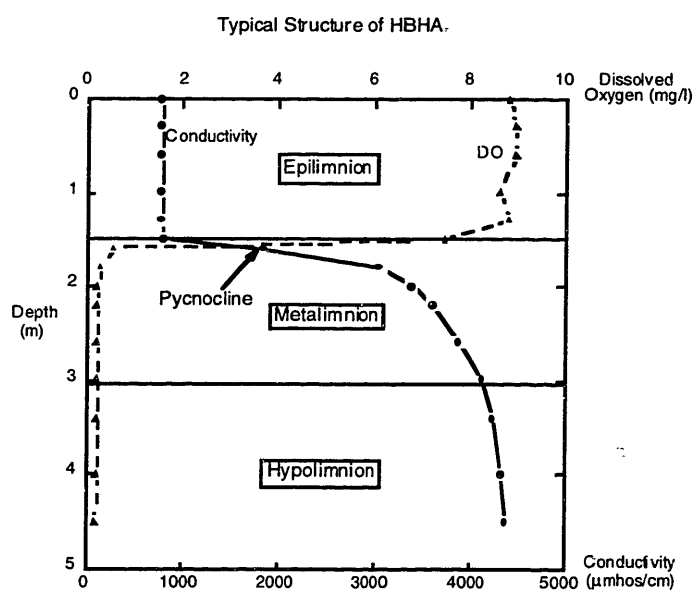

Figure 3.1. Typical structure of HBHA (10/22/97). The epilimnion is the layer of constant low conductivity and high DO concentration. The pycnocline is the plane at the depth of maximum conductivity (density) gradient. It was typically immediately below the epilimnion in HBHA. The metalimnion is the layer of low DO and transitional conductivity. The hypolimnion is the layer of relatively constant conductivity (defined here as ± 5%).

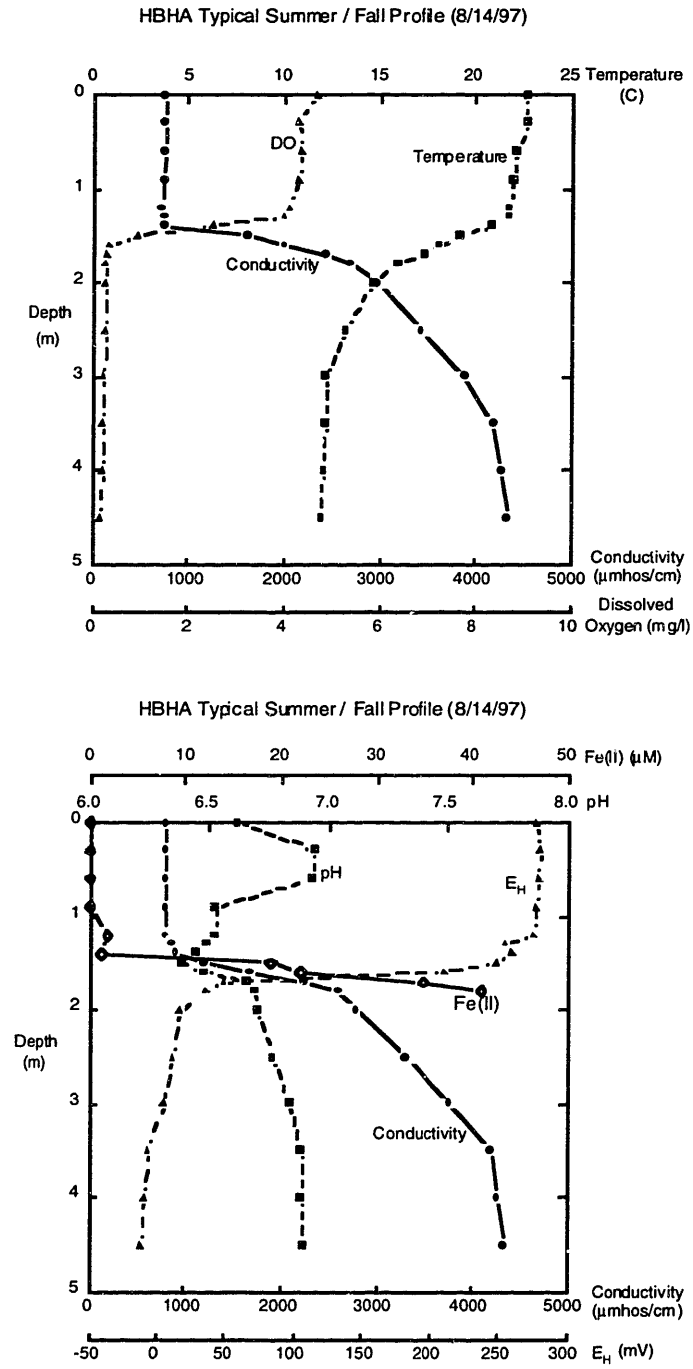

Figure 3.2. Typical summer depth profiles in HBHA. The epilimnion is the surface layer of high dissolved oxygen concentrations, temperature, and redox potential. Below the pycnocline, dissolved oxygen drops steeply, along with redox potential and temperature, and conductivity rises to a maximum of approximately 4500 µmho cm^{-1}. The ferrous iron profile rises rapidly with depth through the metalimnion.

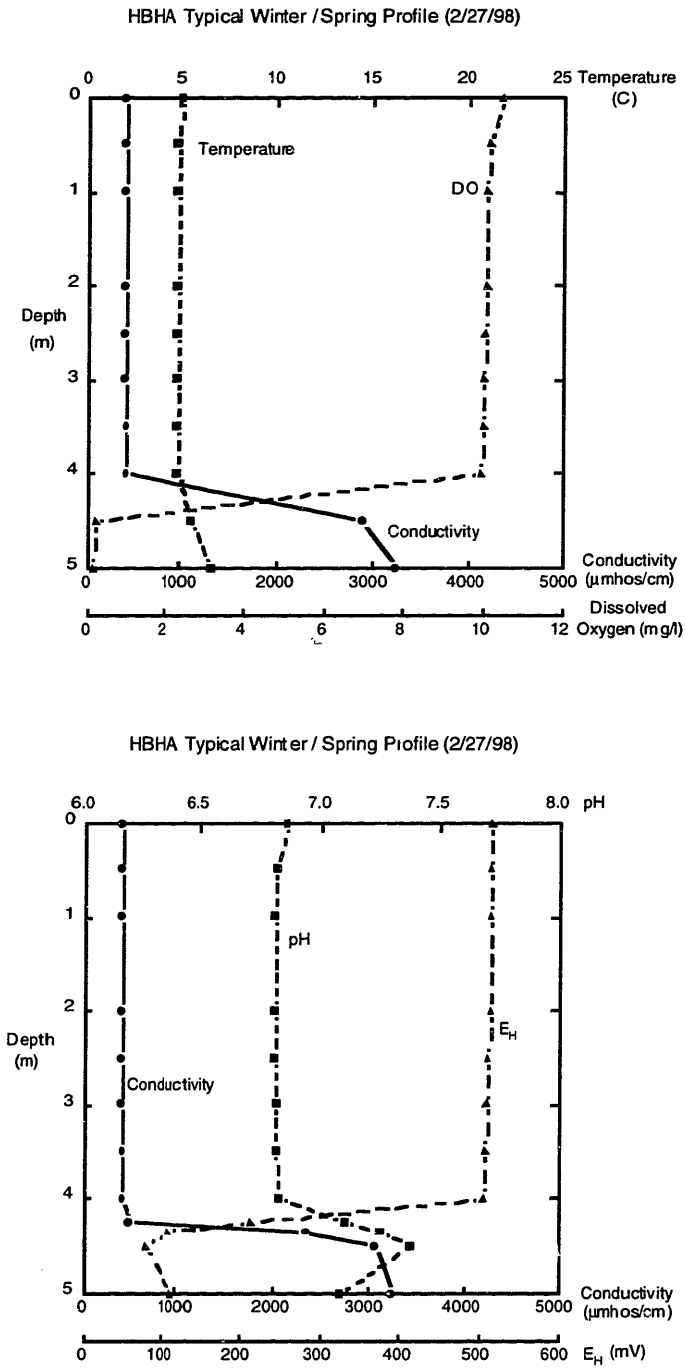

Figure 3.3. Typical winter depth profiles in HBHA. In winter and spring, most of the lake volume is epilimnion, with a low constant conductivity and high redox potential and dissolved oxygen concentration. A small pool of high conductivity, low redox potential, low dissolved oxygen concentration water formed by groundwater inflow remains at the bottom of the lake.

Date	*Total inflow* m^3/*day*	*Cond. of Inflow* *	*Epilimnion Conductivity*	*Total Salt* *µmho/cm*
7/16/97	2500	340	770	77
8/14/97	3720	353	739-764	79
11/20/97	4060		490-500	54
12/17/97	3790	462	650-660	61
1/27/98	25000	412	600	33
2/27/98	45000	421	400	17
3/10/98	120000	198	220	10
4/21/98	23200	357	470-480	24
6/10/98	11500		500	26

* Average conductivity of the surface inflows weighed by the flow rates.

Table 3.2. Inflows, conductivity and total salt in HBHA. "Total salt" is the integral over z of C(z)A(z) dz, where C is the conductivity and A is the area as a function of depth. In general, the total salt is high when the epilimnion conductivity is also high and the total inflow is low. The lowest values for total salt occurred after several days of rain when the inflow was very high (120,000 m^3/day).

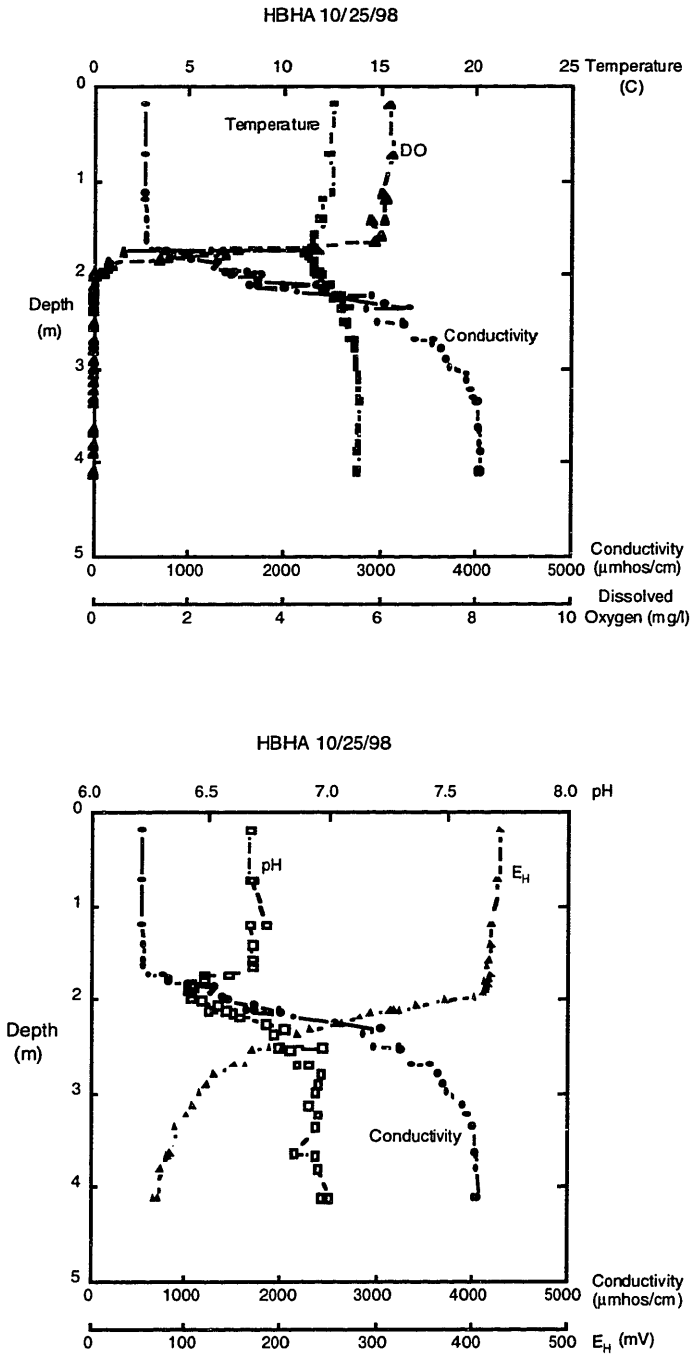

Figure 3.4. Depth profiles in HBHA on October 25, 1998. The profiles are similar to profiles measured during fall of 1997.

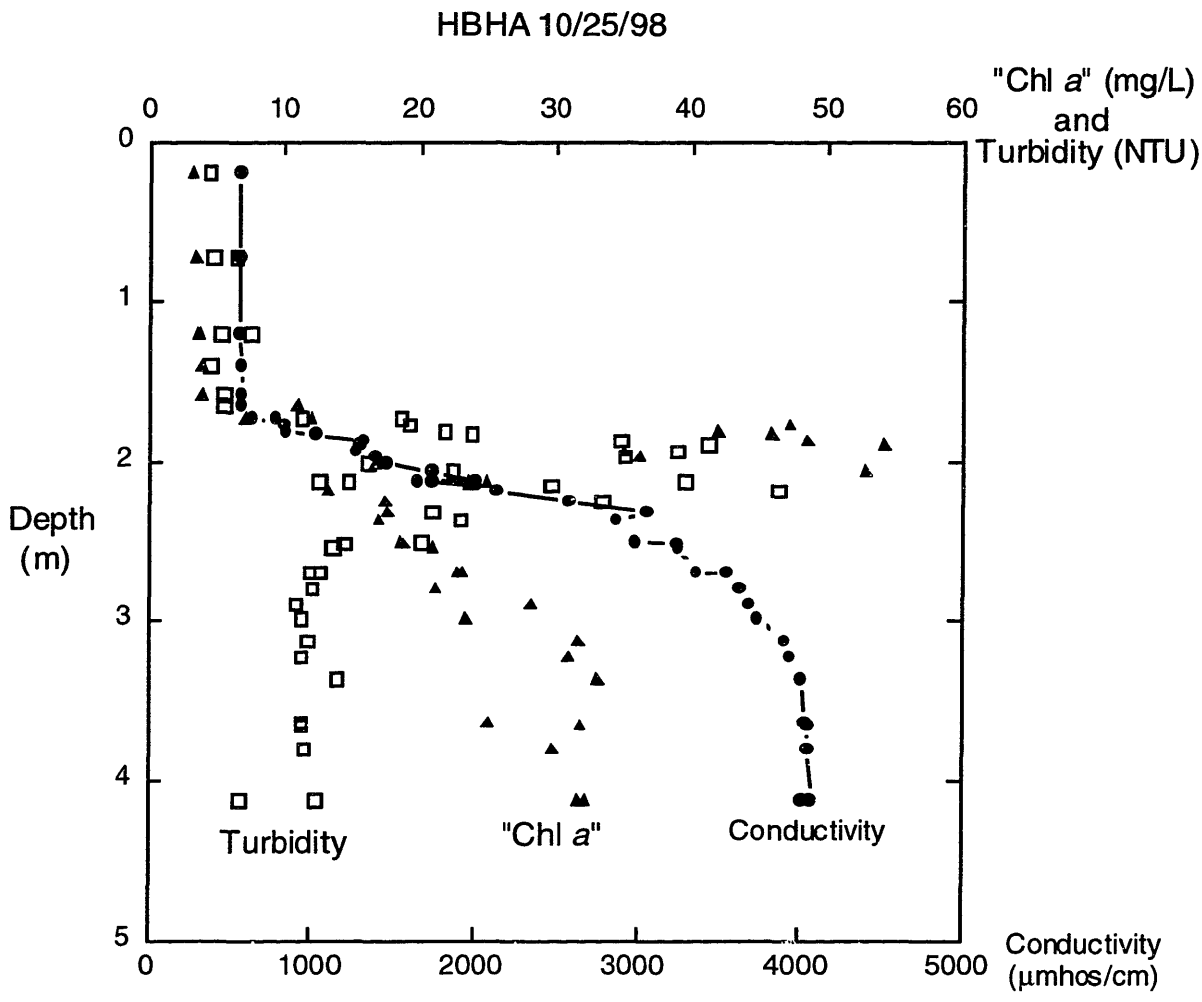

Figure 3.5. Depth profiles of conductivity, turbidity and "chl *a*" in HBHA on October 25, 1998. The peak of both chlorophyll *a* and turbidity in a half meter layer just below the epilimnion suggests that a peak of photosynthetic activity and microbial numbers exists near the pycnocline in HBHA. Much of this peak occurs within a depth interval in which the E_H is still relatively high (> 300 mV) and the oxygen concentration is less than 1 mg/L but non-zero (see Figure 3.4). "Chl a" may remain relatively high in the hypolimnion compared to turbidity due to an interfering fluorophore.

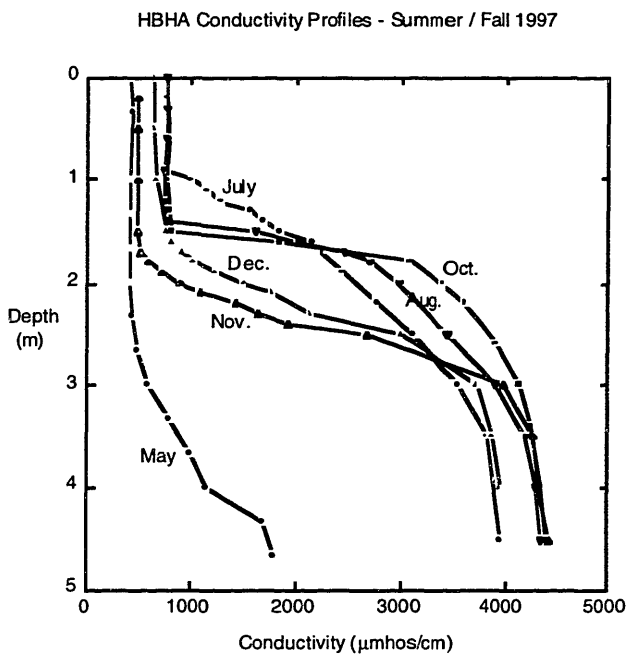

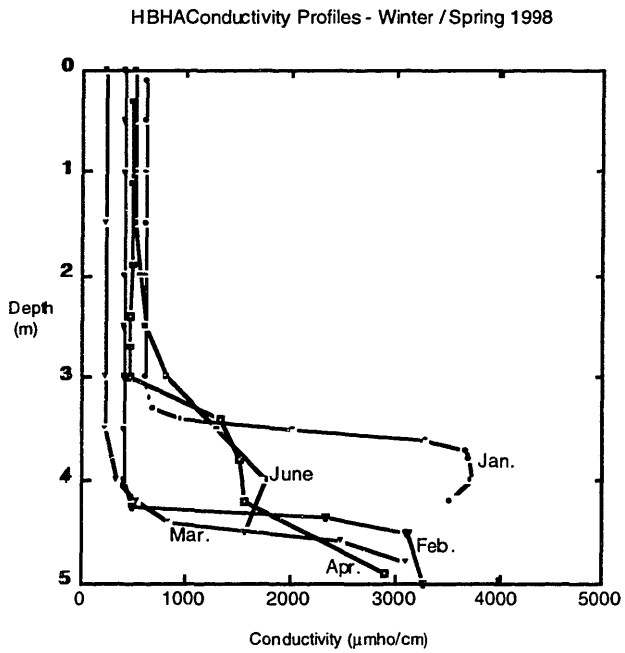

Figure 3.6. Seasonal changes in conductivity vs. depth profiles in HBHA.

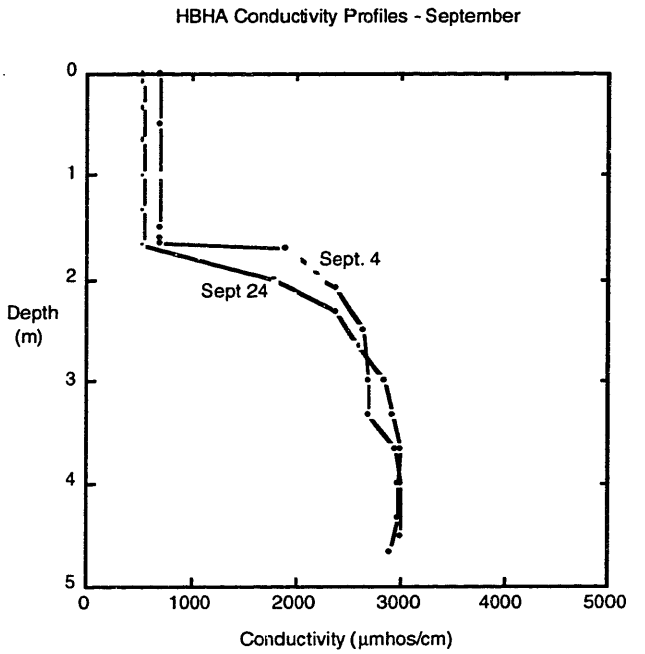

Figure 3.7. September 1997 conductivity vs. depth profiles in HBHA.

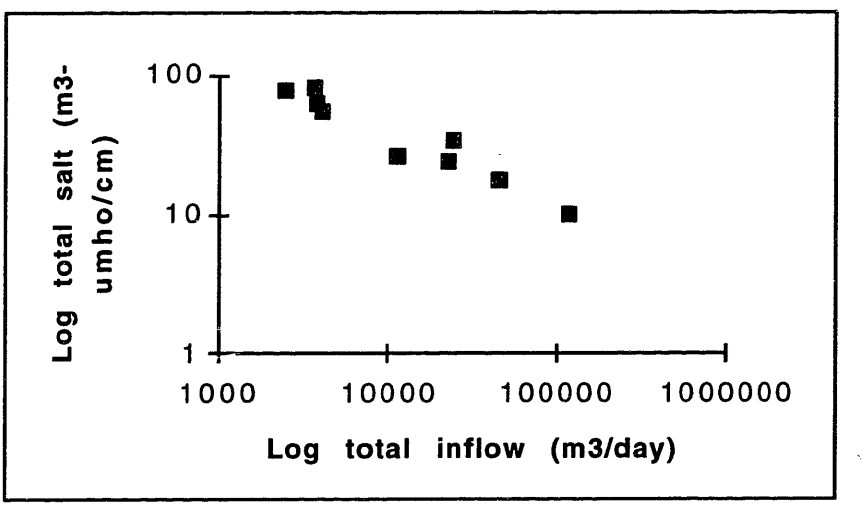

Figure 3.8. Relationship between the log of the total inflow to HBHA and the "total salt" in HBHA. Data from Table 3.2.

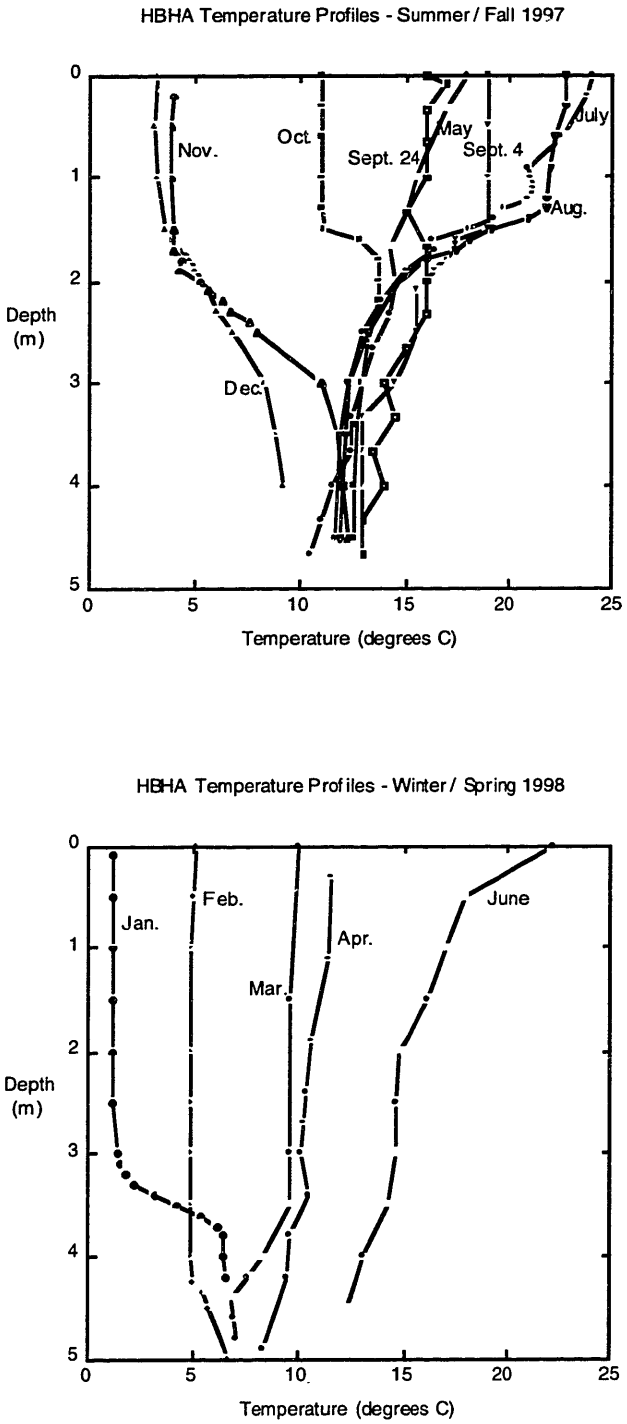

Figure 3.9. Seasonal changes in temperature vs. depth profiles in HBHA.

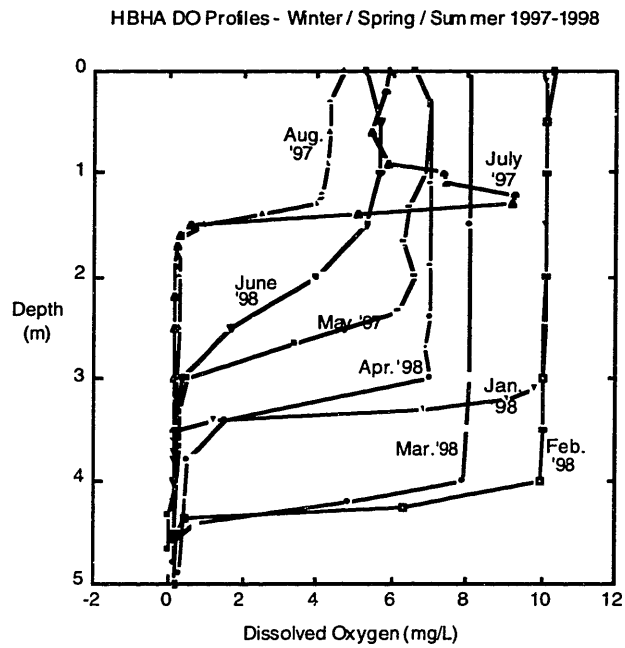

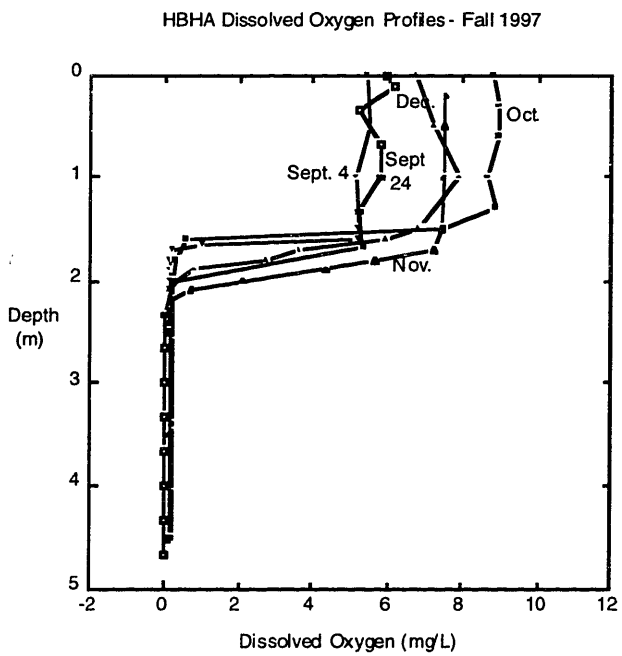

Figure 3.10. Seasonal changes in dissolved oxygen concentration vs. depth profiles in HBHA.

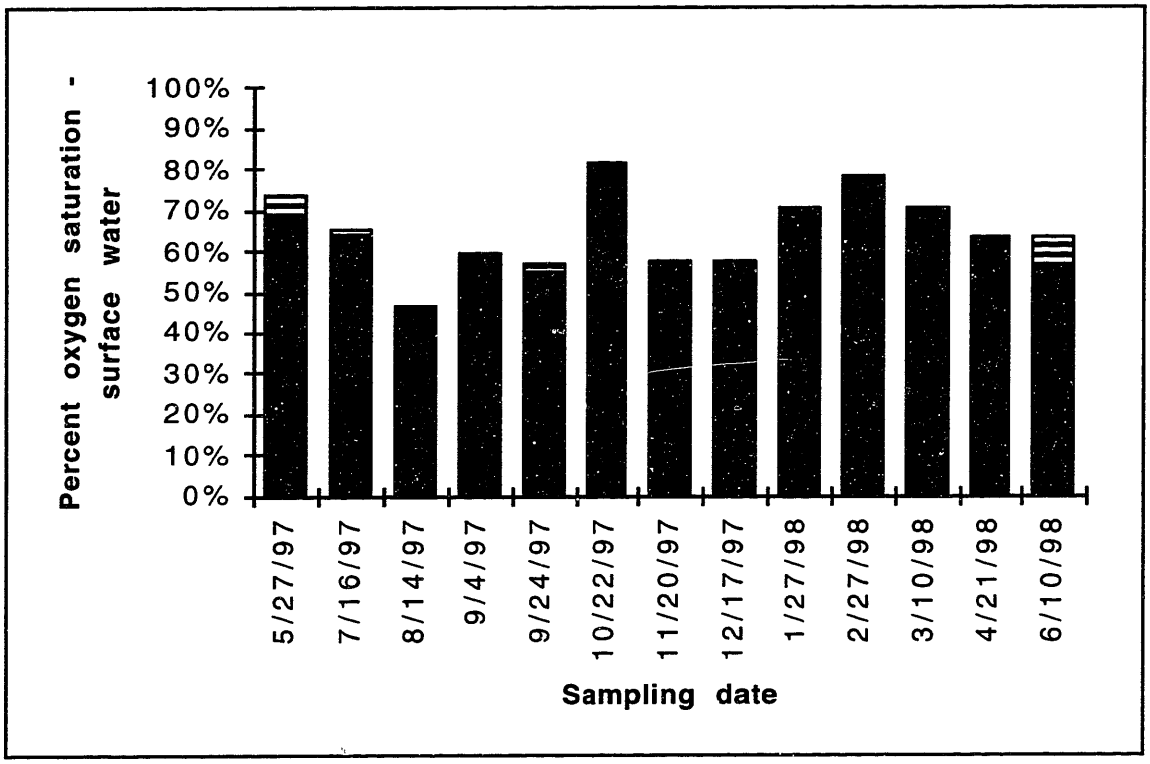

Figure 3.11. The percent oxygen saturation in the surface waters of HBHA. Horizontal bars represent the range of values for each date.

7/16/97

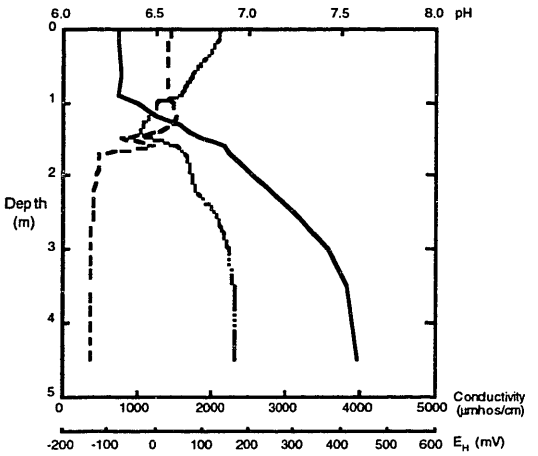

8/14/97

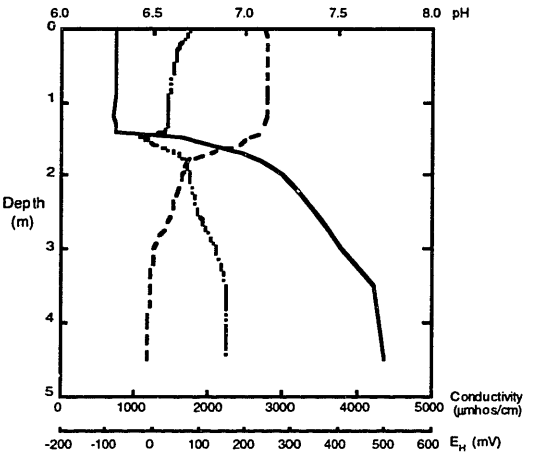

10/22/97

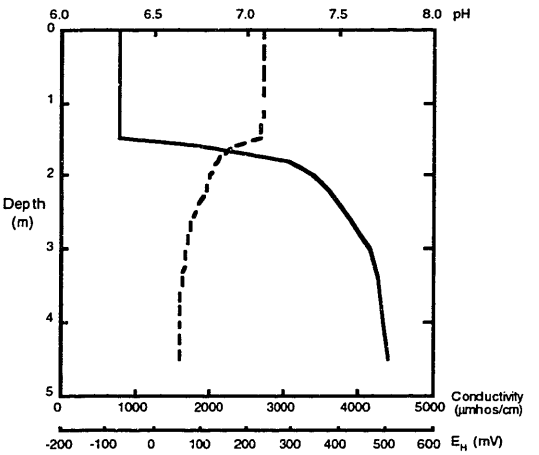

12/17/97

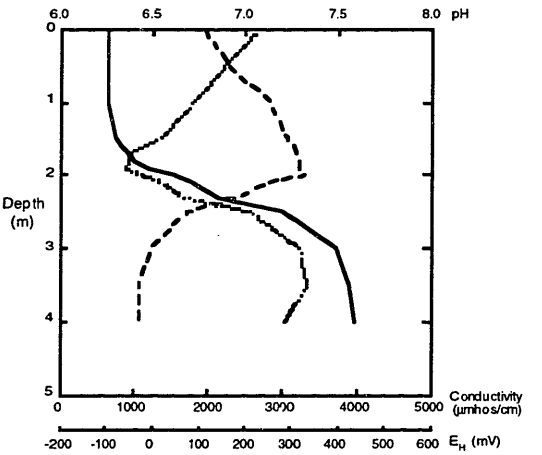

1/27/98

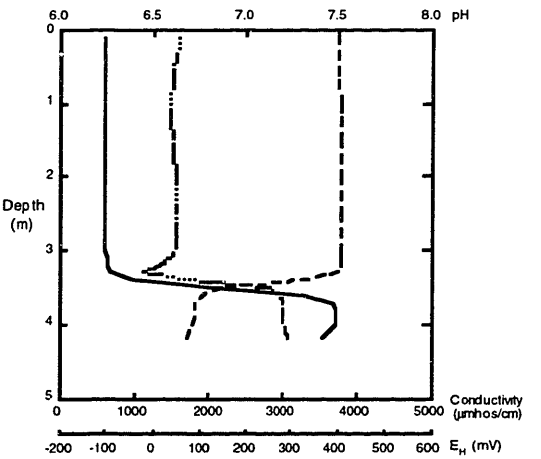

2/27/98

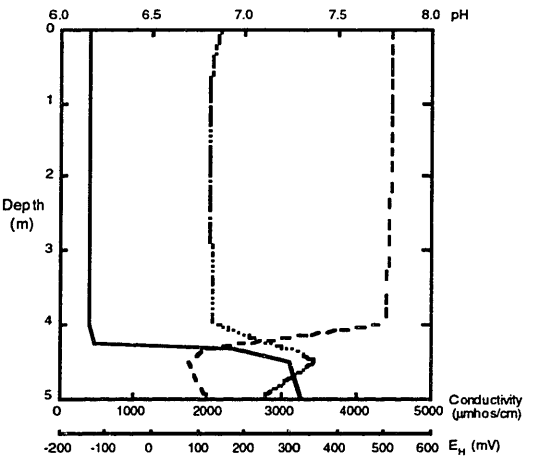

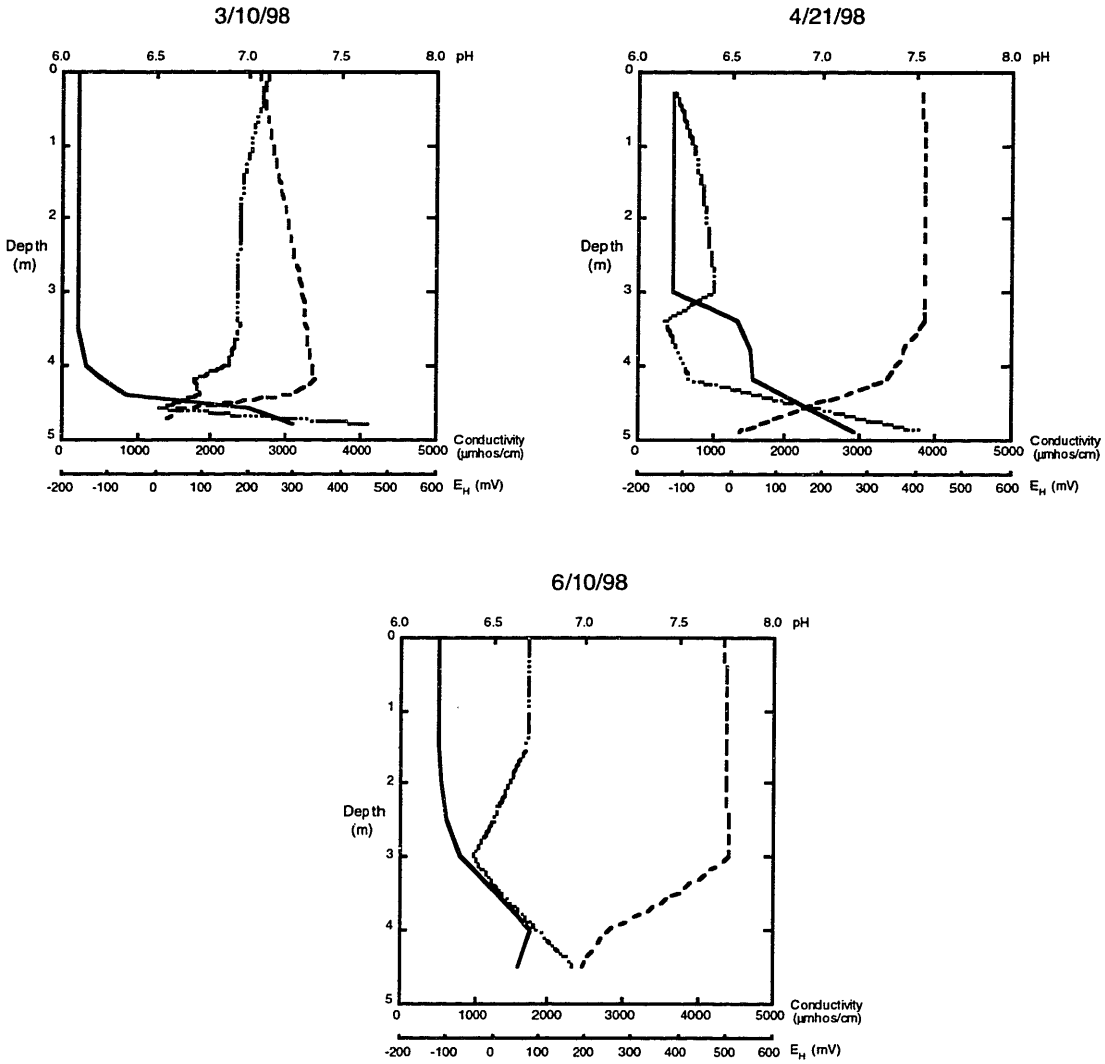

Figure 3.12. Seasonal changes in pH and E_H Profiles. The solid lines are conductivity, the dashed lines are E_H and the dotted lines are pH.

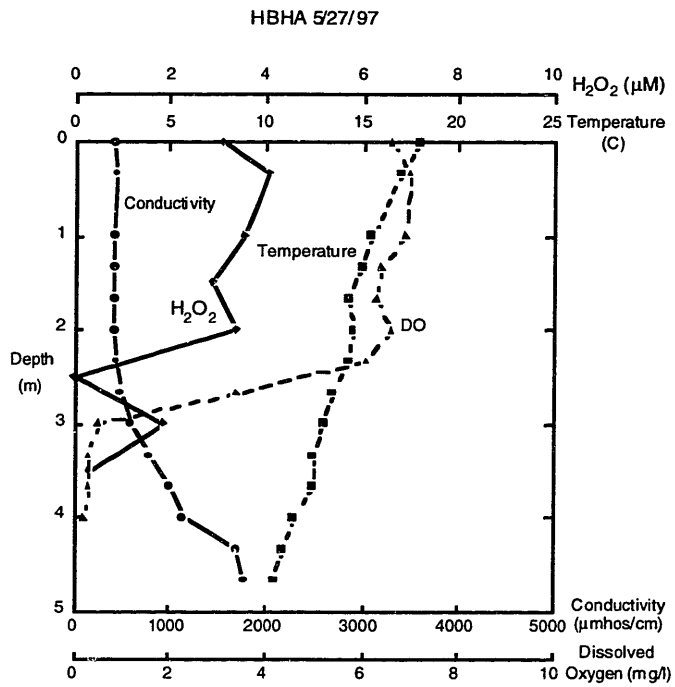

Figure 3.13. May 27, 1997 depth profiles. Hydrogen peroxide was analyzed in the field between noon and 6 p.m. while samples and the spectrometer were exposed to sunlight.

Depth (m)	*[H_2O_2) (µM)*	*Std. Error*
0	3.1	1.5
0.3	4.1	0.6
1	3.6	1.3
1.5	2.9	0.9
2	3.4	1.4
2.5	-0.69	1.3
3	1.9	0.4
3.5	0.3	0.3

Table 3.3. May 27, 1997 hydrogen peroxide data.

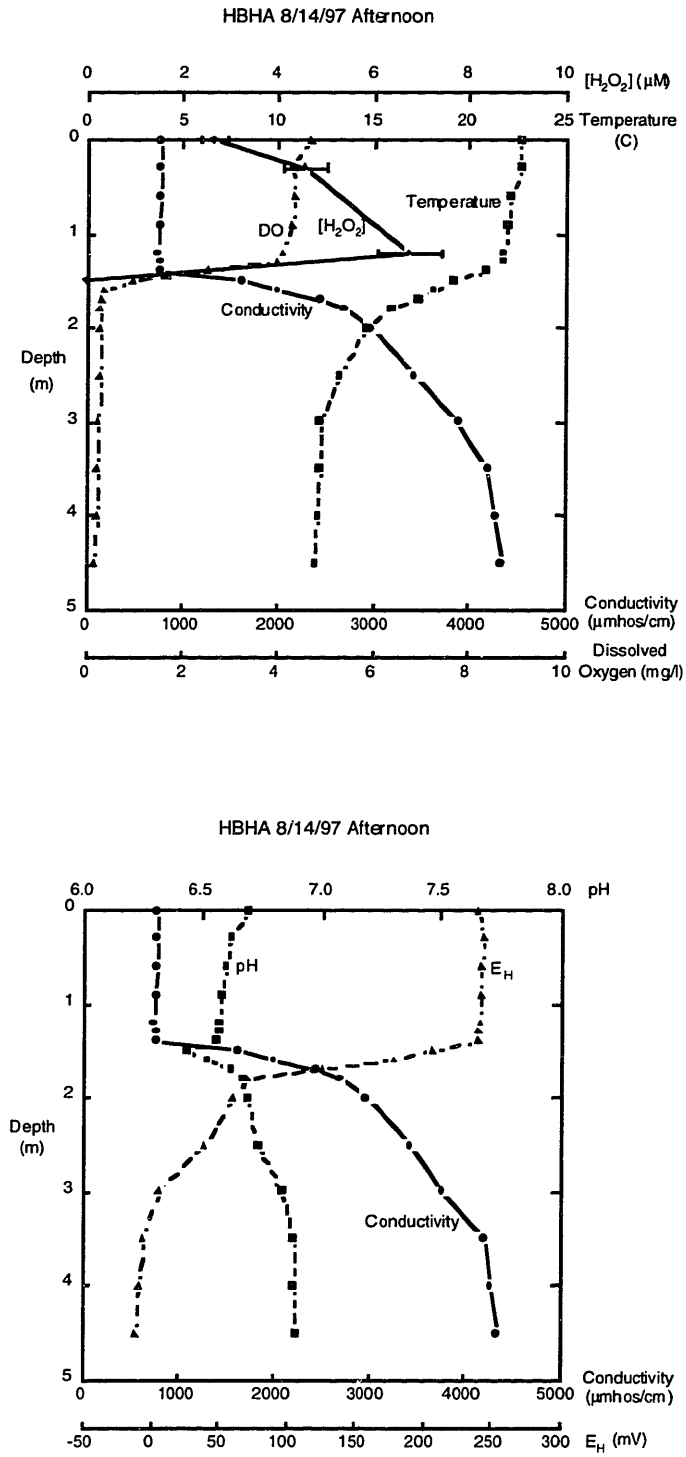

Figure 3.14. August 14, 1997 afternoon depth profiles. Samples were collected for hydrogen peroxide analysis between 4 and 5 p.m.

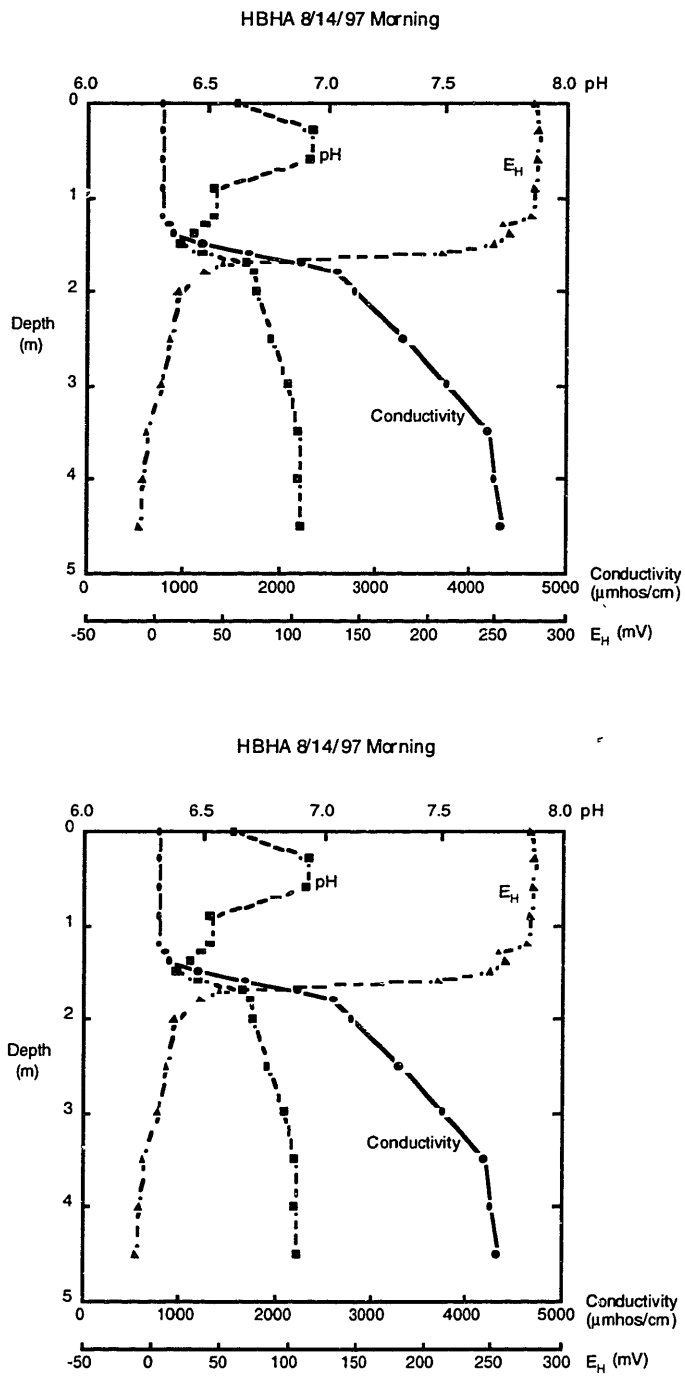

Figure 3.15. August 14, 1997 morning depth profiles. Samples were collected for hydrogen peroxide analysis between 6 and 7 a.m.

Depth (m)	*$[H_2O_2]$ (μM)*	*Std. Error*	*Fe(II) (μM)*
0	0.06	0.68	<0.5
0.6	---	---	<0.5
1.2	0.67	0.07	1.9
1.4	---	---	1.3
1.5	---	---	19
1.6	***	***	22
1.7	---	---	35
1.8	---	---	41

Table 3.4. August 14, 1997 morning hydrogen peroxide and Fe^{2+} data. *** = no detectable hydrogen peroxide, pink color due to Fe^{2+}-bipyridine complexation, and rapid degradation of standard additions of hydrogen peroxide stock solution.

Depth (m)	*$[H_2O_2]$ (μM)*	*Std. Error*
0	2.66	0.27
0.3	4.58	0.46
1.2	6.76	0.68
1.5	***	***

Table 3.5. August 14, 1997 afternoon hydrogen peroxide data. *** = no detectable hydrogen peroxide, pink color due to Fe^{2+}-bipyridine complexation, and rapid degradation of standard additions of hydrogen peroxide stock solution.

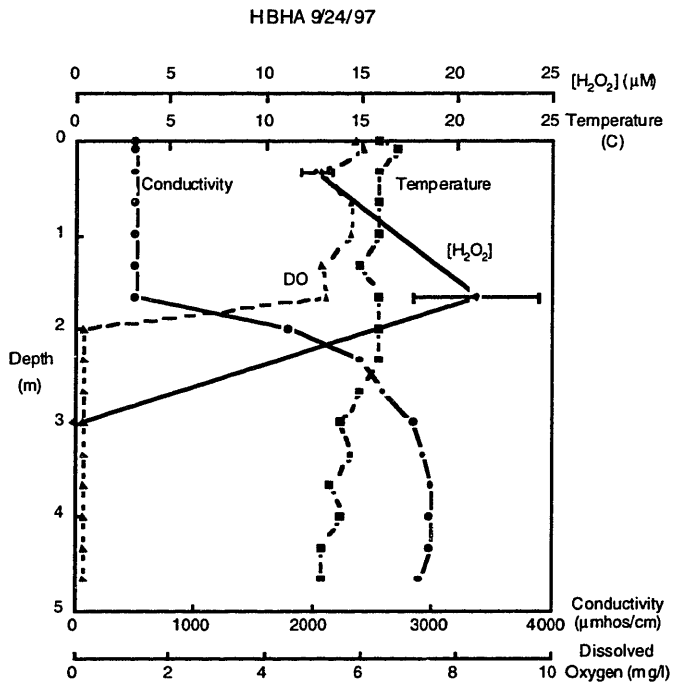

Figure 3.16. September 24, 1997 depth profiles. Samples were collected for hydrogen peroxide analysis between 1 and 2 PM.

Depth (m)	*$[H_2O_2]$ (µM)*	*Std Error*	*$[H_2O_2]$ (µM) Lit. Slope*	*Std. Error Lit Slope*
0.3	13.9	0.7	12.3	0.6
1.7	23.7	1.3	18.6	2.2
1.8	***			

Table 3.6. September 24, 1997 hydrogen peroxide data. Column 2 shows the calculated hydrogen peroxide concentrations using the best fit slope and intercept of each standard addition curve. Column 4 shows the calculated hydrogen peroxide concentrations using the literature value for the slope (21,000 M^{-1} cm^{-1}).

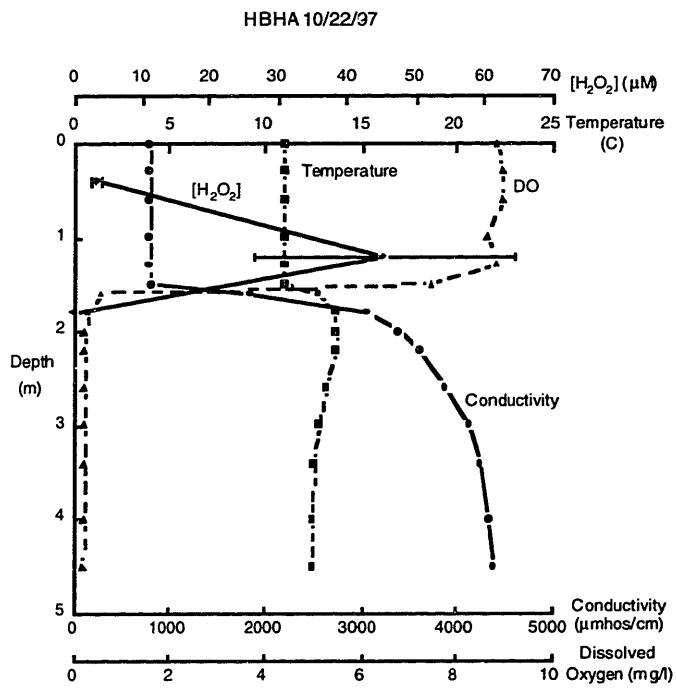

Figure 3.17. October 22, 1997 depth profiles. Samples were collected for hydrogen peroxide analysis between 1 and 2 PM.

Depth (m)	*$[H_2O_2]$ (μM)*	*Std Error*	*$[H_2O_2]$ (μM) Lit. Slope*
0.4	3.4	0.65	3.4
1.2	59	5	32
1.8	***		

Table 3.7. October 22, 1997 hydrogen peroxide data. Column 2 shows the calculated hydrogen peroxide concentrations using the best fit slope and intercept of each standard addition curve. Column 4 shows the calculated hydrogen peroxide concentrations using the literature value for the slope (21,000 M^{-1} cm^{-1}).

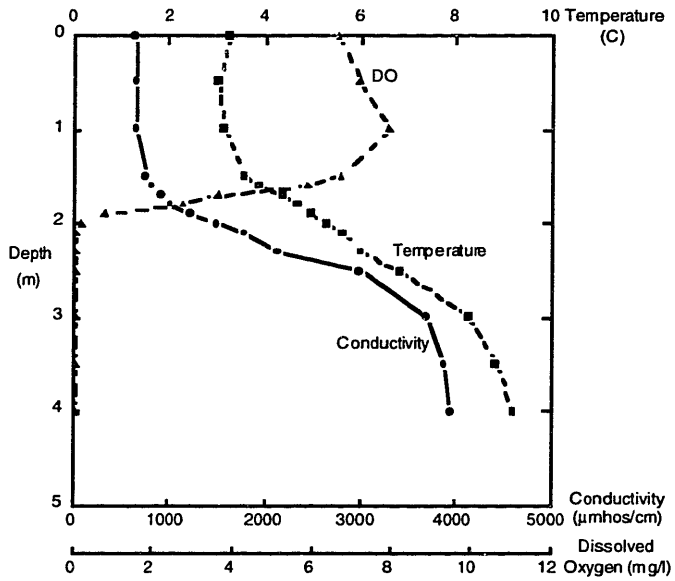

Figure 3.18. December 17, 1997 depth profiles. Samples were collected for hydrogen peroxide analysis between 2 and 3 PM. The southern half of the lake, including the sampling station, was covered by a thin sheet of opaque ice (~ 3 cm).

Depth (m)	*$[H_2O_2]$ (µM)*	*Std. Error*	*Fe(II)*
0.5	0.55	0.17	no
0.5	0.50	0.08	no
1	0.79	0.09	no
1	0.67	0.05	no
1.5	0.66	0.08	no
1.5	0.66	0.08	no
1.7	0.58	0.06	no
1.7	0.66	0.09	no
1.8	0.62	0.23	no
1.9	0.60	0.20	no
2	1.18	0.88	no
2.1	---	---	yes
HB	0.83	0.19	no
ND	1.07	0.21	no

Table 3.8. December 17, 1997 hydrogen peroxide and Fe^{2+} data.

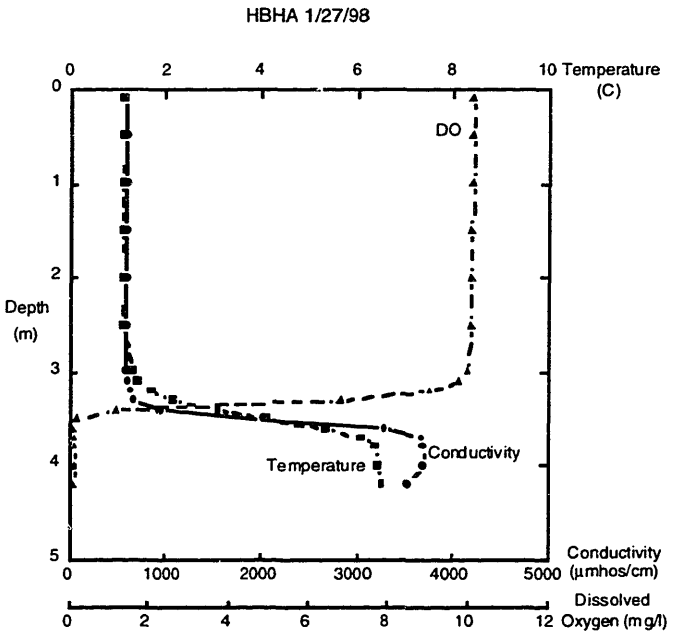

Figure 3.19. January 27, 1998 depth profiles. Samples were collected for hydrogen peroxide analysis between 12 and 2 PM. The southern half of the lake, including the sampling station, was covered by about 6 - 8 cm of opaque ice.

Depth (m)	*$[H_2O_2]$ (µM)*	*Std. Error*	*Fe(II)*
0.6	1.05	0.28	no
1.5	0.40	0.07	no
2.5	0.58	0.14	no
3	0.89	0.11	no
3	0.38	0.16	no
3.1	0.54	0.57	trace
3.3	0.99	0.13	yes
3.4	- - -	- - -	yes
ND	0.66	0.06	no
HB	0.76	0.10	no

Table 3.9. January 27, 1998 hydrogen peroxide and Fe^{2+} data.

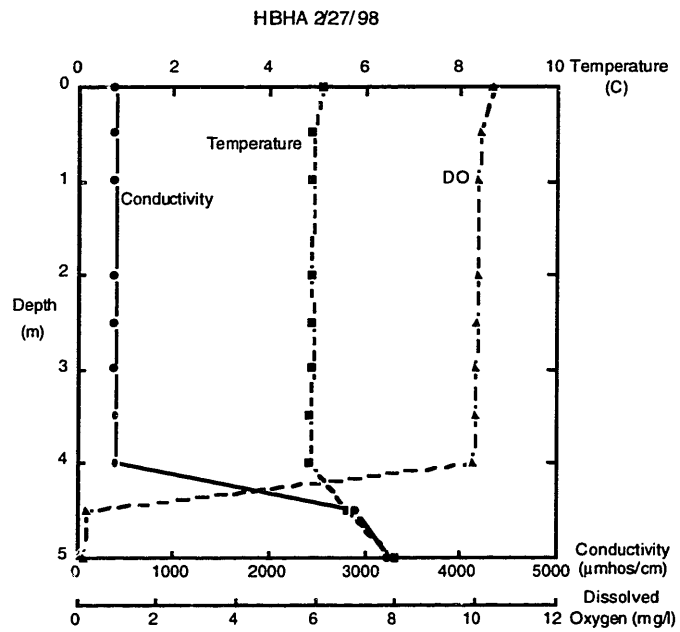

Figure 3.20. February 27, 1998 depth profiles. Samples were collected for hydrogen peroxide analysis between 1 and 2 PM.

Depth (m)	*$[H_2O_2]$ (µM)*	*Std. Error*	*Fe(II)*
0.5	---	---	no
1	0.27	0.25	no
2	0.14	0.12	no
3	0.18	0.13	no
4	0.16	0.26	no
4.25	---	---	yes
ND	0.04	0.12	no
HB	0.18	0.18	no

Table 3.10. February 27, 1998 hydrogen peroxide and Fe^{2+} data.

4. Calculations and Modeling

4.1 Introduction

In order to determine whether observed hydrogen peroxide concentrations in the Halls Brook Holding Area can be explained by processes known to affect hydrogen peroxide in natural waters, a modeling study was carried out. As covered in Chapter One, the major processes thought to control hydrogen peroxide in natural fresh waters are abiotic photochemical production, biological decay, and physical mixing processes. Our degradation results (see Table 3.4) showed that the decay process in epilimnion samples in February was probably abiotic, but also first order with respect to H_2O_2 and similar in magnitude to rates observed for biological degradation in the literature (Cooper et al., 1994 and references therein). Therefore, we replaced pseudo-first order biological decay with the observed first order abiotic decay rate in our model. An additional process that must occur in HBHA is degradation in the anoxic layer below the epilimnion. Since hydrogen peroxide could never be detected below the oxic epilimnion and standard additions of stock H_2O_2 were rapidly degraded in samples from this layer (see section 3.3.3), we assumed a large enough sink below the pycnocline in the model to degrade essentially all of the hydrogen peroxide. Thus, the model includes (1) vertical mixing (2) a photochemical input, (3) a first-order decay, and (4) a rapid decay below the epilimnion. Since we suspect that there must have been an additional source of hydrogen peroxide in late summer and fall, estimates that result in the highest likely concentrations of H_2O_2 in HBHA were used. If the modeled concentrations are still substantially lower than measured concentrations, we can conclude that there is indeed another dominant source of H_2O_2 in HBHA.

4.1.1 CHEMSEE

The modeling program used in this study is known as CHEMSEE (Ulrich, 1994). It is a 1-dimensional vertical model used to describe the behavior of chemicals in lakes

by using mass balance principles. It assumes that the modeled water body is horizontally well-mixed, and divides the lake into a user-defined number of well-mixed horizontal boxes. The physical system is defined by user-entered depth, the area at defined depths, inflow and outflow rates, and vertical diffusion coefficients. Chemical variables are defined along with their initial values. Processes are defined that affect the chemical variables along with their rate constants. CHEMSEE interpolates between the user-entered values with depth to get values for each box of the model. It also interpolates between values defined at different times. The number of well-mixed boxes used by the model, and the amount of relative change in the variables allowable per time step are also set by the user. Thus the user can input all of the known physical parameters and processes affecting a given chemical in a lake, allow the model to run over a given period of time, and compare the resulting profiles of the chemical variable to measured concentrations of the chemical in a lake.

4.1.2 Model Processes

As we had the most complete data set for the August 14, 1997 sampling date, we chose to model this data. In some cases, we had to use data from other dates in our model, and these cases will be discussed in more detail. Abiotic photochemical production of hydrogen peroxide can be estimated using literature values for the apparent quantum yield, solar radiation data, and lakewater absorbance in the epilimnion. Apparent quantum yields and formation efficiencies in solar spectrum light for hydrogen peroxide formation have been determined for a variety of natural waters (Cooper et al., 1988; Scully, et al. 1995). For this study we selected the highest values for a surface freshwater reported (Cooper et al., 1988) [Table 4.1]. Solar radiation data for midsummer (late July) at 40 degrees latitude was used - this should overestimate incident sunlight by less than 10% for the August date. Lakewater absorptivity was not measured on Aug. 14. However, the absorptivity of HBHA epilimnion water is similar for several dates throughout the year, and does not appear to undergo significant seasonal change. Absorptivity data from epilimnion samples collected on Oct. 22,

when the conductivity profile was similar to that observed in August, were used in the model [Table 4.1]. Our estimated production rate, then, was a high-end estimate, even although it is always possible that HBHA dissolved organic carbon is unusually efficient at producing H_2O_2.

The H_2O_2 sink in the epilimnion can be estimated based on measured decay rates of hydrogen peroxide in HBHA water. Decay rates were not measured on the August 14 sampling date, so the February decay rate must be used in our model [Table 2.4]. The actual decay rate in August was most likely larger than the February decay rate due to both the higher water temperature and probable increased biological activity. This, again, should result in an overestimate of hydrogen peroxide concentrations in the model.

Vertical mixing coefficients can be calculated using conductivity and temperature as tracers. In the epilimnion, temperature can be used as a tracer. As the air temperature warms, heat is added to the lake and mixes down into the water column via turbulent mixing. Using the two temperature profiles measured in HBHA on Aug. 14, 1997, the turbulent mixing coefficients required to get from the morning profile to the afternoon profile can be calculated and used in the model (Schnoor, 1996). Heat does not mix across the pycnocline quickly enough to quantify mixing coefficients in this way. Conductivity can be used as a tracer for mixing processes for the rest of the water column instead. Conductivity was assumed to be conservative; the lake was assumed to be horizontally well-mixed and at steady state with respect to inflows and outflows. A groundwater input of conductivity was also required for this calculation, which was estimated by mass balance of both water and conductivity.

4.2 Calculations

4.2.1 Hydrogen Peroxide Input Function

A photochemical input function for hydrogen peroxide in HBHA, PI, was calculated according to the equation:

$$PI = \sum_{\lambda} I(\lambda, t, z)\,\Phi(\lambda) \qquad (1)$$

where I is light intensity as a function of wavelength, λ, time, t, and depth, z, and Φ is the apparent quantum yield of hydrogen peroxide production as a function of wavelength. The apparent quantum yield of hydrogen peroxide as a function of wavelength has been reported in the literature for a number of different water samples. Cooper et al. (1988) determined the apparent quantum yields as a function of wavelength for two lake and four groundwater samples. These values result in calculated hydrogen peroxide production rates within about a factor of five of each other. The values for the higher quantum yield lake were chosen for use in our calculation [Table 4.1].

Light intensity can be further broken down as follows:

$$I(\lambda, t, z_n \text{ to } z_{n+1}) = f(t)Z(\lambda)\left(\left[1-10^{-\alpha_D(\lambda)z_{n+1}}\right]-\left[1-10^{-\alpha_D(\lambda)z_n}\right]\right) \qquad (2)$$

where $Z(\lambda)$ is the light intensity at noon as a function of wavelength. $Z(\lambda)$ values have been tabulated for both noon and for a 24 hour average for a midsummer day (late July; solar inclination of 20°) at sea level at 40°N latitude under clear skies (Zepp and Cline, 1977; Leifer, 1988; Schwarzenbach et al., 1993) [Table 4.1]. The noon values were used for this calculation and the 24-hour-average values were used to scale the sunlight intensity over the day as a parabolic function, $f(t) = 1-x(t-n)^2$ with the maximum value of 1 at $t = n$, where n is solar noon (12:30 PM EDT). The value of x was adjusted such that the average value of f(t) from 0 to 24 hours was equal to the ratio of Σ $Z(\lambda)(\text{noon})\Phi(\lambda)$ to Σ $Z(\lambda)(24, h)\Phi(\lambda)$ [Table 4.2]. This results in scaling of light intensity consistent with both noon and 24-hour average values.

The lakewater absorptivity, $\alpha_d(\lambda)$, was not determined for August 14 samples. However, the epilimnion lakewater absorptivity changed very little between October 1997 and February 1998 and the October 22, 1997 conductivity profile was nearly identical to the conductivity profile on August 14. So lakewater absorptivity values from October 22, 1997 were used in the calculation. Lakewater absorptivity was

constant through the epilimnion, so the average values from 5 depths in the epilimnion were used [Table 4.1].

The values z_1 and z_2 in equation 2 define the boundaries of each vertical box in HBHA. Depth intervals of 0.05 m were used. The 3rd term in equation 2, then, is the fraction of sunlight at the surface of the lake, $Z(\lambda)$, that is absorbed by a given layer of water, between depths z_1 and z_2, as a function of wavelength. Using the values in Table 4.1 and Table 4.2, equations 4.1 and 4.2 were used to calculate an input function with time steps of 1 hour and vertical boxes of 5 cm. The results were used directly in the CHEMSEE model [Table 4.3].

4.2.2 Vertical Diffusion Coefficients

4.2.2.1 Epilimnion

The vertical diffusion coefficients for the epilimnion of HBHA on Aug. 14, 1997 were calculated using temperature profiles determined at 6 AM and at 4 PM. The vertical turbulent diffusivity (E_z), was calculated from (Imboden et al., 1979):

$$E_z = \frac{-\Delta}{A_z \frac{\delta T}{\delta z}} \tag{3}$$

where A_z is the area of the lake as a function of depth, T is temperature, z is depth, and Δ is the change in the heat content with time,

$$\Delta = \int A_{z'} \frac{\delta T}{\delta t} dz' \tag{4}$$

The temperature profiles for 6 AM and 4 PM lie on top of each other below 1.5 m [Figure 4.1]. In the surface water, the temperatures at 4 PM are higher than those at 6 AM and less constant with depth. The arithmetic mean of the points measured at 6 AM between 0 and 1.45 m was calculated to get $T_1(z)$. Two linear fits though the data

points measured at 4 PM were used to find $\delta T/\delta z$ and $\delta T/\delta t$, one from 0 to 1.3 m and the other from 1.3 to 1.45 m. $\delta T/\delta z$ is $T_2(z)$ on the plot and $\delta T/\delta t$ is $(T_2(z) - T_1(z))/\Delta t$, where Δt is 10 hours. Area as a function of depth in HBHA was approximated as a linear interpolation between the known area at the surface and at 1.5 m [Table 3.1].

$$A_z, (m^2) = -387z\ (m) + 17400,\ 0 \leq z \leq 1.45 \tag{5}$$

Solving for E_z: for $0 < z < 1.3$, $E_z = 1 \pm 0.1\ cm^2/s$ and for $1.3 < z < 1.45$, $E_z \cong 0.1 \pm 0.01\ cm^2/s$. These values are at the low end of the range typical for the mixed layer of lakes ($0.1 - 10^4\ cm^2/s$ from calm to storm conditions; Schwarzenbach, 1993). This is what we would expect, since the weather was calm on August 14.

4.2.2.2 Pycnocline

The vertical turbulent diffusivity in HBHA below the epilimnion was determined using a salt balance calculation. The calculation assumes that conductivity is conservative, the conductivity profile is at steady state, and the lake is horizontally well-mixed. We also needed to estimate a value for groundwater inflow. HBHA appeared to receive at least two sources of groundwater: one was salty (conductivity > 12,000 $\mu mho\ cm^{-1}$) that entered the lake on the northeastern side, the other was fresh and probably reflected inputs all around the lake. We estimated the volumes of each groundwater source by using the following mass balance equations, assuming steady state :

$$Q_{HB} + Q_{SGW} + Q_{FGW} = Q_{OUT} \tag{6}$$

$$C_{HB}Q_{HB} + C_{SGW}Q_{SGW} + C_{FGW}Q_{FGW} = C_{OUT}Q_{OUT} \tag{7}$$

Q's are flow rates and C's are conductivities. The subscripts, HB, SGW, FGW, and OUT refer to the flow rate or conductivity of the Halls Brook inflow, the salty groundwater inflow, the fresh groundwater inflow, and the outflow, respectively. We

assumed that the conductivity of the salty groundwater is the same as the conductivity of the water at maximum depth in HBHA and that the conductivity of the fresh groundwater is equal to the conductivity of Halls Brook. For August 14, the following measured values were used:

Q_{HB} = 3720 (m^3/day) C_{HB} = 350 (μmho/cm)

Q_{OUT} = 6250 (m^3/day) C_{OUT} =750(μmho/cm)

and the following values were assumed:

C_{SGW} = 4360 (m^3/day) C_{FGW} = 350(μmho/cm)

Solving equations 6 and 7, Q_{SGW} = 620 m^3/day and Q_{FGW} = 1910 μmho/cm.

We know that the actual salty groundwater conductivity is at least 12,000 μmhos cm^{-1}, so our calculated groundwater flows are not physically correct. Actual salty groundwater flows would be approximately a factor of three less than our calculated value for Q_{SGW}. However, we assume that dense groundwater flows along the bottom of lake, mixing with less salty water as it goes, until it reaches the bottom of the lake at our sampling station. Our operationally calculated salty groundwater, then, should represent this flow that arrives at the bottom of the lake before advecting upwards. The fresh groundwater is assumed to flow into the epilimnion at an unknown depth of equal density.

The water column was divided into vertical boxes, each of which was assumed to be well mixed. Water flows between each box as shown in Figure 4.2. For the bottom box, 1, the groundwater flows in, water flows in from box two, and water flows out of box 1 into box 2. For boxes 2 and higher, flows are exchanges between each box and the boxes immediately above and below each box. In general, we can write the following equations based on the conservation of mass:

$$Q_{n+1,n} = \frac{C_n Q_{n,n-1} + C_n Q_{GW} - C_{n-1} Q_{n-1,n}}{C_{n+1} - C_n} \quad (8)$$

$$Q_{n,n+1} = Q_{GW} + Q_{n+1,n} \quad (9)$$

where C is the conductivity in a given box or in the groundwater and Q is the flow in and out of boxes for which the subscripts refer to box numbers, with box 1 as the bottom box. Subscripts of the form, x,y, indicate flow from box x to box y when associated with Q. For box 1, $C_{n-1}Q_{n-1,n} = C_{GW}Q_{GW}$ and $C_nQ_{n,n-1} = 0$ since there is no flow out of the bottom of box 1. Thus, given the ground water flow rate and conductivity and the conductivity of each box, the flows in and out of each box were calculated. $Q_{n+1,n}$ is due entirely to vertical mixing, whereas $Q_{n,n+1}$ reflects both advection (equal to Q_{GW}) and vertical mixing. The downward flow rates can be used to calculate a diffusive flux,

$$F = \frac{(C_{n+1} - C_n)Q_{n+1,n}}{A_{n,n+1}} = -E_z \frac{dC}{dz} \tag{10}$$

which can then be used to calculate the vertical turbulent diffusion coefficient, E_z. The results of this calculation for August 14, 1998 are shown in Figure 4.3. Values ranges from 2.5×10^{-3} to 1.2×10^{-2} cm^2/s below the pycnocline. As expected, the minimum vertical turbulent diffusion coefficient occurred at the pycnocline (1.5 m).

The consistency of the calculated turbulent diffusion coefficients with the conductivity profile was tested by running a CHEMSEE model. The measured values for conductivity were used as the initial values, and measured or calculated flows and calculated diffusion coefficients were used. After ten model days, there was less than 1% overall deviation from the initial values regardless of the assumed fresh groundwater conductivity (0, 350, and 1000 µmho/cm were each tried). Additionally, the stability frequency,

$$N^2 = \frac{g}{\rho}\frac{d\rho}{dz} \tag{11}$$

where $d\rho/dz$ is the vertical gradient of the water density ρ, and g is the acceleration due to gravity, was calculated by assuming that density due to temperature and to salt concentration is additive. Salt concentrations were calculated by scaling the values determined by Wick and Gschwend (1998) by conductivity. At the pycnocline, where

$E_z = 2.5 \times 10^{-3}$ cm^2/s, N^2 was calculated to be 9×10^{-3} s^{-2}. Based on an extrapolation of the relationship found between N^2 and E_z for another lake (Urnersee) under calm conditions reported in the literature, $N^2 = 9 \times 10^{-3}$ s^{-2} corresponds to an E_z of 10^{-3}, quite similar to our calculated value of 2.5×10^{-3} cm^2/s despite different lake hydrology (Wüest, 1987; Schwarzenbach et al., 1993).

4.3 Modeling

4.3.1 CHEMSEE Set Up

The CHEMSEE program was set up to model conditions in HBHA on August 14, 1997 by entering values for the physical characteristics of HBHA, the inflows and outflows, and the vertical diffusion coefficients as a function of depth [Table 4.4]. Hydrogen peroxide formation and degradation rates were also defined. Photochemical formation was defined as a zeroth order reaction variable over time and depth [Table 4.3] Two degradation processes were also defined. The "epilimnion degradation" was defined as a first order reaction with a half-life of 24 hours over the entire depth of the lake. This represents the observed pseudo-first order reaction rate observed for hydrogen peroxide degradation in HBHA samples. A "pycnocline degradation" process was defined as a first order reaction in H_2O_2 below the pycnocline at arbitrarily high rates [Table 4.4]. The initial value of hydrogen peroxide concentration used in the first iteration of the model was 0. The model was run for a model-time of 1 day, and the concentration profile at the end of one day was used as the initial concentration profile of hydrogen peroxide for the next iteration. This process was continued until steady state was reached.

4.3.2 Results

Each iteration of the model produced values for the hydrogen peroxide concentration in each vertical box for each time step of 0.1 days. Steady state results within 10% was achieved on the second model-day, and within 1% on day 4. The

results of the model for day 5 are shown in Figure 4.4. The maximum value of hydrogen peroxide varied from 1.8 μM to 3.2 μM over the course of a day. Starting at 4 AM, the concentrations drop to a minimum of 1.7 to 2.1 μM by the first time step at 6:24 AM, because degradation is faster than photochemical production at the low sunlight intensities around sunrise. The concentrations increase with time throughout the day, with the fastest increase around solar noon, when the sunlight intensity is greatest, and reaching a maximum at around 4 PM. After 4 PM, sunlight levels fall low enough for photochemical production rates to fall below degradation rates, so hydrogen peroxide concentrations begin to fall. Profiles were relatively constant over the epilimnion (< ±10%), indicating that vertical mixing is faster than photochemcial production, but more constant with depth at night in the absence of photochemical production than in the afternoon. Production alone results in an exponential decay in hydrogen peroxide concentration with depth due to light attenuation, but vertical mixing acts to carry hydrogen peroxide in the surface waters down throughout the epilimnion.

4.3.3 Addition of Source Function

Using the results of the previous model after it had been run for 5 model days, a pycnocline source was added as a zeroth order production term, leaving the other processes the same as in the previous model. The addition of a source near the pycnocline (1.45 m) in the model did not result in a gradient of hydrogen peroxide within the epilimnion. If the source was placed at a level just above the pycnocline (1.3 - 1.5 m), mixing was faster than production, resulting in relatively constant epilimnion profiles [Figure 4.5]. If the source was placed slightly deeper in the water column (between 1.39 m and 1.5 m with the maximum at 1.44 m), large amounts (~16 μM) of hydrogen peroxide built up in the pycnocline, with smaller amounts escaping into the epilimnion. The resulting profiles were constant through the epilimnion with a sudden spike in the pycnocline. When a large source strength was used (1000 μM day^{-1}, about 8 times as large as the photochemical source over the entire epilimnion),

hydrogen peroxide that made it into the epilimnion was still mixed faster than it was supplied to the bottom of the epilimnion, resulting in high concentrations at the pycnocline and constant concentrations in the epilimnion [Figure 4.6].

4.4 Discussion

4.4.1 Comparison to Data

The modeled data without a pycnocline source is of the same order of magnitude as the data from August 14. Modeled values were higher than observed values in the morning: 1.6 - 1.8 μM for the model at 6:24 AM as compared to less than 1 μM at 6 AM [Figure 4.4]. This may indicate that the modeled degradation rate was too slow or that the photochemical production term was too high. Model data were also more constant than observed values in the afternoon (2.7 - 3.2 μM at 4 PM in the model as compared to 2 - 7 μM) [Figure 4.4]. Additionally, hydrogen peroxide concentrations were either uniform with depth in the epilimnion or they fall slightly with depth, depending on the time of day. The data shows an increase with depth on Aug. 14. In September and October, the photochemical production should decrease due to shorter days and lower solar inclinations, and we would expect even lower concentrations of hydrogen peroxide. However, we continued to see even higher concentrations at HBHA on those dates with an even more extreme increase with depth [Figure 3.16 and Figure 3.17].

An additional source was not be successfully modeled using our estimated parameters. These results were highly sensitive to the depth at which the source was placed due to large differences in the vertical mixing coefficients over small changes in depth. Our calculated mixing coefficients in the epilimnion were based on only two temperature profiles, one taken in the early morning and one in mid-afternoon. The mixing coefficients were most likely changing throughout the day as the prevailing winds changed. If the vertical turbulent mixing coefficients at the bottom of the lake were lower than calculated over most of the day, this might allow for a build up of

hydrogen peroxide at the bottom of the epilimnion. The vertical resolution of vertical diffusion coefficients is also very important to the result. Our data was taken at a maximum resolution of 0.1 m, and better resolution than this may be needed.

An additional problem is that the vertical mixing across the pycnocline as calculated by the conductivity profile is uncertain. The least certain value was the conductivity of fresh groundwater. Fortunately, changing this value from 0 to 1000 μmho/cm results in only a factor of three difference in calculated E_z values and the range of results was consistent with the steady state conductivity profile. We also know that the salty groundwater is not in fact coming in the deepest part of the lake (where we measured all the profiles in this study), but at the northern end of the lake. The conductivity of this groundwater is at least 12000 μmho cm^{-1}. It may, however, be a reasonable assumption that the water flowing up from the bottom of the profiling spot in some combination of salty and fresh groundwater that flows to the deepest part of the lake before advecting upwards. The assumption that HBHA is horizontally well mixed and that vertical profiles were controlled by turbulent vertical mixing may also be faulty. Vertical mixing may have occurred faster at the sides of the lake, before diffusing horizontally to the rest of the lake. However, past work has shown that HBHA seems to be well mixed from west to east, and reasonably well mixed from north to south (Wick et al., 1998).

4.4.2 Possible Additional Sources

Several possibilities for additional hydrogen peroxide sources exist. The quantum yield of hydrogen peroxide formation could be higher in HBHA water than what has been reported in the literature, but this would not change the shape of the modeled profiles. This would also result in higher concentrations throughout the year and not just the late summer and fall as we saw in HBHA. Rainwater could introduce hydrogen peroxide to HBHA, but it had not rained in several days on any of the dates when high hydrogen peroxide concentrations were observed. High hydrogen peroxide concentrations could possibly enter with the surface water inputs, that is,

Halls Brook. If hydrogen peroxide was being dumped into the river, extremely high concentrations in Halls Brook would be needed to explain the concentrations observed in HBHA.

A chemical source at the pycnocline could be due to reduced metal oxidation by molecular oxygen. The oxidation of the metal by oxygen to form superoxide (and then H_2O_2) (equation 1.10) would have to occur at faster rates than its oxidation by hydrogen peroxide (equation 1.11) in order to act as a net source of H_2O_2. The kinetics for this sort of process appear unfavorable in the case of iron, but possible in the case of copper (see section 1.5). Since the oxidation kinetics of metals such as iron and copper are dependent on the presence of iron oxide surfaces and biological reactions, it is difficult to extrapolate rates of hydrogen peroxide formation and degradation due to redox processes in HBHA from laboratory kinetic studies. However, a redox chemistry source does not seem justified by the data, because it would not be expected to exist only in late summer and fall, but not in winter.

The most likely possibility for an additional source of hydrogen peroxide in HBHA is a biological source. A layer of high microbial activity at the pycnocline might be expected due to the opposing gradients of light levels and oxygen on the one side and nutrient concentrations coming in with the groundwater on the other side. Indeed, a chlorophyll *a* and turbidity peak was observed at the pycnocline in October 1998 [Figure 3.5]. The algae and cyanobacteria studied to date do not seem to produce hydrogen peroxide fast enough to account for the concentrations observed at HBHA. Up to ~ 50 mmol m^{-3} day^{-1} at 1000 mg chl a m^{-3} has been observed *in vitro* (Zepp et al., 1987; see section 1.5) as compared to the photochemical source used in the model of ~ 60 mmol m^{-3} day^{-1} near the surface at noon. The only chlorophyll *a* concentrations observed in HBHA were about 60 mg chl a m^{-3}, and at these concentrations algae similar to those studies by Zepp et al. would not produce enough hydrogen peroxide. However, it is possible that other species are capable of producing more H_2O_2 and/or that a larger bloom of algae existed in HBHA during the fall of 1997. Under appropriate environmental conditions, a hydrogen peroxide-

producing community of microorganisms may have become dominant in HBHA in late summer and fall of 1997.

4.5 References

Cooper, W. J., Zika, R. G., Petasne, R. G. and Plane, J. M. C., 1988. Photochemical formation of H_2O_2 in natural waters exposed to sunlight. *Environ. Sci. Technol.*, **22**: 1156-1160.

Cooper, W. J., Shao, C., Lean, D. R. S., Gordon, A. S. and Scully, F. E., Jr., 1994. Factors affecting the distribution of H_2O_2 in surface waters. Environmental Chemistry of Lakes and Reservoirs. L. A. Baker. Washington D.C., ACS. **237:** 390-422.

Imboden, D. M., Eid, B. S. F., Joller,T., Schuster, M. and Wetzel, J. 1979. MELIMEX, an experimental heavy-metal pollution study. 2. Vertical mixing in a large limnocorral *Schweiz. Z. Hydrol.*, **47**: 177-189.

Leifer, A. 1988. The Kinetics of Environmental Aquatic Photochemistry. Washington, DC, American Chemical Society.

Schnoor, J. L. 1996. Environmental Modeling. Fate and Transport of Pollutants in Water, Air, and Soil. New York, John Wiley & Sons.

Schwarzenbach, R. P., Gschwend, P. M. and Imboden, D. M., 1993. Photochemical Transformation Reactions. Environmental Organic Chemistry. New York, Wiley: 436-484.

Scully, N. M., Lean, D. R. S., McQueen, D. J. and Cooper, W. J., 1995. Photochemical formation of hydrogen peroxide in lakes: effects of dissolved organic carbon and ultraviolet radiation. *Can. J. Fish. Aquat. Sci.*, **52**: 2675-2681.

Ulrich, Markus, 1994. CHEMSEE: A model construction kit for the simulation of dynamic processes in lakes. User's Guide. 2nd version.

Wick, L. Y., McNeill, K., Diez, S., Southworth, B., and Gschwend, P.M., 1996-1998, Unpublished results.

Wüest, A., 1987. *Ursprung und Grösse von Mischungsprozessen im Hypolimnion von Seen*, Dissertation ETH, Zurich.

Zepp, R. G. and Cline, D. M. 1977. Rates of direct photolysis in aquatic environment. *Environ. Sci. Technol.*, **11**: 359-366.

Zepp, R. G., Skurlatov, Y. I. and Pierce, J. T., 1987. Algal-induced decay and formation of hydrogen peroxide in water: its possible role in oxidation of anilines by algae. Photochemistry of Environmental Aquatic Systems. R. G. Zika and W. J. Cooper. Washington, D.C., American Chemical Society: 215-224.

4.6 Figures and Tables

λ (nm)	Z(noon, λ) mE cm^{-2} s^{-1}	Z(24 hr, λ) mE cm^{-2} d^{-1}	$\alpha_D(\lambda)$ cm^{-1}	Φ(λ)
297.5	1.19E-09	2.68E-05	0.107	0.0015
300	3.99E-09	1.17E-04	0.103	0.0013
302.5	1.21E-08	3.60E-04	0.099	0.0012
305	3.01E-08	8.47E-04	0.094	0.0011
307.5	5.06E-08	1.62E-03	0.091	0.00097
310	8.23E-08	2.68E-03	0.087	0.00085
312.5	1.19E-07	3.94E-03	0.084	0.00074
315	1.60E-07	5.30E-03	0.081	0.0007
317.5	1.91E-07	6.73E-03	0.078	0.00069
320	2.24E-07	8.12E-03	0.075	0.00067
323.1	4.18E-07	1.45E-02	0.073	0.00065
330	1.41E-06	5.03E-02	0.076	0.0006
340	1.60E-06	6.34E-02	0.061	0.00055
350	1.71E-06	7.03E-02	0.054	0.0005
360	1.83E-06	7.77E-02	0.046	0.00045
370	2.03E-06	8.29E-02	0.038	0.00041
380	2.24E-06	8.86E-02	0.031	0.00037
390	2.68E-06	8.38E-02	0.025	0.00032
400	3.84E-06	1.20E-01	0.021	0.00007
420	1.51E-05	4.77E-01	0.015	0.00007
450	1.90E-05	6.04E-01	0.010	0.00007
480	2.04E-05	6.52E-01	0.008	0.00007
510	2.12E-05	6.82E-01	0.006	0.000026
540	2.22E-05	7.09E-01	0.004	0.000024
570	2.25E-05	7.14E-01	0.003	0.000024
600	2.24E-05	7.19E-01	0.002	0.000024
640	3.72E-05	1.22	0.001	0.000006

Table 4.1. Sunlight intensity, absorbance of HBHA epilimnion water , and apparent quantum yields of hydrogen peroxide formation as a function of wavelength. These values were used for the photochemical input of H_2O_2 calculation.

EDT	f(t)	EDT	f(t)
1:00	0	13:00	1.00
2:00	0	14:00	0.96
3:00	0	15:00	0.89
4:00	0	16:00	0.79
5:00	0.04	17:00	0.66
6:00	0.28	18:00	0.49
7:00	0.49	19:00	0.28
8:00	0.66	20:00	0.04
9:00	0.79	21:00	0
10:00	0.89	22:00	0
11:00	0.96	23:00	0
12:00	1.00	0:00	0

Table 4.2. Attenuation of noon sunlight intensity as a function of time. f(t) is the scaling factor vs. Eastern Daylight Time. Sunrise occurred at approximately 5:40 AM and sunset at 7:40 PM on August 14.

	0	0.04	0.08	0.13	0.17	0.21	0.25	0.29	0.33	0.38	0.42	0.46	0.50	0.54	0.58	0.63	0.67	0.71	0.95
0	0.0	2.5	17.3	30.3	40.8	48.9	55.1	59.4	61.9	61.9	59.4	55.1	48.9	40.8	30.3	17.3	2.5	0.0	0.0
0.05	0.0	1.5	10.2	17.9	24.0	28.8	32.4	35.0	36.4	36.4	35.0	32.4	28.8	24.0	17.9	10.2	1.5	0.0	0.0
0.1	0.0	0.9	6.5	11.4	15.3	18.3	20.6	22.3	23.2	23.2	22.3	20.6	18.3	15.3	11.4	6.5	0.9	0.0	0.0
0.15	0.0	0.6	4.4	7.8	10.5	12.6	14.1	15.3	15.9	15.9	15.3	14.1	12.6	10.5	7.8	4.4	0.6	0.0	0.0
0.2	0.0	0.5	3.2	5.7	7.7	9.2	10.3	11.1	11.6	11.6	11.1	10.3	9.2	7.7	5.7	3.2	0.5	0.0	0.0
0.25	0.0	0.4	2.5	4.4	5.9	7.0	7.9	8.6	8.9	8.9	8.6	7.9	7.0	5.9	4.4	2.5	0.4	0.0	0.0
0.3	0.0	0.3	2.0	3.5	4.7	5.6	6.3	6.8	7.1	7.1	6.8	6.3	5.6	4.7	3.5	2.0	0.3	0.0	0.0
0.35	0.0	0.2	1.6	2.9	3.9	4.6	5.2	5.6	5.9	5.9	5.6	5.2	4.6	3.9	2.9	1.6	0.2	0.0	0.0
0.4	0.0	0.2	1.4	2.4	3.3	3.9	4.4	4.8	5.0	5.0	4.8	4.4	3.9	3.3	2.4	1.4	0.2	0.0	0.0
0.5	0.0	0.1	1.0	1.8	2.5	2.9	3.3	3.6	3.7	3.7	3.6	3.3	2.9	2.5	1.8	1.0	0.1	0.0	0.0
0.6	0.0	0.1	0.8	1.4	1.9	2.3	2.6	2.8	2.9	2.9	2.8	2.6	2.3	1.9	1.4	0.8	0.1	0.0	0.0
0.7	0.0	0.1	0.7	1.1	1.5	1.9	2.1	2.3	2.3	2.3	2.3	2.1	1.9	1.5	1.1	0.7	0.1	0.0	0.0
0.8	0.0	0.1	0.5	0.9	1.3	1.5	1.7	1.9	1.9	1.9	1.9	1.7	1.5	1.3	0.9	0.5	0.1	0.0	0.0
0.9	0.0	0.1	0.5	0.8	1.1	1.3	1.4	1.5	1.6	1.6	1.5	1.4	1.3	1.1	0.8	0.5	0.1	0.0	0.0
1	0.0	0.1	0.4	0.7	0.9	1.1	1.2	1.3	1.4	1.4	1.3	1.2	1.1	0.9	0.7	0.4	0.1	0.0	0.0
1.1	0.0	0.0	0.3	0.6	0.8	0.9	1.0	1.1	1.2	1.2	1.1	1.0	0.9	0.8	0.6	0.3	0.0	0.0	0.0
1.2	0.0	0.0	0.3	0.5	0.7	0.8	0.9	1.0	1.0	1.0	1.0	0.9	0.8	0.7	0.5	0.3	0.0	0.0	0.0
1.3	0.0	0.0	0.2	0.4	0.6	0.7	0.8	0.8	0.9	0.9	0.8	0.8	0.7	0.6	0.4	0.2	0.0	0.0	0.0
1.4	0.0	0.0	0.2	0.4	0.5	0.6	0.7	0.7	0.8	0.8	0.7	0.7	0.6	0.5	0.4	0.2	0.0	0.0	0.0
1.5	0.0	0.0	0.2	0.3	0.4	0.5	0.6	0.6	0.7	0.7	0.6	0.6	0.5	0.4	0.3	0.2	0.0	0.0	0.0

Table 4.3. Model photochemical production input as a function of time and depth. Depth (m) is in the first column of the table, and time (days) is in the first row, where t=0 corresponds to 4 AM. Production values are in units of mmol H_2O_2 m^{-3} day^{-1}.

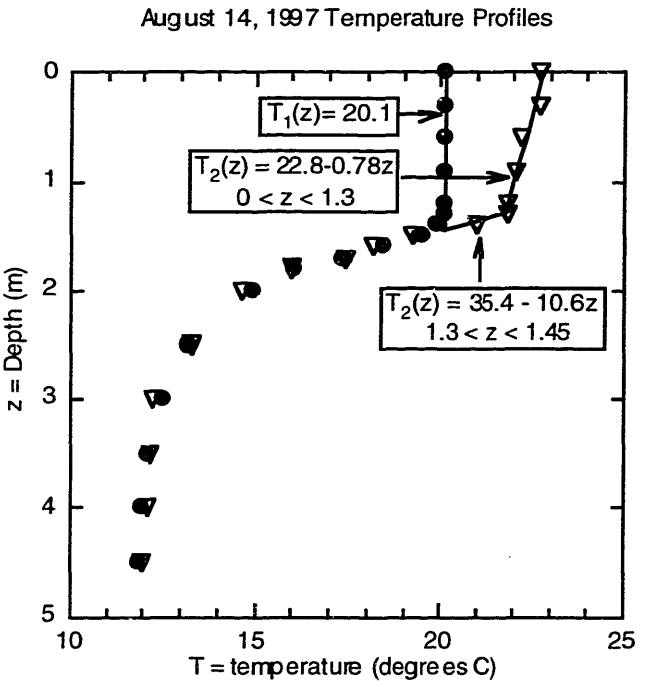

Figure 4.1. Temperature profiles used for vertical turbulent diffusion coefficient calculation in the epilimnion of HBHA for 8/14/98. The equations represent the best-fit lines drawn through the data, where T is in degrees Celsius and z is in meters.

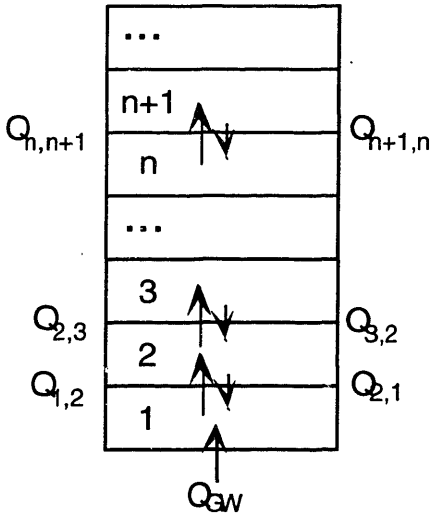

Figure 4.2. Flows into and out of each box in HBHA. Q_{GW} represents the flow of groundwater into the bottom box. $Q_{x,y}$ represents the flow from box x to box y.

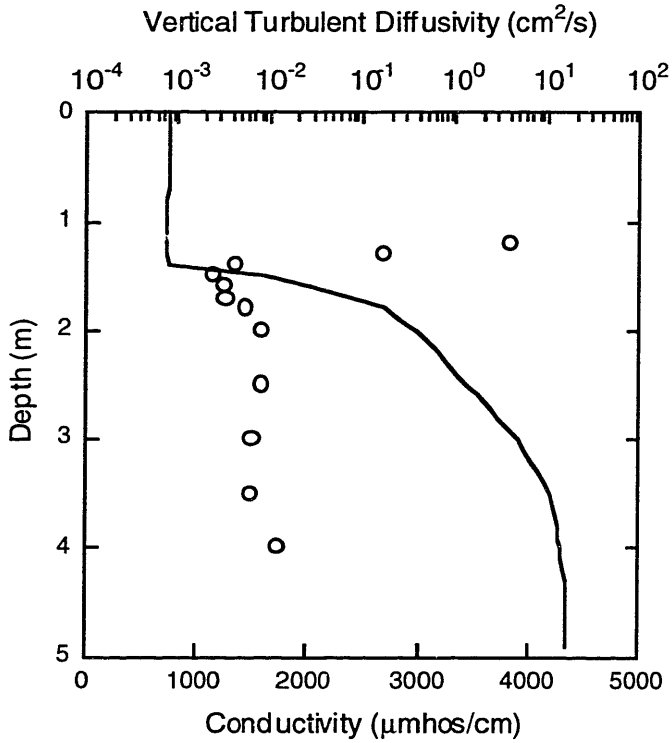

Figure 4.3. Conductivity profile (line) used for calculation of vertical turbulent diffusion coefficients below the epilimnion in HBHA (8/14/98), and calculation results for the vertical turbulent diffusivity (circles).

Table 4.4. CHEMSEE model inputs

Maximum Depth (m) 4.9

Area

Depth (m)	Area (m^3)
0.0	17000
1.5	11600
3.0	5990
4.0	2250

Inflows (m^3/s)	From (m)	To (m)
Q_{HB}=0.04[illegible]	0.0	0.5
Q_{FGW}=0.022	0.5	1.0
Q_{SGW}=0.007	4.5	4.9
Outflows		
Q_{OUT}=0.072	0.0	0.5

Vertical turbulent diffusion coefficient

Depth (m)	E_z (m^2 day^{-1})
0.0	7.8
1.2	10.7
1.3	5.9
1.4	0.037
1.5	0.022
1.6	0.028
1.7	0.029
1.8	0.048
2	0.073
2.5	0.074
3	0.057
3.5	0.056
4	0.106

Pycnocline Degradation

Depth	Rate (day^{-1})
0.0	0
1.0	0
1.4	0
1.5	-100
1.6	-1000
4.9	-1000

Epilimnion Degradation

-0.7 day^{-1}

Model Parameters

Number of Boxes	90
Relative change per timestep	5%
Maximum timestep	10^{-4} days
Minimum timestep	10^{-7} days
Run time	1 day
Output interval	0.1 days

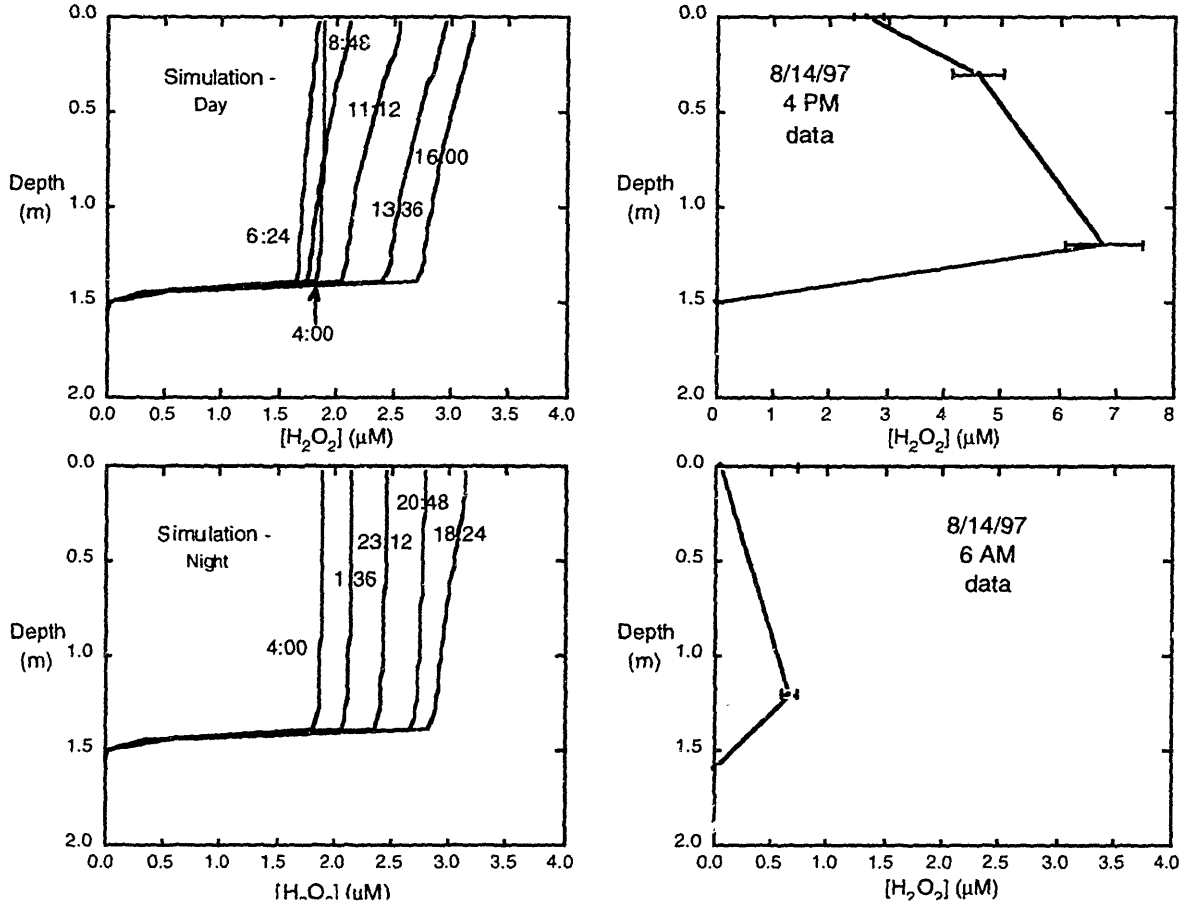

Figure 4.4. Steady state model results after an 5-day simulation compared to August 14, 1997 data. Approximate time of day is indicated for each model profile. Note the x-axis scale difference for the afternoon data (8/14/97 4 PM).

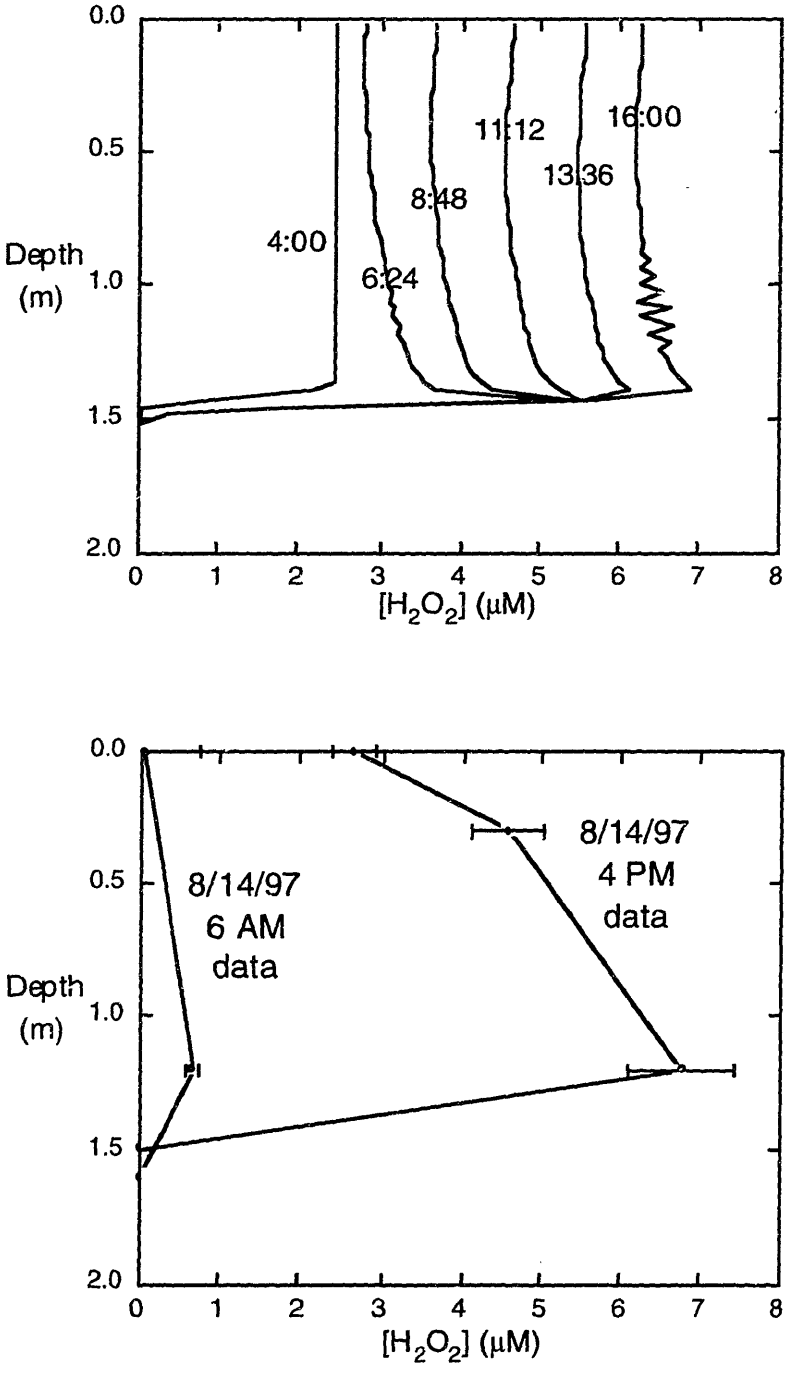

Figure 4.5. Example results for the addition of a H_2O_2 source above the pycnocline compared to data from 8/14/97. The zeroth order source (200 μM H_2O_2 d^{-1}) was located at 1.4 m and went to zero above 1.3 m and below 1.5 m.

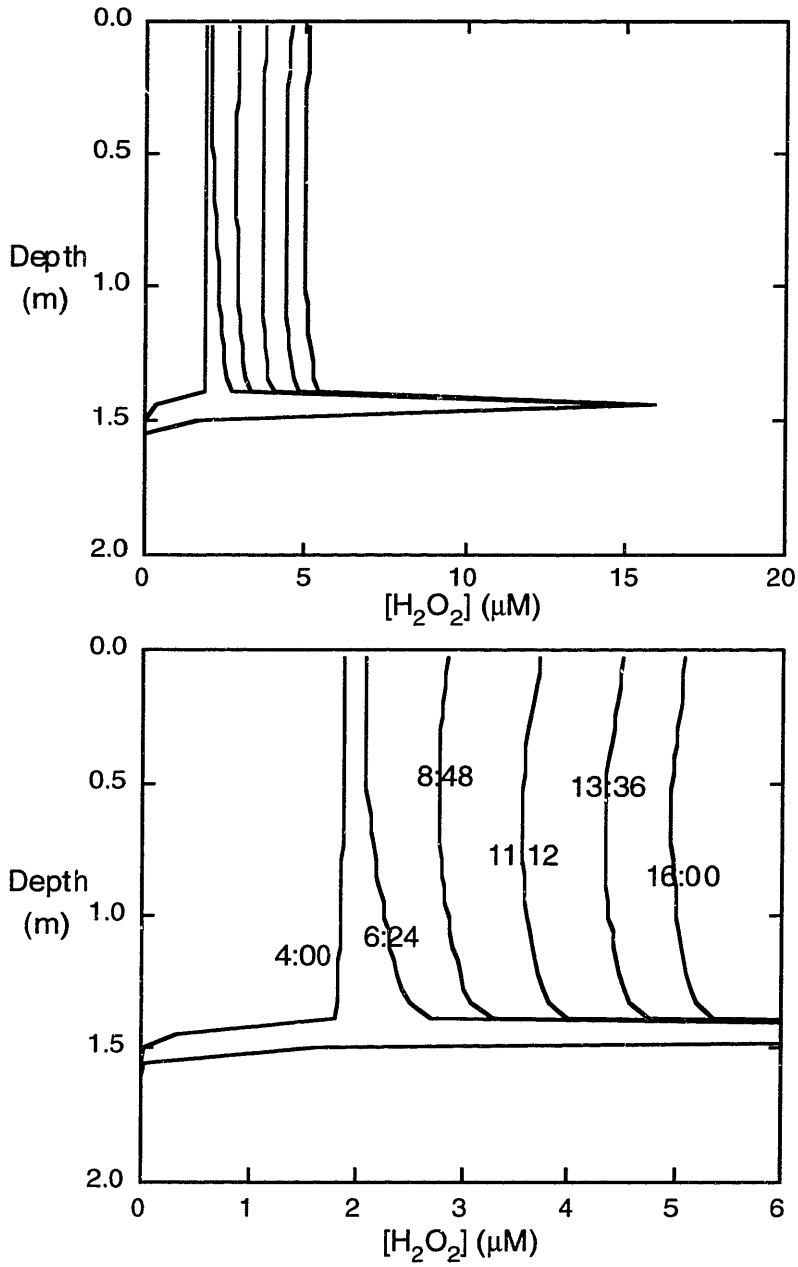

Figure 4.6. Example results of adding an H_2O_2 source at the pycnocline to the model. The zeroth order source (1000 μM H_2O_2 d^{-1}) was located at 1.44 m and went to zero above 1.39 m and below 1.5 m. The second plot is the same as the first, but with an expanded y-axis scale.

5. Conclusions and Future Work

Hydrogen peroxide distributions observed in the Halls Brook Holding Area between May 1997 and February 1998 could not be explained by the formation and decay processes previously observed for lakes reported in the literature. Higher concentrations (up to 80 μM) were observed at HBHA as compared to the highest previously reported value of 3 μM. These high concentrations were observed on three dates from August to October 1997. Low and insignificant (compared to method blanks) concentrations were observed in May 1997 and from December to February 1997-1998. When high concentrations were observed, the maximum concentration occurred at the bottom of the epilimnion. This sort of profile is inconsistent with an abiotic photochemical source only. A seasonal biological source seems like the most likely source of additional hydrogen peroxide at the bottom of the epilimnion.

The addition of a pycnocline source to our model did not result in profiles similar to observed hydrogen peroxide gradients. This may be due to insufficient resolution of vertical diffusion coefficients over time and space. Better resolution of conductivity and temperature data should be readily achievable during future field studies. Turbulent vertical mixing above the pycnocline most likely changes throughout the day as heat is added to the lake, and these changes could greatly affect hydrogen peroxide profiles and should be incorporated into the modeling work.

Additionally, an improved hydrogen peroxide measurement technique would be useful. Flow injection analysis of samples could allow for continuous monitoring of hydrogen peroxide concentrations over the course of a day, while avoiding the possibility of degradation during transit to the lab. The issue of declining standard curves with increasing concentrations of hydrogen peroxide will also need to be resolved in order to get more accurate values for the hydrogen peroxide concentrations. Hydrogen peroxide data with a high degree of spatial and temporal resolution should help resolve the location and the possible diurnal nature of a source other than non-abiotic photochemistry.

More accurate estimates of abiotic photochemical formation of hydrogen peroxide can be achieved by measuring the apparent quantum yields of hydrogen peroxide formation in HBHA as a function of wavelength instead of relying on literature values. Alternatively, formation under a solar simulator could be measured to get a gross formation rate. More accurate estimates of sunlight intensity on a particular date can be obtained from the computer program, GCSOLAR.

The decay rate of hydrogen peroxide in HBHA also needs to be investigated. This could be done by suspending bottles containing HBHA water at the depth from which they were collected and measuring concentrations of H_2O_2 over time. Bottles could be covered to prevent photochemical production or poisoned or filtered to prevent biological processes. This could also help to discriminate between the different sources and sinks in HBHA and help to identify the nature of the pycnocline source. Quartz bottles could also be suspended so that *in situ* photochemical formation could be observed as a check on the calculated photochemical production rates.

Once the processes that control hydrogen peroxide concentrations in HBHA are more fully understood, we plan to investigate the role of hydrogen peroxide in the potential production of hydroxyl radical. As a first estimate, we could calculate the amount of hydrogen peroxide that mixes across the pycnocline and assume that all of this hydrogen peroxide reacts to form hydroxyl radical. The distributions of organic compounds such as trichloroethylene (TCE) that do not appear to undergo biological degradation, but should be degraded by hydroxyl radical, could be studied to see if their behavior is consistent with the calculated hydroxyl radical concentrations. With the high concentrations of hydrogen peroxide that must be produced very close to the pycnocline in order to result in the observed hydrogen peroxide profiles and the high concentrations of ferrous iron below the pycnocline, we suspect that hydroxyl radical production should have a significant impact on organic pollutants in HBHA.

Appendix A: Field Data

5/27/97

Depth (m)	*Temperature (°C)*	*Conductivity (µmho/cm)*	*DO (mg/L)*
0.0	18.0	420	6.6
0.3	17.0	430	7.0
1.0	15.5	415	6.9
1.3	15.0	415	6.4
1.7	14.3	418	6.3
2.0	14.5	420	6.6
2.3	14.3	430	6.1
2.7	13.5	480	3.4
3.0	13.0	590	0.5
3.3	12.5	790	0.3
3.7	12.5	1010	0.3
4.0	11.5	1150	0.2
4.3	11.0	1700	0.2
4.7	10.5	1800	0.2

7/16/97

Depth (m)	*Temperature (°C)*	*Conductivity (µmho/cm)*	*DO (mg/L)*	*pH*	E_H *(mV)*
0.0	24.06	769	5.89	6.85	30
0.2	23.81	769	5.75	6.83	27
0.6	22.56	790	5.40	6.70	26
0.9	20.97	769	5.86	6.63	22
1.0	21.11	1012	7.34	6.50	35
1.1	21.26	1143	7.41	6.50	36
1.2	20.94	1279	9.23	6.46	45
1.3	19.74	1559	9.15	6.43	38
1.4	19.34	1691	5.03	6.42	9
1.5	18.08	1848	0.60	6.45	-72
1.6	16.33	2155	0.28	6.61	-1.7
1.7	16.45	2240	0.21	6.65	-119
1.9	15.02	2434	0.17	6.68	-119
2.2	13.85	2765	0.16	6.71	-129
2.5	12.94	3119	0.15	6.82	-132
3.0	12.33	3558	0.12	6.89	-139
3.5	11.92	3824	0.14	6.92	-139
4.5	11.69	3958	0.13	6.92	-136

8/14/1997 6 AM

Depth (m)	*Temperature (°C)*	*Conductivity (µmho/cm)*	*DO (mg/L)*	*pH*	*E_H (mV)*
0.0	20.10	798	3.89	6.62	278
0.3	20.11	799	3.59	6.94	281
0.6	20.11	799	3.39	6.93	280
0.9	20.11	800	3.40	6.53	278
1.2	20.11	800	3.37	6.53	276
1.3	20.09	868	2.31	6.49	256
1.4	19.90	904	1.60	6.45	260
1.5	19.50	1197	0.26	6.39	249
1.6	18.45	1677	0.23	6.48	211
1.7	17.40	2244	0.12	6.66	49
1.8	16.03	2602	0.09	6.69	36
2.0	14.96	2790	0.10	6.71	17
2.5	13.20	3322	0.10	6.77	12
3.0	12.55	3773	0.10	6.84	5
3.5	12.13	4222	0.10	6.89	-6
4.0	11.98	4275	0.10	6.89	-8
4.5	11.91	4355	0.10	6.90	-11

8/14/1997 4 PM

Depth (m)	*Temperature (°C)*	*Conductivity (µmho/cm)*	*DO (mg/L)*	*pH*	*E_H (mV)*
0.0	22.74	764	4.71	6.69	240
0.3	22.75	761	4.33	6.62	244
0.6	22.21	755	4.36	6.60	243
0.9	22.05	745	4.31	6.58	243
1.2	21.86	739	4.11	6.57	242
1.3	21.83	742	4.01	6.57	241
1.4	20.99	763	2.52	6.56	241
1.5	19.23	1622	0.95	6.44	207
1.6	18.19	2010	0.39	6.52	179
1.7	17.45	2452	0.32	6.62	126
1.8	16.00	2702	0.28	6.67	71
2.0	14.68	2978	0.27	6.69	61
2.5	13.27	3441	0.27	6.74	39
3.0	12.28	3903	0.25	6.84	5
3.5	12.23	4203	0.22	6.89	-6
4.0	12.11	4291	0.23	6.89	-8
4.5	12.00	4357	0.19	6.90	-11

9/4/97

Depth (m)	*Temperature (°C)*	*Conductivity (µmho/cm)*	*DO (mg/L)*
0.0	19.0	680	5.4
0.5	19.0	680	5.5
1.0	19.0	680	5.1
1.5	19.0	680	5.2
1.6	17.5	680	5.2
1.7	17.5	700	1.0
1.7	17.5	1900	0.2
1.8	17.0	2000	0.1
1.9	16.5	2150	0.1
2.0	16.0	2250	0.1
2.1	15.5	2400	0.1
2.5	15.5	2650	0.1
3.0	14.5	2700	0.1
3.3	13.0	2700	0.1
3.7	13.0	2950	0.1
4.0	13.0	3000	0.1
4.5	13.0	3000	0.1

9/24/97

Depth (m)	*Temperature (°C)*	*Conductivity (µmho/cm)*	*DO (mg/L)*
0.0	16	520	5.9
0.1	17	520	6.1
0.3	16	520	5.2
0.7	16	520	5.8
1.0	16	520	5.8
1.3	15	520	5.2
1.7	16	520	5.3
2.0	16	1800	0.2
2.3	16	2400	0.2
2.7	15	2600	0.2
3.0	14	2850	0.2
3.3	14.5	2925	0.2
3.7	13.5	3000	0.2
4.0	14	2990	0.2
4.3	13	2990	0.2
4.7	13	2900	0.2

10/22/97

Depth (m)	*Temperature (°C)*	*Conductivity (µmho/cm)*	*DO (mg/L)*	E_H *(mV)*
0.0	11.03	780	8.83	233
0.3	11.04	780	8.97	231
0.6	11.04	781	8.96	230
1.0	11.04	781	8.66	230
1.3	11.07	782	8.85	229
1.5	11.12	812	7.50	224
1.6	12.82	1845	0.58	164
1.8	13.72	3075	0.30	134
2.0	13.78	3401	0.24	117
2.2	13.69	3614	0.22	109
2.6	13.28	3895	0.23	79
3.0	12.93	4139	0.22	67
3.4	12.66	4250	0.22	59
4.0	12.54	4343	0.22	55
4.5	12.56	4401	0.21	52

11/20/97

Depth (m)	*Temperature (°C)*	*Conductivity (µmho/cm)*	*DO (mg/L)*
0.2	3.95	486	7.53
0.5	3.90	486	7.49
1.0	3.88	486	7.47
1.5	3.91	490	7.41
1.7	4.02	499	7.21
1.8	4.34	588	5.62
1.9	4.19	721	4.37
2.0	5.24	895	2.10
2.1	5.69	1090	0.70
2.2	6.23	1418	0.17
2.3	6.65	1646	0.14
2.4	7.60	1926	0.11
2.5	7.90	2674	0.13
3.0	11.03	3989	0.13
3.5	11.87	4270	0.11
4.0	12.10	4328	0.12
4.5	12.28	4428	0.11

12/17/97

Depth (m)	*Temperature (°C)*	*Conductivity (µmho/cm)*	*DO (mg/L)*	*pH*	E_H *(mV)*
0.0	3.27	650	6.69	7.07	110
0.5	3.04	654	7.20	6.89	164
1.0	3.16	664	7.95	6.72	250
1.5	3.57	760	6.76	6.54	289
1.6	3.87	826	5.91	6.47	304
1.7	4.37	921	3.64	6.38	310
1.8	4.69	1020	2.78	6.37	314
1.9	4.97	1234	0.81	6.36	315
2.0	5.34	1500	0.26	6.44	325
2.1	5.68	1785	0.12	6.55	250
2.3	6.04	2136	0.13	6.65	175
2.5	6.84	3005	0.11	7.02	70
3.0	8.30	3710	0.13	7.29	-3
3.5	8.89	3893	0.12	7.33	-26
4.0	9.24	3951	0.11	7.22	-28

1/27/98

Depth (m)	*Temperature (°C)*	*Conductivity (µmho/cm)*	*DO (mg/L)*	*pH*	E_H *(mV)*
0.1	1.18	600	10.13	6.64	398
0.5	1.18	601	10.13	6.61	400
1.0	1.17	602	10.11	6.59	405
1.5	1.17	602	10.10	6.60	405
2.0	1.18	602	10.10	6.62	407
2.5	1.17	602	10.08	6.62	407
3.0	1.35	612	10.00	6.62	409
3.1	1.45	629	9.79	6.59	409
3.2	1.71	653	9.06	6.54	405
3.3	2.18	686	6.81	6.44	402
3.4	3.11	966	1.21	6.69	312
3.5	4.15	2040	0.23	7.12	152
3.6	5.37	3297	0.13	7.18	108
3.7	6.12	3684	0.14	7.20	92
3.8	6.41	3707	0.14	7.20	89
4.0	6.43	3713	0.14	7.20	86
4.2	6.53	3536	0.13	7.23	72

2/27/98

Depth (m)	*Temperature (°C)*	*Conductivity (µmho/cm)*	*DO (mg/L)*	*pH*	*E_H (mV)*
0.0	5.15	395	10.45	6.86	516
0.5	4.96	396	10.14	6.82	514
1.0	4.94	396	10.10	6.81	513
2.0	4.93	396	10.08	6.81	513
2.5	4.94	397	10.05	6.81	511
3.0	4.94	397	10.02	6.82	509
3.5	4.91	399	10.03	6.82	508
4.0	4.90	399	9.98	6.83	506
4.25	4.98	482	6.30	7.11	215
4.35	5.42	2344	0.45	7.26	110
4.5	5.63	2917	0.24	7.38	80
5.0	6.68	3262	0.17	7.09	114

3/10/98

Depth (m)	*Temperature (°C)*	*Conductivity (µmho/cm)*	*DO (mg/L)*	*pH*	*E_H (mV)*
0.0	10.00	221	8.03	7.10	221
1.5	9.67	220	8.07	6.96	264
3.0	9.68	221	8.04	6.94	316
3.5	9.64	222	8.02	6.95	324
4.0	8.28	334	7.90	6.89	336
4.2	7.55	540	4.85	6.71	343
4.4	6.78	850	0.77	6.74	294
4.6	6.93	2500	0.15	6.52	50
4.8	7.04	3115	0.14	7.64	16

4/21/98

Depth (m)	*Temperature (°C)*	*Conductivity (µmho/cm)*	*DO (mg/L)*	*pH*	*EH (mV)*
0.3	11.59	481	7.00	6.20	415
1.1	11.42	480	7.01	6.31	418
1.9	10.66	479	6.99	6.36	419
2.4	10.33	469	6.99	6.38	420
2.7	10.28	470	6.88	6.40	421
3.0	10.18	471	6.96	6.41	421
3.4	10.53	1334	1.50	6.14	417
3.8	9.60	1502	0.52	6.21	374
4.2	9.47	1561	0.45	6.28	337
4.9	8.31	2913	0.27	7.52	18

6/10/98

Depth (m)	*Temperature (°C)*	*Conductivity (µmho/cm)*	*DO (mg/L)*	*pH*	E_H *(mV)*
0.0	22.26	495	5.22	6.70	496
0.5	18.08	495	5.63	6.69	498
1.0	17.05	496	5.65	6.69	498
1.5	16.21	501	5.30	6.68	498
2.0	14.83	559	3.93	6.58	500
2.5	14.65	621	1.62	6.50	503
3.0	14.58	808	0.35	6.39	504
3.5	14.24	1312	0.16	6.54	399
4.0	13.10	1784	0.15	6.74	251
4.5	12.26	1580	0.13	6.93	190

10/25/98

Depth (m)	*Temperature (°C)*	*Conductivity (µmho/cm)*	*DO (mg/L)*	*pH*	E_H *(mV)*	*Turbidity (NTU)*	*"Chl a" (mg/L)*
0.20	12.66	559.4	6.19	6.67	429	4.4	3.2
0.73	12.44	559.5	6.25	6.67	427	4.7	3.5
0.72	12.32	558.9	6.25	6.68	425	6.3	3.5
1.20	12.15	560.5	6.14	6.74	422	7.4	3.7
1.20	12.01	562.9	6.10	6.67	421	5.3	3.8
1.41	11.93	565.4	6.09	6.68	420	4.5	3.9
1.58	11.67	567.4	6.01	6.68	419	5.5	4.0
1.65	11.54	570.9	5.91	6.68	417	5.5	11.1
1.74	11.39	635.7	4.71	6.58	421	11.3	12.2
1.74	11.24	789.8	3.03	6.48	420	18.6	7.1
1.78	11.12	830.8	2.79	6.48	419	19.3	47.4
1.81	11.32	849.8	1.59	6.48	414	21.8	42.1
1.84	11.42	1032	1.41	6.43	418	23.8	46.0
1.88	11.68	1328	0.33	6.44	417	34.8	48.6
1.90	11.65	1307	0.38	6.41	415	41.4	54.4
1.94	11.63	1275	0.31	6.42	413	39.0	35.2
1.98	11.72	1408	0.22	6.43	403	35.1	36.2
2.02	11.74	1460	0.05	6.47	372	16.2	16.9
2.06	12.02	1750	0.03	6.54	342	22.5	53.1
2.13	12.21	2013	0.02	6.57	324	39.6	23.6
2.13	11.99	1741	0.00	6.50	319	12.6	25.0
2.13	11.85	1653	0.00	6.50	314	14.7	24.1
2.15	12.02	2015	0.00	6.60	295	29.7	23.7
2.19	12.19	2149	0.01	6.63	284	46.6	13.3
2.26	12.66	2586	0.01	6.74	264	33.5	17.6
2.32	13.12	3063	0.00	6.82	232	20.9	17.8
2.37	12.99	2884	0.00	6.78	218	23.0	17.1
2.51	13.12	2999	0.00	6.80	203	20.1	18.6

2.52	13.32	3241	0.00	6.98	189	14.4	18.9
2.54	13.36	3260	0.00	6.84	172	13.6	21.1
2.69	13.44	3370	0.00	6.87	164	12.8	22.9
2.70	13.68	3561	0.00	6.92	152	12.0	23.2
2.80	13.75	3653	0.00	6.97	132	12.1	21.3
2.90	13.84	3702	0.00	6.96	124	10.9	28.4
2.99	13.85	3752	0.00	6.95	116	11.3	23.5
3.12	13.93	3910	0.00	6.92	109	11.8	31.8
3.23	13.97	3953	0.00	6.96	102	11.4	31.0
3.37	13.99	4012	0.00	6.95	91	13.9	33.2
3.64	13.97	4039	0.00	6.86	86	11.3	25.1
3.65	13.95	4052	0.00	6.95	83	11.3	32.0
3.81	13.94	4056	0.00	6.96	76	11.6	29.9
4.12	13.92	4078	0.00	7.00	73	12.5	32.3
4.12	13.92	4032	0.00	6.98	68	6.7	31.8

Depth (m)	*Temperature (°C)*	*Conductivity (µmho/cm)*	*DO (mg/L)*
4.09	13.90	4042	0.00
4.08	13.90	4071	0.00
3.88	13.92	4063	0.00
3.35	13.96	4037	0.00
3.31	13.98	3979	0.00
3.06	13.95	3913	0.00
2.75	13.68	3548	0.00
2.35	13.45	3319	0.00
2.23	13.02	2929	0.00
2.21	12.70	2629	0.00
2.11	12.45	2346	0.00
2.02	11.98	1765	0.00
2.02	12.05	1709	0.00
1.97	11.92	1627	0.00
1.97	11.59	1484	0.20
1.97	11.57	1488	0.24
1.97	11.76	1500	0.12
1.75	11.58	1253	0.63
1.73	11.67	691.6	2.70
1.42	12.12	563.5	5.84
1.14	12.54	560.1	6.07

THESIS PROCESSING SLIP

FIXED FIELD: ill. _____ name _____

index _____ biblio _____

► COPIES: (Archives) Aero Dewey (Eng) Hum

Lindgren Music Rotch Science

TITLE VARIES: ► ☐ _____

NAME VARIES: ► ☑ Anne _____

IMPRINT: (COPYRIGHT) _____

► COLLATION: 122 ℓ

► ADD: DEGREE: _____ ► DEPT.: _____

SUPERVISORS: _____

NOTES:

cat'r: date:

page: F 37

► DEPT: C. E.

► YEAR: 1999 ► DEGREE: S. M.

► NAME: SOUTHWORTH, Barbara A.